Pacific Northwest
NATIONAL LABORATORY

PNNL-28846
73793-RPT-0001, Rev 0.0

Carbon Tetrachloride: Evaluation of Biotic Degradation Mechanisms and Rates

June 2019

CE Bagwell
C Johnson
G Wang
I Demirkanli
M Truex

U.S. DEPARTMENT OF ENERGY

Prepared for the U.S. Department of Energy
under Contract DE-AC05-76RL01830

DISCLAIMER

PACIFIC NORTHWEST NATIONAL LABORATORY
operated by
BATTELLE
for the
UNITED STATES DEPARTMENT OF ENERGY
under Contract DE-AC05-76RL01830

Printed in the United States of America

Available to DOE and DOE contractors from the
Office of Scientific and Technical Information,
P.O. Box 62, Oak Ridge, TN 37831-0062;
ph: (865) 576-8401
fax: (865) 576-5728
email: reports@adonis.osti.gov

Available to the public from the National Technical Information Service
5301 Shawnee Rd., Alexandria, VA 22312
ph: (800) 553-NTIS (6847)
email: orders@ntis.gov <https://www.ntis.gov/about>
Online ordering: http://www.ntis.gov

PNNL-28846
73793-RPT-0001, Rev 0.0

Carbon Tetrachloride: Evaluation of Biotic Degradation Mechanisms and Rates

June 2019

CE Bagwell
C Johnson
G Wang
I Demirkanli
M Truex

Prepared for
the U.S. Department of Energy
under Contract DE-AC05-76RL01830

Pacific Northwest National Laboratory
Richland, Washington 99354

Executive Summary

Quantitative information about *in situ* natural degradation mechanisms and rates for carbon tetrachloride (CT) is needed to support remedy implementation with respect to the operational lifetime of the 200 West Groundwater Treatment Facility (200W P&T system) and transition to monitored natural attenuation. Laboratory studies estimated the hydrolysis half-lives of CT and chloroform (CF) under Hanford groundwater conditions (pH 7.8, 16 °C) to be 630 and 3,400 years, respectively. This rate of CT hydrolytic degradation is too slow and will not have a consequential impact on groundwater CT remediation. Biotic and coupled biotic-abiotic mechanisms of natural CT degradation have not been evaluated or measured with respect to a natural attenuation remedy for 200 West Area aquifer (200W aquifer) conditions.

Summarized in this report are biotic and abiotic reductive degradation mechanisms for CT, as well as chlorinated byproducts, along with normalized reaction rates for each mechanism based on published values from controlled laboratory studies and field trials. In addition to hydrolysis, CT can degrade via three other mechanisms: (1) biotic hydrogenolysis, where CF accumulates as an intermediate byproduct; (2) a biotic dichlorocarbene pathway to CO_2, with no measureable intermediate byproducts; and (3) abiotic degradation by reactive minerals, where CF and a range of other compounds may be intermediate byproducts. Published reaction rate data are for conditions where biostimulation amendments have been added or reactive minerals are present; thus, this information is only useful in assessing relative rates of CT and byproduct degradation, not for absolute rates of natural attenuation in the 200W aquifer. Previous field trials have demonstrated that the Hanford subsurface microbial populations can degrade CT during respiratory nitrate reduction (denitrification) when a labile organic carbon substrate is available. The coincident presence of CF with CT in the aquifer near the disposal areas is another indicator that reductive dechlorination (hydrogenolysis) occurred historically when CT was co-disposed with organic carbon wastes. There is ample evidence to demonstrating that, under the appropriate conditions, biotic and abiotic-biotic reductive degradation of CT (and CF) can occur in the 200W aquifer.

CT degradation mechanisms were used to identify indicators of degradation activity. 200 West Area groundwater data and the relative significance of measured trends in groundwater chemistry were evaluated, taking into account the effect of 200W P&T activities on monitoring well data. Examination of available groundwater data throughout the plume over the period from 1986 to the present provides evidence that biotic CT degradation has taken place and continues to occur in the 200W aquifer. Briefly, the multiple lines of evidence for continuing *in situ* biotic CT degradation are as follows.

- Anaerobic reductive dechlorination (hydrogenolysis) of CT in the 200 West groundwater is indicated by the detection of dichloromethane (DCM) across a wide spatial area and into recent time. DCM only originates from the degradation of CT (and CF) occurring in anoxic/reduced zones by reductive dechlorination. DCM is a reliable indicator of more recent degradation activity because DCM is quickly metabolized to CO_2 in oxic groundwater (which is the predominant condition in the bulk 200W aquifer). Thus, detection of DCM in groundwater indicates recent biotic degradation in anoxic/reduced zones that must be within proximity to the wells where DCM is detected (i.e., not from historical degradation near a source zone with co-disposed organic waste).
- The detection, and in certain cases the accumulation, of nitrite is clear evidence of microbial catalyzed nitrate reduction to nitrite. Nitrite is evidence of incomplete nitrate reduction (as the first step in the pathway). There is ample evidence in the literature (including site-specific data) that shows nitrate degradation is positively correlated with anaerobic degradation of CT. Nitrite is a reliable indicator of recent denitrification activity in anoxic/reduced zones because nitrite is highly unstable in oxic groundwater and will quickly oxidize back to nitrate. Thus the detection of nitrite in a monitoring well is evidence of recent denitrification activity within close proximity to the wells

where it is detected. The nitrite detection limit is high because of the high nitrate concentrations in many wells. Therefore, it may be that nitrite is more ubiquitous at low concentrations, but is not being detected against the high background concentrations of nitrate.

- CF concentration trends are also an indicator of CT degradation by reductive dechlorination. CF can only be derived by the anaerobic degradation of CT in anoxic, reduced zones within the aquifer. At monitoring wells, concentrations of CT and CF are affected by aquifer heterogeneity, plume migration, adsorption, and degradation. However, based on a relative rate analysis for CT and CF, increasing CF concentrations and an increasing CF/CT ratio are indicators for CT degradation that can be used in conjunction with the above indicators. For monitoring data away from the source area, these trends are indicative of more recent degradation activity. The widespread presence of CF in the aquifer is an indication that reductive dechlorination (hydrogenolysis) occurred in the past, which was likely driven in large part by the co-disposal of organic waste at the primary CT disposal areas.

Mechanisms and pathways for CT/CF degradation are well established in the literature. There is a wealth of site-specific data (experimental, field, and monitoring) that supports biotic degradation of CT and conditions suitable for abiotic-biotic reductive degradation in the 200W aquifer. The analysis of 200 West Area groundwater data revealed numerous well locations distributed throughout the aquifer where multiple indicators of local anoxic/reduced conditions and CT degradation pathway products (DCM) coincide. The analysis was restricted to well locations that have not been influenced by any P&T operations in the 200 West Area. More than three decades of groundwater data reveals a pattern of persistent *in situ* CT degradation activity. The sustainability of biotic and coupled biotic-abiotic processes depends on anoxic, reduced conditions and a supply of organic carbon. An organic carbon energy source is required to fuel microbiological pathways, and the metabolism of organic carbon generates anoxic, reduced conditions that propagate anaerobic degradation and sustain reducing power for abiotic processes. Organic carbon is the single most important driver (or rate limiting factor) of CT degradation in the 200W aquifer. Indicators of recent anoxic activity demonstrate that there is a flux of organic carbon into anoxic zones that supports continued denitrification and CT degradation.

The oxic conditions of the bulk aquifer are not conducive to biotic degradation of CT or CF. DCM and CM degradation would be expected within high permeability flow paths where oxic conditions dominate. The conceptual model of CT degradation in the 200 West Area aquifer is based on CT and CF degradation occurring in anoxic, reduced zones of low permeability (e.g., silt and clay lenses or possibly the RLM unit) which will comprise only a portion of the total aquifer volume. There are adequate indicators that these zones exist and that CT and CF degradation is currently occurring. However, for remediation purposes, a bulk aquifer degradation rate is needed to evaluate the overall impact that biotic and abiotic degradation pathways are having on the CT plume.

Reductive dechlorination (hydrogenolysis) is a coupled rate process for CT→CF→DCM→CM under the anaerobic conditions required for the reaction to proceed. Microcosm tests consistently show CF accumulation as an intermediate for reductive dechlorination, which would occur even with CT and CF rates being similar, if the CT concentration is higher than the CF concentration. The CT and CF responses can be estimated based on relative degradation rates over a range of initial concentrations. When the CT concentration is high (~100 µg/L and higher), even a moderate rate of CT reductive dechlorination (hydrogenolysis) will cause the CF concentration to increase when the CF degradation rate is similar to or even faster than the CT rate. At locations where CT is in the 100-1000 µg/L range and the degradation rate of CT has a half-life between 100 and 400 years, CF concentrations would be expected to increase over time with a noticeable increase in just 10- to 20-years. At groundwater monitoring wells, CT and CF concentrations are affected by changing geochemical conditions, plume migration, and a variable degradation rate. Thus, the strongest indicator for potential CT degradation would be increasing concentrations of CF and an increasing CF/CT ratio. There are 16 groundwater well locations in the

studied area of the 200W aquifer where DCM, nitrite, and CF-based indicators and visual inspection of trends offer convincing evidence of reductive dechlorination (hydrogenolysis).

In the absence of site-specific laboratory rate data, CF concentration data can be used to approximate the rate of CT reductive dechlorination (hydrogenolysis). From the rate estimate evaluation, it is unlikely that biotic degradation of CT to CF would support a half-life projection of 100 years or less. If that were the case, CF concentration would be increasing in areas where CT concentration is above 100 µg/L. However, biotic degradation of CT to CF could support a bulk aquifer half life of less than 400 years, and be consistent with the available site groundwater data.

For the purposes of the rate assessment summarized above, reductive dechlorination (hydrogenolysis) of CT to CF was the only degradation pathway considered. It is important to note that abiotic pathways and other biotic degradation pathways may not lead to the accumulation of CF. Thus, the contributions of these degradation pathways are not captured by a CF-based rate estimate or the presence of DCM. Evidence of anoxic, reduced geochemical conditions (the same indicators that were used for reductive dechlorination) do however, imply that these other pathways are clearly possible at the site. There are a large set of locations (58) where the presence of DCM and nitrite indicate anoxic zones in the region of the monitoring well.

The effect of these pathways on the bulk rate of CT degradation is uncertain because direct indicators such as CF are not available for these other pathways. However, the biotic pathway for CT degradation without accumulation of CF requires specific conditions in the Hanford subsurface that may be less likely than conditions conducive to the pathway leading to accumulation of CF. Abiotic pathways depend on the presence of appropriate surface-phase minerals in a reduced oxidation state. These surface phases would be possible in the portion of the aquifer with anoxic conditions. This situation is conceivable in a heterogenous system where geochemically distinct zones could be conducive to a variety of distinct degradation pathways. Given the more specialized conditions needed for these alternative CT degradation mechanisms it is assumed that their contribution to the overall CT degradation rate would be equal to or less than the contribution by the pathway of CT degradation to CF. Thus, the additional pathways would not result in an overall CT degradation half-life of equal to or less than 100 years, if the half-life from the CT to CF degradation pathway is on the order of 400 years. Collectively, though, the biotic and abiotic-biotic mechanisms could result in a half-life that is considerably less than 400 years. Additional efforts could be applied to determine a more specific estimate of the half-life value (i.e., a more specific value between 100 and 400 years). The need for these efforts depends on the impact that a more specific estimate of this rate would have on remedy decisions for the CT in the Ringold Unit E (Rwie) and Ringold Unit A (Rwia) formations of the 200W aquifer. In particular, because of the slower transport velocity in the Rwia formation, a half-life greater than 100 years may still be of significance for attenuating the Rwia CT plume.

If laboratory tests were conducted, they would focus on quantifying CT degradation processes and rates in the low permeability zones (silt and clay lenses) where we anticipate anoxic conditions may occur. Appropriate laboratory data would be needed to estimate the rate of CT degradation in these zones and then scaling would be used to estimate a bulk biotic/reductive CT degradation rate.

Acronyms and Abbreviations

CF	chloroform
CT	carbon tetrachloride
CM	chloromethane
DBP	di-butyl phosphate
DCM	dichloromethane
DNRB	dissimilatory nitrate reducing bacteria
FRB	iron reducing bacteria
NOM	natural organic matter
OC	organic carbon
ORP	oxidation reduction potential
OU	operable unit
PCE	tetrachloroethylene
PFP	Plutonium Finishing Plant
RAO	Remedial Action Objective
RAWR	Remedial Action Work Plan
RD/RA	Remedial Design/Remedial Action
ROD	Record of Decision
RLM	Ringold lower mud
Rwie	Ringold Unit E
Rwia	Ringold Unit A
SRB	sulfate reducing bacteria
TBP	tri-butyl phosphate
TCE	trichloroethylene
TOC	total organic carbon
VOC	volatile organic carbon

Contents

Figures

Tables

1.0 Introduction

The 200 West Area carbon tetrachloride (CT) plume and associated chloroform (CF) (along with comingled contaminants such as nitrate, hexavalent chromium, iodine-129, technetium-99, trichloroethene, and tritium) are currently being remediated by a pump-and-treat (P&T) system. Quantitative information about *in situ* natural degradation mechanisms and rates for CT is needed to support remedy implementation with respect to the operational lifetime of the 200 West Groundwater Treatment Facility (200W P&T system) and the transition to monitored natural attenuation (MNA) as the final remedy step for achieving the identified remedial action objectives. Prior laboratory studies estimated the half-life for hydrolysis of CT under Hanford groundwater conditions (pH 7.8, 16 °C) to be 630 years (Amonette et al., 2012). This rate of CT hydrolysis is slow, and will not have a consequential impact on groundwater CT remediation. Other mechanisms of natural CT degradation, specifically biotic and abiotic-biotic reductive degradation processes, have not been evaluated or measured for 200 West Area groundwater conditions.

Because direct measures of CT natural degradation by biotic or abiotic-biotic reductive degradation processes are not available, lines of evidence need to be evaluated to assess the potential significance of these processes in the 200 West Area aquifer (200W aquifer). The lines of evidence include literature information about CT degradation processes, and site monitoring data for CT, degradation products, and indicators of conditions favorable for CT degradation processes. The goal of this work is to evaluate existing literature for information about possible CT degradation processes and to use this information to interpret site monitoring data in terms of natural attenuation of CT in the 200W aquifer. The targeted outcomes are 1) determination of whether CT degradation by biotic or abiotic-biotic processes is currently occurring in the aquifer, 2) indication of the spatial distribution and prevalence of these CT degradation processes, and 3) estimation of the rate at which these processes are occurring in terms of a CT half-life. Estimating the rate of CT degradation processes will need to consider the type of information available and the uncertainties related to quantifying rates in the field versus rates in the laboratory. However, it is important to identify reasonable bounding values for the estimated field CT degradation rate because this rate is needed for predictive modeling of CT as input to remedy management and transition of the P&T system to MNA. For this purpose, determination of whether the CT degradation half-life is likely to be equal to or less than 100 years is of interest because a 100 year half-life was used in Remedial Design/Remedial Action Work Plan (RD/RAWP) predictive simulations for remedy design and is on the same order as the current timeframe identified in the Record of Decision (ROD) for reaching the remedial action objectives (RAOs) for CT. A CT degradation half-life longer than 100 years may still be significant for natural attenuation of the plume. However, half-life values greater than several hundred years become insignificant in the expected timeframe of the remedy.

The report is organized into the following sections. Section 2.0 provides a brief background for the 200W Area CT plume, and summarizes groundwater data, geochemical conditions and reliable indicators for interpreting CT degradation processes and rates. Section 3.0 covers site relevant biotic and abiotic reactive degradation processes. Section 4.0 summarizes the analysis of the historical data set performed within context of the geochemical requirements for potential degradation mechanisms. Finally, Section 5.0 provides a concise plan for additional field sampling and laboratory experiments needed to generate a more precise measurement of CT degradation rates in the 200W aquifer.

2.0 History, Approach, and Field Data

Groundwater CT concentrations in 200 West Area of the Central Plateau on the Hanford Site are affected by historical disposal practices (i.e., the contamination source), transport processes (advection, diffusion) that vary with site geology and external influences (artificial recharge, pumping/injection), and attenuation processes. This section describes the disposal history of the CT waste streams, activities that have significantly affected groundwater flow, as well as the overall conditions and constituent concentrations in the unconfined aquifer. Theoretical analysis of CT and CF degradation rates for a batch system are used to determine the concentration response characteristics under varying degradation rate and concentration conditions as a metric for assessing trends in existing data. Indicators are identified for analysis of the field data to provide lines of evidence for CT degradation. Collectively, this information is used to evaluate the relative significance of biotic or abiotic-biotic degradation in the 200W aquifer.

2.1 Carbon Tetrachloride Disposal History

At Hanford's Plutonium Finishing Plant (PFP; also referred to as Z Plant) in the south-central portion of the 200 West Area, liquid waste streams generated by the chemical processes used to recover plutonium were discharged to three nearby subsurface disposal facilities. This aqueous waste stream was principally a concentrated, acidic solution of sodium nitrate, though an estimated 5 vol% consisted of organics. The main organic constituents were carbon tetrachloride (CT), tributyl phosphate (TBP), and dibutyl butyl phosphonate (DBBP), plus lesser amounts of dibutyl phosphate (DBP), monobutyl phosphate (MBP), and lard oil (Last and Rohay, 1991; Truex et al., 2001). Between 1955 and 1973, it is estimated that up to 750,000 kg of CT and 13×10^6 L of aqueous waste were discharged from the PFP facility. The resultant dissolved-phase CT groundwater plume spans an aerial footprint of 10 km². Figure 1 shows the CT plume contours for 2017. The nature of the disposed waste stream has impacts relevant to the development of the CT plume. For example, the co-disposed hydrocarbons likely facilitated anaerobic conditions in the subsurface and associated degradation of CT to CF. Also, the volume of water disposed in the 200 West Area resulted in a significant groundwater mound that influenced groundwater flow directions in the unconfined aquifer.

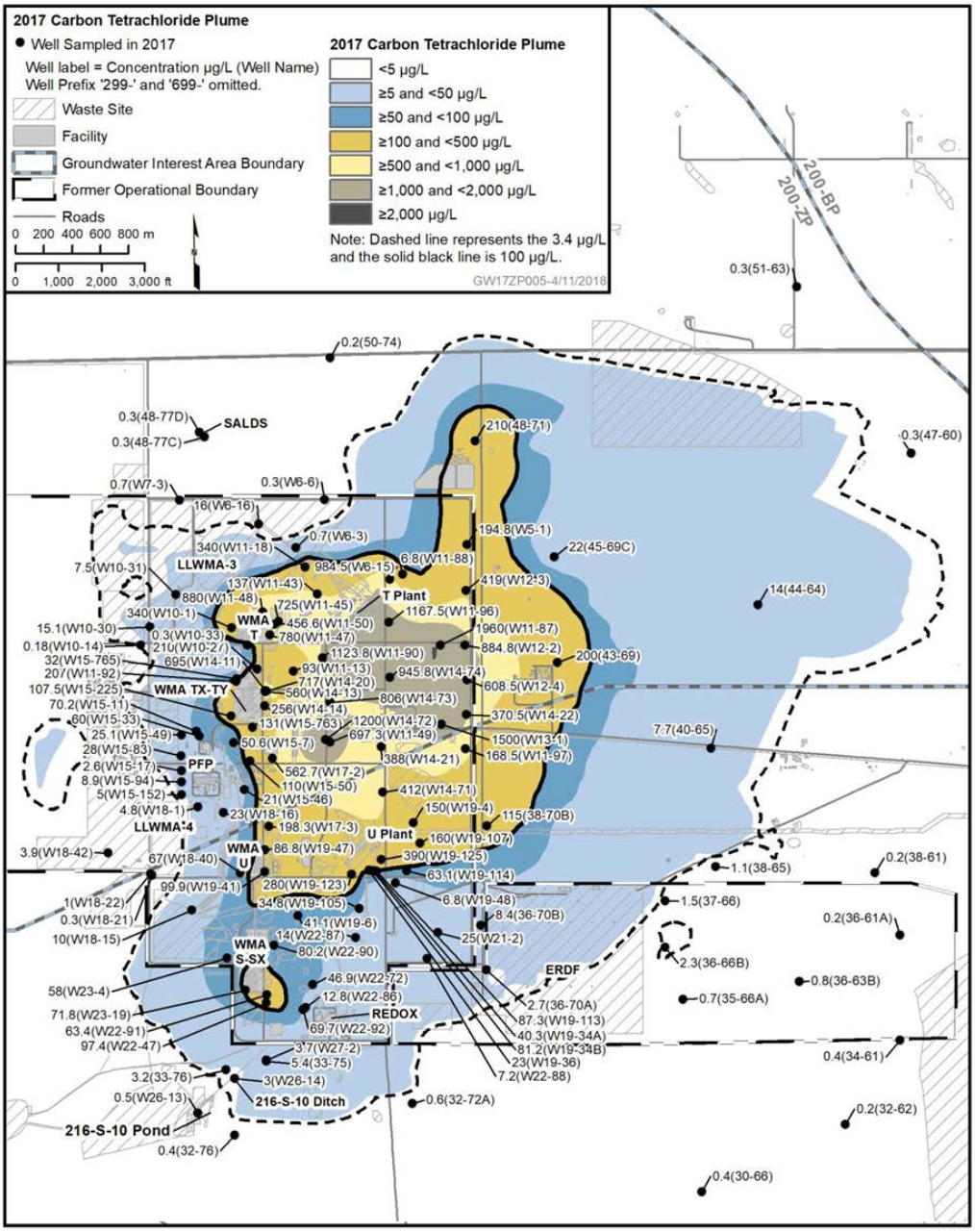

Figure 1. Carbon tetrachloride plume contours for 2017 in the 200 West Area (DOE, 2018a).

2.2 Selection of Zones and Wells for Evaluation

There are three regimes of groundwater flow that are relevant to evaluating groundwater concentration data from the 200 West Area: 1) the time period prior to active groundwater remediation, 2) the time period for the Interim Remedial Action (IRA), and 3) the present time period for the remedial action specified in the Record of Decision (ROD). Appendix A provides a synopsis of information on wells involved in the P&T systems and groundwater hydraulic conditions for these three regimes. This information on predominant features of groundwater flow and the operation of P&T extraction/injection wells provides important context for the interpretation of 200 West Area groundwater concentration data.

Specifically, the P&T information indicated which areas were impacted by P&T; wells outside of those areas are categorically identified as potentially reliable for evaluating groundwater chemistry data.

The nominal zones impacted by IRA and present day P&T systems are shown in Figures 2 and 3, respectively. Monitoring wells outside of the impacted areas are candidates for data analysis of attenuation processes and rates in this study. Based on the zones impacted by IRA and present day P&T, two sets of groundwater wells, a northern group and a southern group, were identified for assessment of CT degradation and related chemistry data. As depicted in Figure 4, the southern group is valid for all time frames, while the northern group is only relevant through the end of IRA P&T activities.

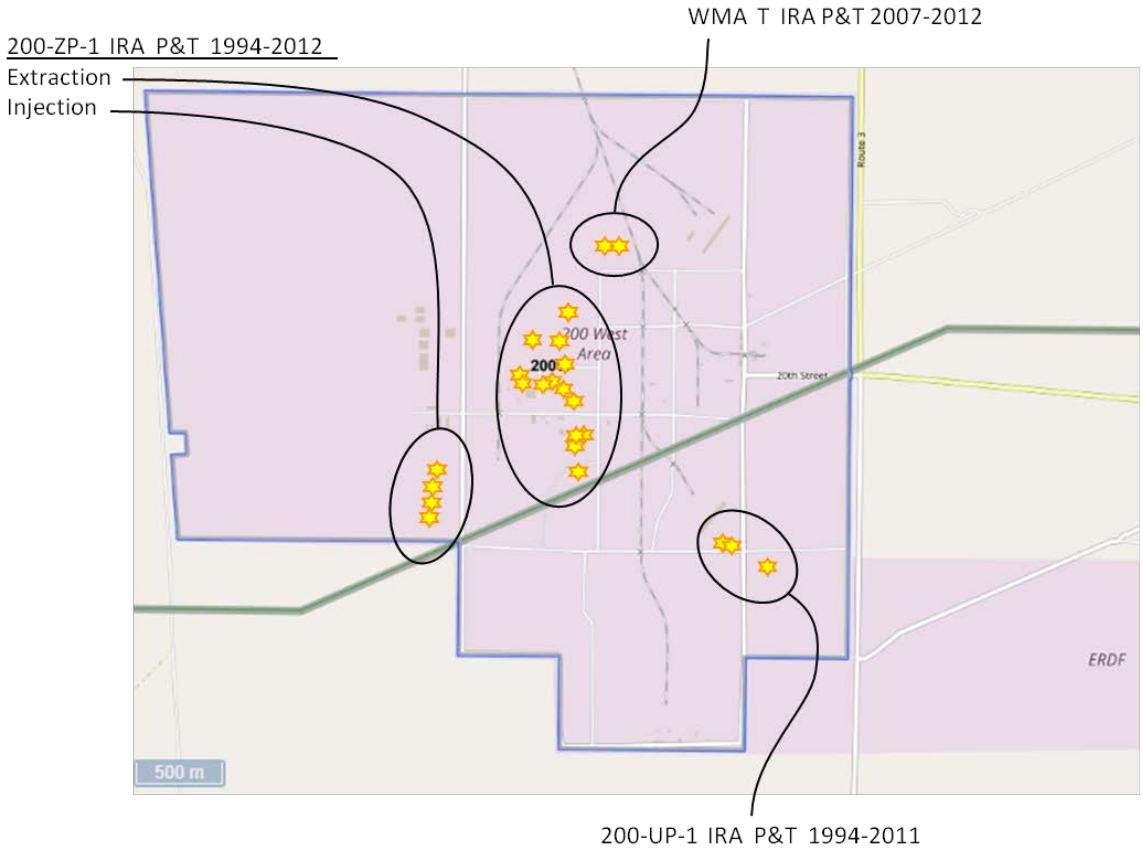

Figure 2. Locations of wells used for Interim Remedial Action P&T systems in the 200 West Area.

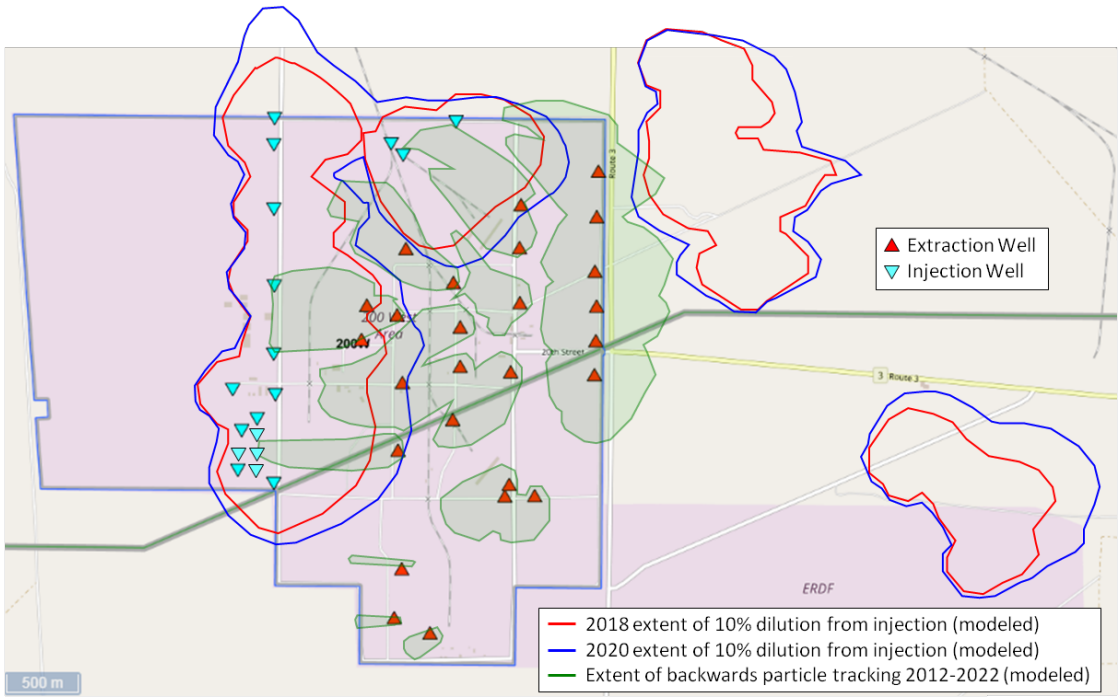

Figure 3. Locations of extraction wells (red triangles) and injection wells (inverted cyan triangles) for the present-day 200W P&T system. (Adapted from information provided by the site contractor modeling team for particle tracking results and dilution zone calculations that were derived from simulations using the Central Plateau Groundwater Model (CP-47631)

In Figure 3, red and blue outlines show numerical model results for the extent of 10% diluted groundwater in 2018 (red) and 2020 (blue). The green shaded zones depict the extent of numerical model results for backwards particle tracking for the period of June 2012 to October 2022. Locations outside of these zones would have been less impacted from the 200W P&T system.

As depicted in Figure 4, the southern group is valid for all time frames, while the northern group is only relevant through the end of IRA P&T activities.

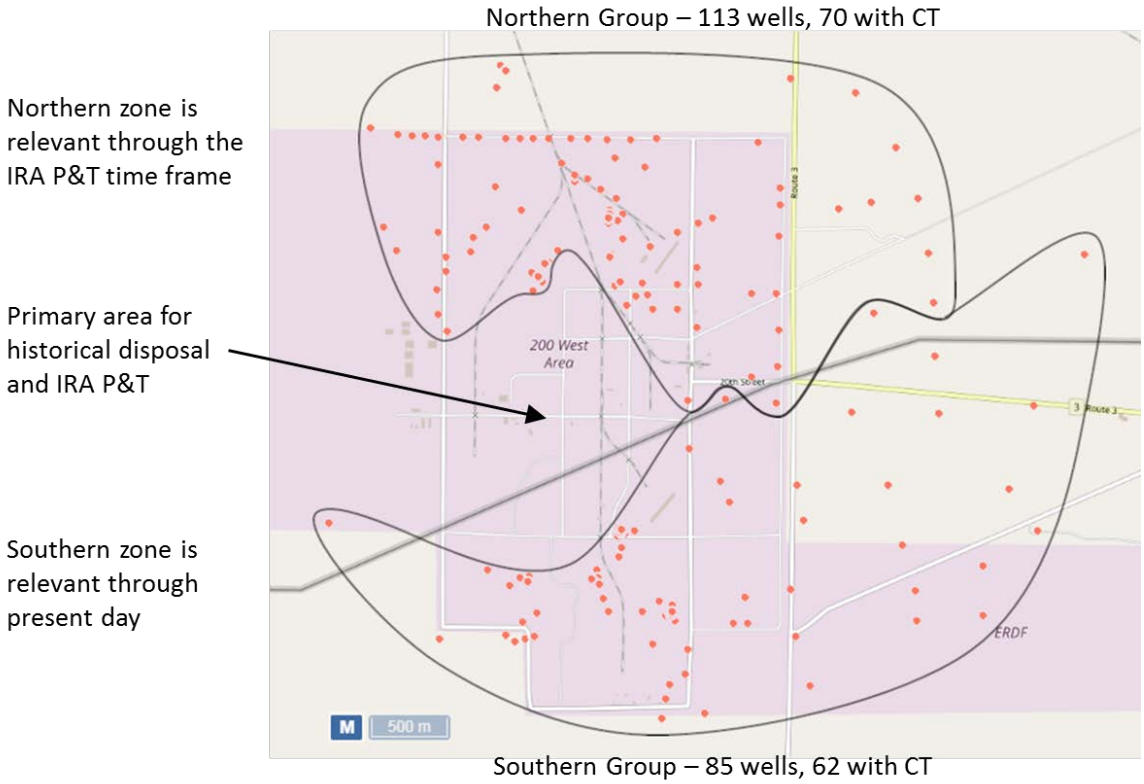

Figure 4. Depiction of the wells relevant to data assessment during IRA P&T and present day P&T activities.

2.3 Groundwater Monitoring Data

The Hanford Environmental Information System (HEIS) is a database repository for groundwater concentration data (and a variety of other Hanford-related environmental data). Groundwater data can be retrieved through web-based tools such as the Environmental Dashboard Application (EDA, https://ehs.hanford.gov/eda) and SOCRATES (https://socrates.pnnl.gov/). Data not flagged as "non-detect" were retrieved from HEIS for CT and degradation products (CF, dichloromethane [DCM; methylene dichloride], chloromethane), co-contaminants (nitrate), and geochemical indicators (nitrite, dissolved oxygen, sulfate, ferrous iron) for wells in the northern and southern groups .

Geochemical indicators are described here to provide the broader context of groundwater in the 200 West Area, setting the stage for identifying attenuation indicators.

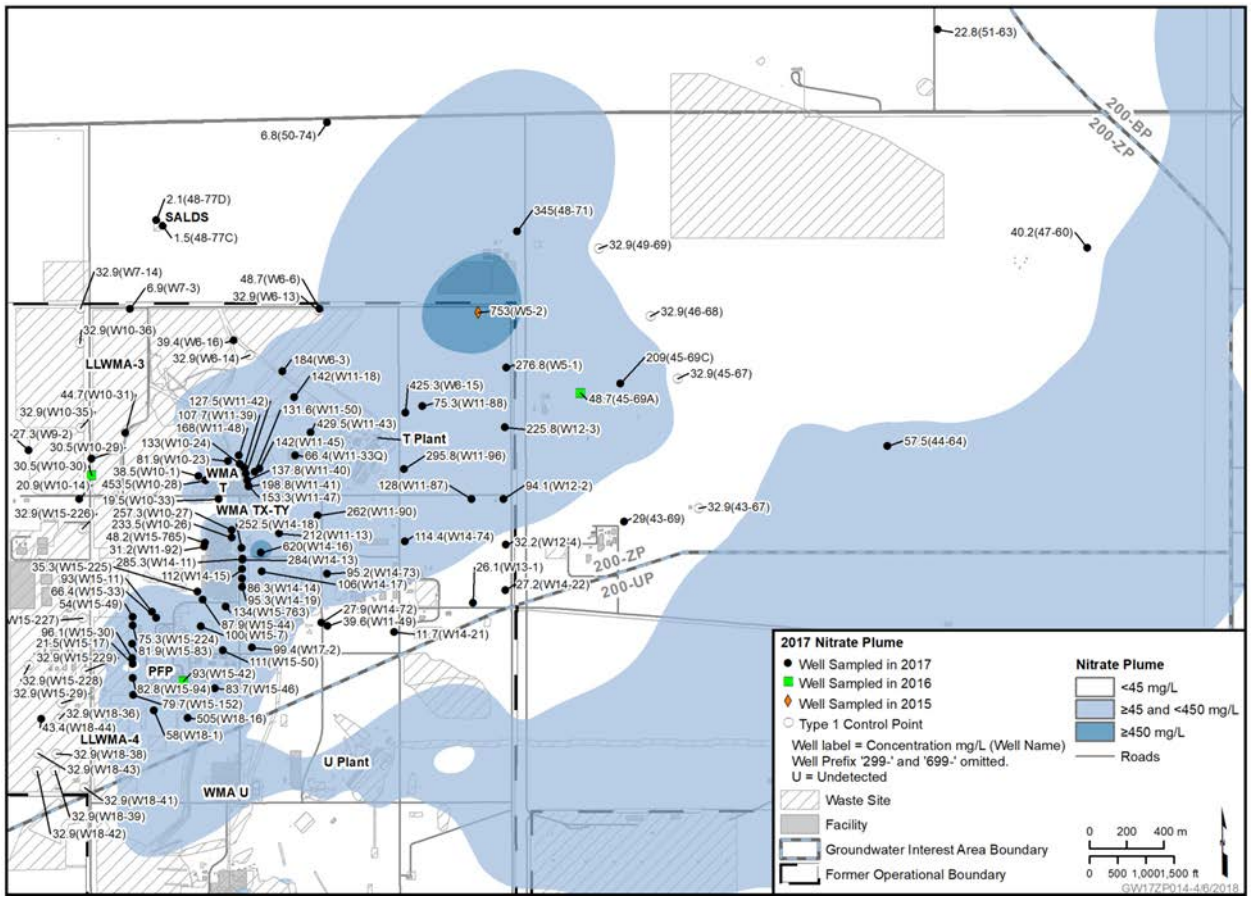

Figure 5. Nitrate plume contours for 2017 in the 200 West Area (DOE, 2018a).

2.3.1 Geochemical Conditions

Review of geochemical parameter data for 200 West Area wells (Figure 4) provided general information about the unconfined aquifer conditions. Dissolved oxygen data is stable over time and tends to range from 7 to 11 mg/L. Sulfate data is also stable over time at relatively high concentrations, ranging from 10 to 70 mg/L, depending on the well. Essentially no ferrous iron data is available because it has not typically been measured. While manganese has been measured, speciation information is not available. Total organic carbon (TOC) measurements provide nonspecific information on organic carbon (i.e., no information on the nature of the carbon). TOC detections are relatively sparse over time, with values ranging from about 0.1 to 10 mg/L, indicating that some form of organic carbon can be found in some locations.

The key outcome from the review of geochemical data is that the bulk unconfined aquifer is aerobic and has relatively high sulfate levels. Other geochemical parameters lack sufficient data or detail to be useful. Under these bulk conditions, degradation of CT and nitrate would not occur (see Section 3.0). Consequently, the degradation of CT would be constrained to localized zones where anoxic conditions (Section 3.0) can establish and persist.

2.4 Carbon Tetrachloride and Chloroform Dechlorination Behavior

As discussed in Section 3.0, reductive dechlorination (hydrogenolysis) is a potentially important CT degradation mechanism. Degradation of contaminants is typically modeled as a first-order rate process.

Thus, it is possible to perform a coupled rate analysis for reductive dechlorination (CT → CF → DCM) using a range of hypothetical half-lives for CT and CF degradation. Such an analysis provides insight into the expected behavior of contaminant concentrations over time in a "batch" system (i.e., uninfluenced by transport processes or other factors). Figure 6 shows the results of the coupled rate analysis for three different initial concentrations of CT [1000 (a-c), 100 (d-f), or 10 (g-i) µg/L], three different CT half-lives [400 y (a, d, g), 200 y (b, e, h), and 100 y (c, f, i)], and four different CF half-lives [400, 200, 100, and 50 y.]. At high CT concentrations (1000 µg/L), there is significant buildup of CF concentration, even at the slowest CT degradation rate (400 year half-life). At moderate CT concentrations (100 µg/L), CF concentrations increase (by small to moderate amounts) in all cases except for the combination of the slowest CT rate (half-life of 400 years) and the fastest CF degradation rate (half-life of 50 years), for which CF concentrations remain stable. When the CT concentration is low (10 µg/L), CF concentrations exhibit a range of results from small increases (e.g., fastest CT degradation rate and slower CF degradation rate) to small decreases (e.g., in the fastest CF degradation rate cases), with stable concentrations for in between cases.

The tested range of half-lives most generally results in an increase in CF concentrations. However, field observations of groundwater concentrations have complicating factors (e.g., bulk concentrations collected from long well screens, inherent variability in sample results, ongoing transport processes) and, thus, delineating degradation rates is not as definitive as portrayed by the behavior of the "batch" system model.

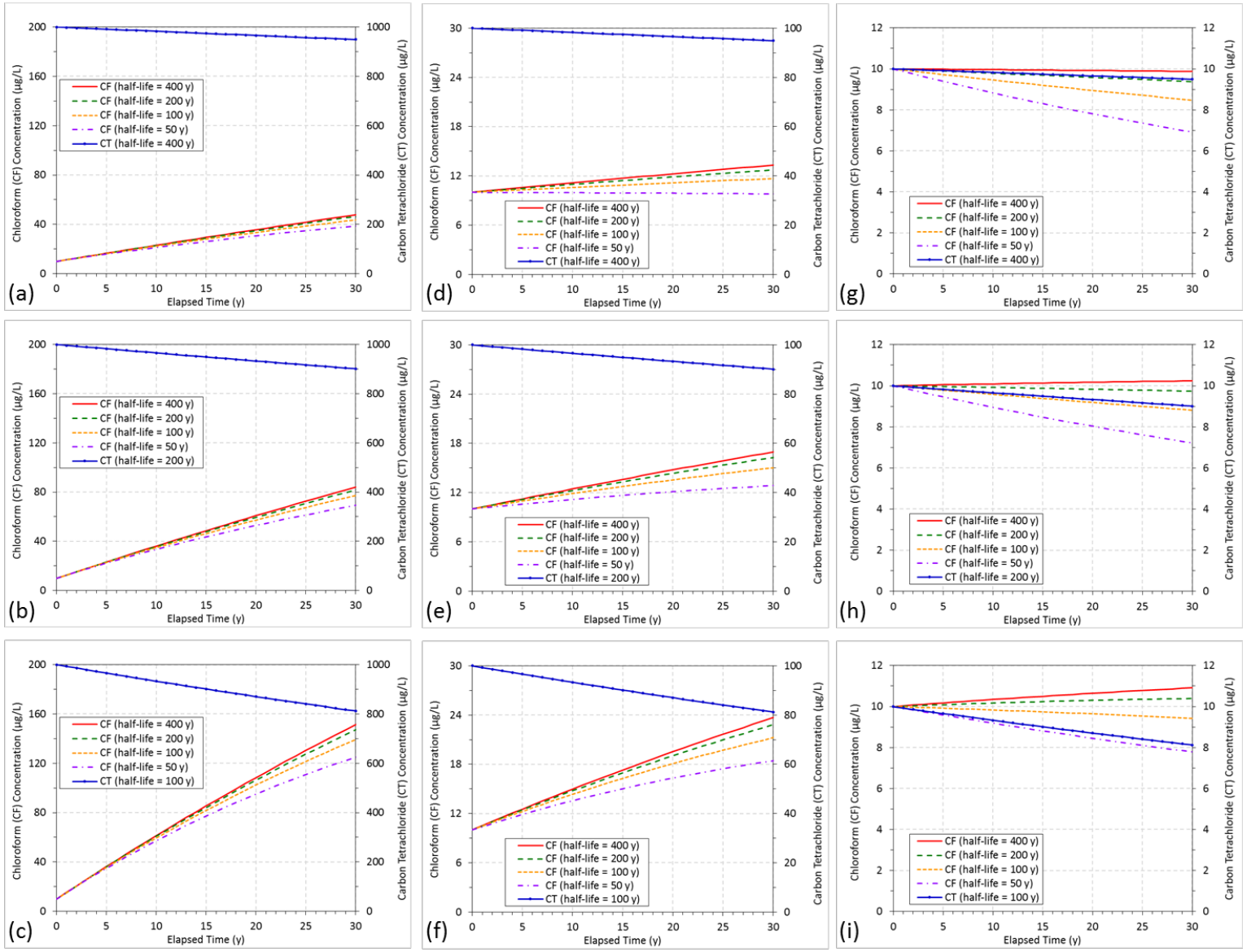

Figure 6. Theoretical first-order reductive dechlorination for a range of initial CT concentrations, CT half-lives, and CF half-lives.

2.5 Attenuation Indicators

The Hanford subsurface is a complex hydrogeologic system. Geological stratification and variations in subsurface permeability will affect contaminant migration. Detailed information on the 200 West subsurface characteristics can be found in *200 West Area 200-ZP-1 Pump and Treat Remedial Design/Remedial Action Work Plan*. DOE/RL-2008-78, Rev. 0 (DOE, 2009). Low permeability zones (e.g., silt and clay layers, Ringold A, Ringold Lower Mud [RLM]) can contribute to the formation of *in situ* groundwater chemistries that are different from the bulk aquifer conditions and may not be reliably captured by groundwater sampling from long-screened monitoring wells. Natural degradation rates are inherently difficult to measure because subsurface conditions are so highly heterogeneous, and contaminant degradation is the product of many competing processes that are being performed separately by many different types of microorganisms and interactions with sediment surface chemistry. Rates of microbial degradation of CT would most likely be the highest at the interface between high and low permeability zones in the Hanford subsurface and in anaerobic microhabitats that could establish principally in low permeability materials (Last and Rohay, 1991; Last et al., 1991; McCarty and Semprini, 1994; Streile et al., 1991).

Based on the aquifer setting and conditions needed for CT degradation, if degradation were occurring, it would be associated with silt/clay lenses or features in the bulk aquifer where anoxic conditions can be generated. Because monitoring wells do not directly measure these zones, data from monitoring wells must be interpreted for these assumed degradation conditions for small anoxic zones occurring within an overall oxic bulk aquifer. Thus degradation products from the anoxic zones would 1) be diluted when measured at monitoring wells and 2) potentially be affected by the bulk oxic conditions if the products can be transformed aerobically. This same type of scaling needs to be considered for degradation rates (Section 2.4). Rates of degradation in a silt zone represent only a portion of the total aquifer volume and CT mass. Thus, the rate in the silt zone is scaled to be slower when considering the overall rate in the bulk zone.

Field data can be evaluated for indicators of CT degradation using the approaches described in Table 1. Of these candidate indicators, the combination of CT, CF, and DCM concentration detections/trends, the CF/CT ratios, and nitrite concentration detections/trends are the most significant indicators. These indicators are used in this assessment of existing site data (Section 2.6). Data are not sufficient to develop plume contours over time for CF, DCM, and nitrite, thus data at individual wells is examined.

Table 1. Groundwater indicators for CT degradation; those with bolded text are considered the strongest indicators

Indicator	Justification	Limitation
CT, CF, DCM, CM concentrations	Primary contaminants and reductive dechlorination (hydrogenolysis) products	Changes in CT concentrations could be caused by hydrogeological phenomena and/or degradation. Thus, CT concentration changes alone are an insufficient indicator of degradation on a meaningful time scale. CF can be present as a remnant of historical in situ CT reductive dechlorination (hydrogenolysis) near the disposal area when co-disposed organic compounds were present. CF concentration trends in later years and away from the disposal zone can be from hydrogeological phenomena and/or degradation. However, based on a coupled rate analysis interpretation, an increasing CF trend can be an indicator of continued CT degradation (beyond the initial disposal timeframe). Detection of reductive dechlorination degradation products DCM or CM are strong indicators of local (or more recent) degradation activity because these products are metabolized to CO_2 quickly in oxic groundwater. In the oxic bulk Hanford groundwater, DCM and CM would have a very short half-life.
CF/CT ratio	Temporal change in ratio of compounds could indicate degradation	Based on a coupled rate analysis interpretation for CT and CF, an increase in CF concentrations is an indicator of CT degradation, especially when a corresponding increase in the CF/CT ratio is also observed. However, concentration changes can be from hydrogeological phenomena and/or degradation, so other indicators must also be used in conjunction with this indicator.
NO_2^- concentration	Product of denitrification	Nitrite is an intermediate product of denitrification that typically builds up under anoxic conditions during the denitrification process. When nitrite transports to oxic zones (or an anoxic zone becomes oxic), nitrite is rapidly converted back to nitrate. Thus, nitrite is not stable in oxic groundwater and, if it is detected at a well within an oxic aquifer, denitrification would need to have occurred recently and locally to the monitoring well. Presence of nitrite, therefore, may be a good indicator of denitrification. Note that the nitrite detection limit is high because of the high nitrate concentrations in many wells. Therefore, it may be that nitrite is more ubiquitous at low concentrations, but detection is masked by the high detection limits.
NO_2^-/NO_3^- ratio	Relative changes would indicate nitrate reduction	Nitrite is a frequently observed intermediate product of denitrification and increasing concentrations of nitrite compared to nitrate would be an indication of denitrification. This indicator is stronger for the 200W aquifer monitoring well data because nitrite is rapidly degraded in the oxic groundwater sampled by the monitoring wells. Because nitrate concentrations are very high and observed nitrite concentrations are very low, use of the ratio can be difficult and, for this reason, detection of nitrite was selected as an appropriate indicator of denitrification activity.
CT/SO_4^{2-} (or H_2S) ratio	Corresponding change could suggest CT cometabolism by sulfate reduction	CT cometabolism is nonspecific, and doesn't correlate exactly with SO_4^{2-} reduction. Because of the weak correlation, this measure is a poor indicator of degradation.

Indicator	Justification	Limitation
TOC concentration or composition	Organic carbon fuels microbial activity and growth, resulting in changes to concentration or composition of OC	OC composition has not been properly characterized and is not monitored consistently or in sufficient detail to detect changes.
Cl^-, pH concentrations	Dechlorination of chlorinated methanes generates Cl- (and corresponding formation of HCl)	Low rates of activity over a large, dilute plume area are unlikely to result in a significant pH shift. Background chloride may be too high for changes in chloride to be used as an effective measure of degradation.
Redox (E_h)	Responsive to microbial activity; anaerobic CT degradation pathways require E_h = -700 to -430 mV	Accurate measurements are difficult to collect because changes are likely occurring at spatially discrete areas or zones not easily accessible by groundwater sampling or in situ sensors in monitoring wells with long screens. This metric is a poor indicator for degradation because measurement is difficult for low permeability zones.
DO concentration	Lower (or decreasing) dissolved oxygen levels reflect microbial activity (or abiotic reactants) and conditions conducive to anaerobic pathways; DO < 2 mg/L is appropriate for CT degradation	The bulk aquifer is oxygenated and maintains a high DO background. Significant changes would most likely be restricted to spatially discrete areas or zones not easily accessible by groundwater sampling from monitoring wells with long screens. This metric is a poor indicator for degradation because measurement is difficult for low permeability zones.
CT/$Mn^{+4/+3}$, CT/$Fe^{+3/+2}$ ratios	Relative changes in reactants could indicate coupled abiotic-biotic processes for CT degradation	Solid-phase reactions would be heterogeneously distributed but not reliably captured by groundwater sampling from monitoring wells with long screens. Limited information exists for Fe and Mn chemistry. These metrics are poor indicators for degradation because measurement is difficult for low permeability zones.

2.6 Field Data and Attenuation Indicators

Field data from HEIS for the set of wells identified in Section 2.2 were evaluated for the degradation indicators identified in Section 2.5. Groundwater data was evaluated in several steps. First, the north and south well sets were culled to just those wells having CT detections (excluding characterization data collected at the time of the well installation). Those wells were examined to determine which wells had detections of CF, DCM, and nitrite, or which had only CF and DCM or only CF and nitrite. Figure 7 shows locations with CT and CF detections, plus detections of one or both DCM and nitrite. From this figure, there is clearly a broad distribution of detections of these degradation indicators. In the northern group, 28 wells had detections of all species (out of 70 wells with CT detections), 8 wells had detections of nitrite but not DCM, and 28 wells had detections of DCM, but not nitrite. In the southern group, 33 wells had detections of all species (out of 62 wells with CT detections), 10 wells had detections of nitrite but not DCM, and 12 wells had detections of DCM, but not nitrite. Note that the nitrite detection limit is high because nitrate concentration is very high in many wells. Therefore, it may be that nitrite is more ubiquitous at low concentrations, but detection is masked by the high background concentration of nitrate.

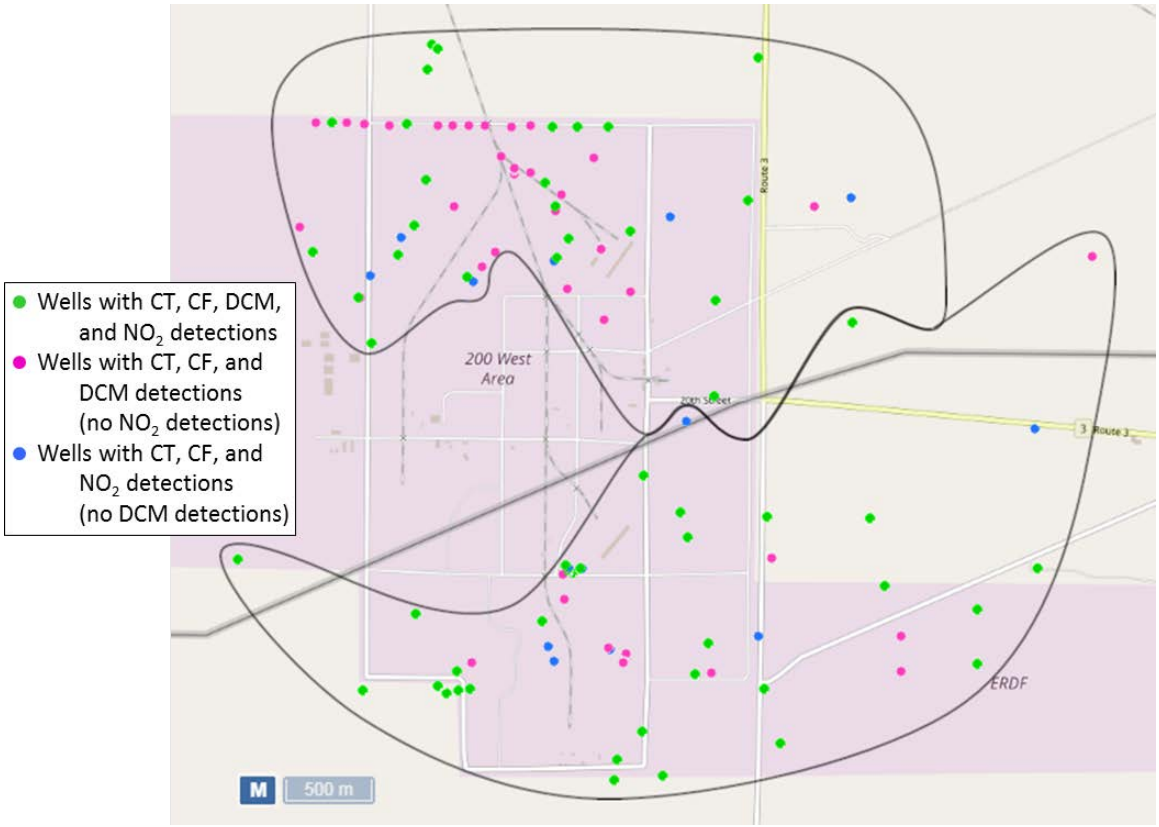

Figure 7. Locations of wells with detections of CT, CF, DCM, and/or nitrite.

The data for wells with CF, DCM, and nitrite detections are compiled in tabular form in Table 2, along with the slope of the CF/CT ratio (where coincident data were collected). Because the flow characteristics and, potentially, the reaction characteristics of the Ringold A formation in the 200W aquifer may be more conducive to CT degradation, wells screened only within the Ringold A unit are also pulled out separately in Table 3. Tables for wells with detections for DCM but no nitrite, nitrite but no DCM, or neither DCM nor nitrite are presented in Appendix B.

Table 2. Detection and CF/CT slope indicator data for the North (shaded) and South (unshaded) well groups for three time periods, from January 1986 through (A) February 1994, (B) June 2012, and (C) January 2019, where both DCM and nitrite were detected during the relevant time frames for the specified well group.

	Number of Detections of …																		
	CF			DCM			Nitrite			CF			DCM			Nitrite			CF/CT
Well	AB		C	AB		C	AB		C	A	B	C	A	B	C	A	B	C	Slope
299-W10-1	2	23	29	0	3	3	0	5	8	100.0	92.0	93.5	0.0	12.0	9.7	0.0	8.9	11.9	-3.6 E-06
299-W10-19	5	24	24	4	9	9	0	1	1	71.4	85.7	85.7	57.1	32.1	32.1	0.0	2.8	2.8	1.3 E-05
299-W11-10	2	27	27	1	3	3	0	1	1	100.0	100.0	100.0	50.0	11.1	11.1	0.0	4.2	4.2	8.0 E-07
299-W11-18	3	20	25	1	4	4	0	2	2	100.0	90.9	92.6	33.3	18.2	14.8	0.0	8.3	6.9	5.9 E-07
299-W11-30	4	12	12	3	4	4	3	5	5	100.0	100.0	100.0	75.0	57.1	57.1	60.0	62.5	62.5	-6.0 E-04
299-W11-37	0	24	24	0	2	2	0	2	2	--	96.0	96.0	--	8.0	8.0	--	8.0	8.0	5.3 E-06
299-W11-43	0	26	33	0	1	1	0	3	4	--	100.0	100.0	--	3.8	3.0	--	12.0	12.5	-2.3 E-05
299-W12-1	3	22	22	2	10	10	0	5	5	75.0	78.6	78.6	50.0	35.7	35.7	0.0	21.7	21.7	3.2 E-04
299-W15-2	1	13	13	0	2	2	0	1	1	100.0	86.7	86.7	0.0	15.4	15.4	0.0	7.7	7.7	-2.7 E-06
299-W6-3	4	11	15	1	1	1	5	6	6	57.1	78.6	78.9	14.3	7.1	5.3	71.4	42.9	31.6	3.2 E-04
299-W6-7	7	14	14	1	3	3	1	1	1	100.0	100.0	100.0	14.3	21.4	21.4	14.3	7.1	7.1	4.7 E-06
299-W7-3	4	31	37	2	6	6	0	2	3	22.2	63.3	66.1	11.1	12.2	10.7	0.0	3.9	5.2	1.5 E-04
299-W7-4	19	44	44	6	13	13	0	1	1	95.0	93.6	93.6	30.0	27.7	27.7	0.0	2.3	2.3	-3.4 E-07
299-W7-9	2	11	11	4	7	7	7	8	8	14.3	37.9	37.9	28.6	24.1	24.1	53.8	27.6	27.6	3.6 E-05
299-W13-1	0	38	44	0	5	5	0	1	1	--	97.4	97.8	--	15.6	13.2	--	3.6	2.9	-2.7 E-05
299-W6-11	3	7	7	1	1	1	0	1	1	50.0	70.0	70.0	16.7	10.0	10.0	0.0	10.0	9.1	5.8 E-07
299-W6-4	7	11	11	2	2	2	3	3	3	100.0	100.0	100.0	28.6	18.2	18.2	42.9	11.5	11.5	-7.2 E-06
299-W6-5	5	10	10	1	2	2	1	1	1	100.0	100.0	100.0	20.0	25.0	25.0	20.0	12.5	12.5	-4.6 E-05
299-W10-14	2	4	4	3	5	5	0	1	1	10.5	7.8	7.1	15.8	10.2	9.3	0.0	2.1	1.9	
299-W9-2	0	3	3	0	1	1	0	3	4	--	100.0	100.0	--	33.3	33.3	--	100.0	30.8	5.2 E-05
299-W10-20	1	37	37	1	12	12	1	2	2	100.0	94.9	94.9	100.0	30.8	30.8	100.0	5.7	5.7	-5.8 E-07
299-W11-32	3	3	3	1	1	1	3	3	3	100.0	100.0	100.0	33.3	33.3	33.3	75.0	75.0	75.0	-1.3 E-02
299-W6-6	0	4	4	1	1	1	1	5	5	0.0	28.6	20.0	14.3	7.1	5.0	14.3	35.7	25.0	
299-W7-2	5	8	8	2	2	2	1	1	1	26.3	34.8	34.8	10.5	8.7	8.7	6.3	5.0	5.0	-1.4 E-03
699-48-71	1	31	37	0	6	6	0	1	3	20.0	88.6	90.2	0.0	17.1	14.6	0.0	2.9	7.3	-7.7 E-04
699-48-77A	0	5	5	0	7	7	0	2	2	0.0	4.7	4.7	0.0	6.8	6.8	0.0	2.0	2.0	-1.0 E-04
699-48-77C	0	12	13	0	7	8	0	5	13	--	13.2	10.7	--	8.0	6.7	--	5.6	10.8	6.3 E-05
699-48-77D	0	5	6	0	8	8	0	6	11	--	5.7	5.3	--	9.3	7.1	--	7.0	9.9	2.9 E-04
299-W17-1	0	4	4	0	4	4	0	2	4	--	16.0	16.0	--	19.0	19.0	--	9.5	13.8	
299-W19-3	6	9	9	1	2	2	0	3	3	50.0	52.9	52.9	8.3	14.3	14.3	0.0	21.4	21.4	-4.1 E-06
299-W19-4	1	18	23	0	6	6	0	1	1	100.0	94.7	95.8	0.0	31.6	25.0	0.0	6.7	5.0	3.1 E-06
299-W22-20	14	28	28	1	5	5	0	2	2	100.0	80.0	80.0	7.1	14.3	14.3	0.0	6.1	6.1	1.0 E-03
299-W23-9	1	9	9	0	3	3	5	9	9	33.3	56.3	56.3	0.0	18.8	18.8	100.0	36.0	36.0	2.5 E-04
699-35-78A	1	13	18	1	5	5	0	3	3	33.3	61.9	64.3	33.3	23.8	17.9	0.0	15.0	13.0	-1.3 E-06
699-36-70A	0	33	50	0	18	20	0	7	8	--	60.0	67.6	--	32.7	27.0	--	9.2	8.6	1.4 E-05
699-38-68A	0	10	15	0	4	4	0	4	5	--	90.9	88.2	--	36.4	23.5	--	36.4	31.3	1.4 E-06
299-W14-71	0	26	33	0	2	3	0	2	2	--	100.0	100.0	--	11.1	12.0	--	13.3	12.5	-7.4 E-06
299-W23-21	0	42	47	0	0	1	0	5	7	--	100.0	100.0	--	0.0	2.1	--	9.4	10.4	-1.0 E-05
699-38-70C	0	26	33	0	2	2	0	2	3	--	89.7	91.7	--	8.0	6.3	--	8.7	9.7	8.2 E-06
699-43-69	0	14	20	0	2	2	0	4	5	--	93.3	95.2	--	13.3	9.5	--	26.7	23.8	1.2 E-06
299-W18-15	4	34	37	0	4	4	0	3	4	44.4	87.2	86.0	0.0	10.3	9.3	0.0	9.7	11.1	-1.0 E-05

Well	Number of Detections of … CF A	B	C	DCM A	B	C	Nitrite A	B	C	Percent of All Samples … CF A	B	C	DCM A	B	C	Nitrite A	B	C	CF/CT Slope
299-W19-107	0	22	28	0	1	1	0	3	4	--	100.0	100.0	--	5.9	4.3	--	17.6	17.4	-1.8 E-05
299-W22-88	0	1	6	0	1	1	0	3	4	--	20.0	60.0	--	20.0	10.0	--	25.0	25.0	-2.1 E-05
299-W23-10	0	16	16	0	4	4	0	3	3	0.0	61.5	61.5	0.0	15.4	15.4	0.0	16.7	16.7	-1.7 E-06
699-34-72	0	9	12	0	1	1	0	3	4	--	100.0	100.0	--	11.1	8.3	--	33.3	28.6	1.7 E-04
699-36-66B	0	0	16	0	3	4	0	0	1	--	0.0	50.0	--	21.4	12.5	--	0.0	4.2	1.1 E-05
699-37-66	0	0	18	0	1	1	0	0	2	--	0.0	51.4	--	7.1	2.9	--	0.0	8.0	8.7 E-06
699-38-65	0	7	14	1	2	2	0	2	2	0.0	58.3	70.0	33.3	16.7	10.0	0.0	6.9	5.4	-6.4 E-05
699-38-70B	0	31	37	0	3	3	0	3	3	--	96.9	97.4	--	12.0	9.7	--	11.5	10.0	1.8 E-06
299-W19-11	2	4	4	1	1	1	0	1	1	28.6	44.4	44.4	14.3	11.1	11.1	0.0	16.7	16.7	-1.2 E-06
699-35-70	0	7	7	0	2	2	0	1	1	0.0	53.8	53.8	0.0	15.4	15.4	0.0	3.0	3.0	1.8 E-05
299-W19-16	7	8	8	2	2	2	0	4	4	58.3	61.5	61.5	16.7	15.4	15.4	0.0	33.3	33.3	-1.5 E-05
299-W19-6	0	1	6	0	0	1	0	1	2	--	100.0	100.0	--	0.0	16.7	--	100.0	40.0	-3.1 E-06
299-W19-9	3	9	9	0	3	3	0	1	1	30.0	56.3	56.3	0.0	18.8	18.8	0.0	9.1	9.1	-5.2 E-06
299-W21-2	0	21	27	0	1	1	0	3	4	--	72.4	77.1	--	5.3	4.0	--	11.5	12.5	-4.0 E-05
299-W22-9	1	1	1	1	5	5	1	5	5	100.0	8.3	8.3	100.0	41.7	41.7	25.0	38.5	38.5	
299-W23-11	1	1	1	1	1	1	1	1	1	33.3	33.3	33.3	33.3	33.3	33.3	33.3	20.0	20.0	
299-W23-14	1	4	4	0	1	1	0	1	1	33.3	57.1	57.1	0.0	14.3	14.3	0.0	4.0	4.0	-1.9 E-05
299-W23-4	0	24	32	0	3	3	0	3	4	--	72.7	78.0	--	9.1	7.3	0.0	9.4	10.0	-4.7 E-06
299-W27-1	14	27	27	3	5	5	0	4	4	73.7	81.8	81.8	15.8	15.2	15.2	0.0	9.8	9.8	-3.0 E-02
299-W19-18	3	27	27	1	6	6	0	1	1	42.9	73.0	71.1	14.3	18.8	18.2	0.0	4.3	4.2	-3.0 E-06

Table 3. Detection and CF/CT slope indicator data for wells in the North (shaded) and South (unshaded) well groups that are screened in the Ringold A unit. Values for number of detections and percent of all samples with detections are shown for three time periods, from January 1986 through (A) February 1994, (B) June 2012, and (C) January 2019. Both DCM and nitrite were detected during the relevant time frames for the specified well group (north or south) for three of the five wells. Two wells had detections of nitrite but not DCM.

Well	Number of Detections of … CF A	B	C	DCM A	B	C	Nitrite A	B	C	Percent of All Samples … CF A	B	C	DCM A	B	C	Nitrite A	B	C	CF/CT Slope
299-W11-43	0	26	33	0	1	1	0	3	4	--	100.0	100.0	--	3.8	3.0	--	12.0	12.5	-2.3 E-05
299-W11-88	0	2	8	0	0	0	0	5	6	--	16.7	40.0	--	0.0	0.0	--	41.7	30.0	
299-W7-3	4	31	37	2	6	6	0	2	3	22.2	63.3	66.1	11.1	12.2	10.7	0.0	3.9	5.2	1.5 E-04
699-45-69C	0	3	7	0	0	0	0	1	2	--	33.3	43.8	--	0.0	0.0	--	11.1	12.5	-1.3 E-05
699-43-69	0	14	20	0	2	2	0	4	5	--	93.3	95.2	--	13.3	9.5	--	26.7	23.8	1.2 E-06

Figures 8 to 11 show examples of the CT, CF, nitrate, and nitrite concentration trend data for selected wells with positive indicators of attenuation. These figures also show the trend for the CF/CT ratio and a correlation plot for normalized concentration data. These are some examples of wells where the CF/CT ratio shows an increase, DCM is present, and there is at least one detection of nitrite. Examination of the monitoring well data did not reveal any instances with CT concentrations near 1000 µg/L where CF concentrations were increasing substantially over a period of 10-20 years. Based on the scenarios and outcomes presented in Figure 6, this observation supports an interpretation of a CT half-life that is greater than 100 years.

There are 25 well locations having both DCM and nitrite detection indicators, as well as a positive slope for the CF/CT ratio trend (Table 2), though the slope is above 1×10^{-5} for only 14 of those wells. Visual inspection of the concentration and CF/CT ratio trends suggests that 11 groundwater well locations in the southern group of wells and 5 locations for the northern group of wells have DCM, nitrite, and CF-based indicators that offer convincing evidence of reductive dechlorination (hydrogenolysis). Plots for all of these wells are shown in Appendix B.

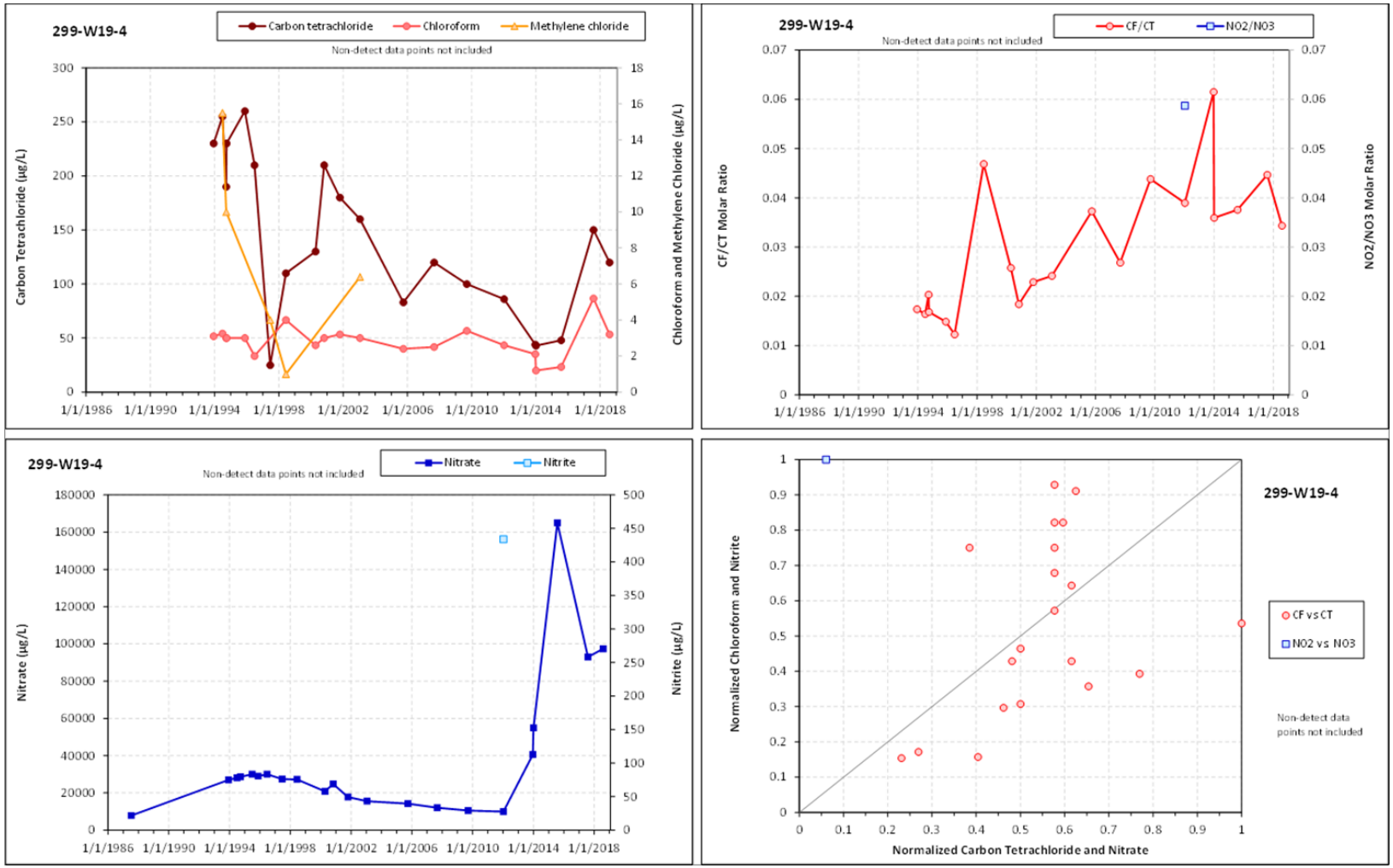

Figure 8. CT, CF, nitrate, and nitrite concentration trends and CF/CT ratio trend over time for well 299-W19-4. Also shown is a correlation plot for normalized concentration data.

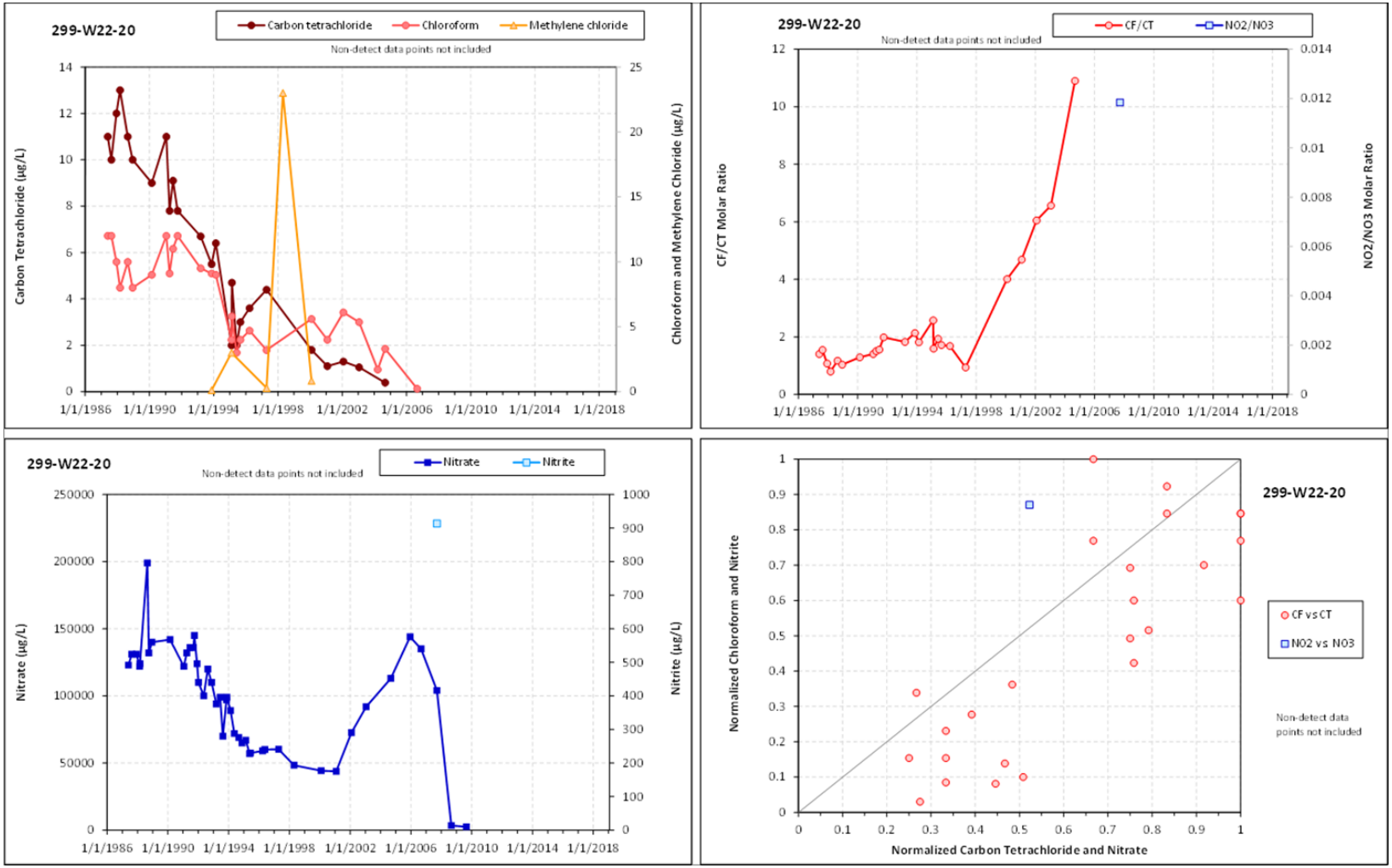

Figure 9. CT, CF, nitrate, and nitrite concentration trends and CF/CT ratio trend over time for well 299-W22-20. Also shown is a correlation plot for normalized concentration data.

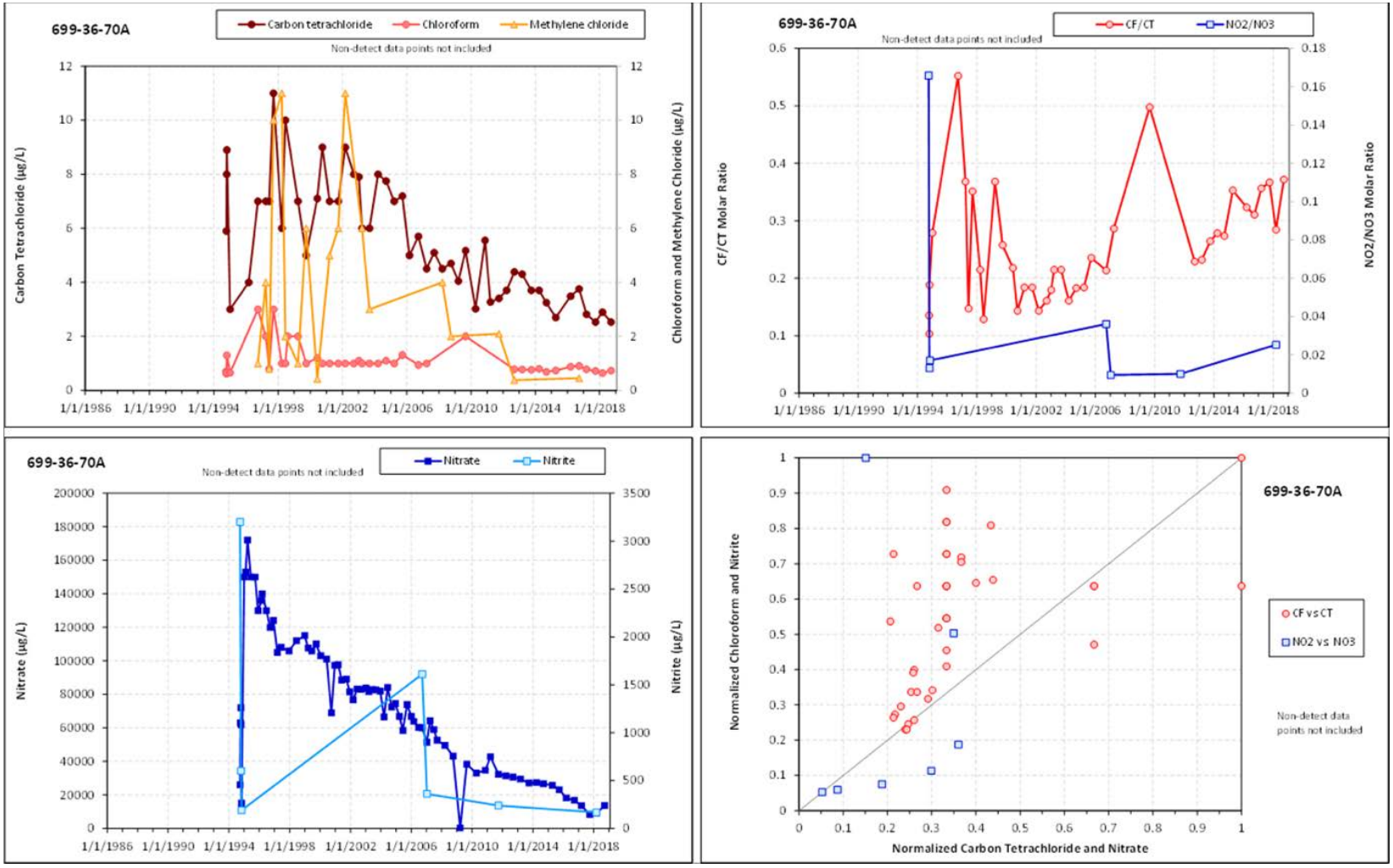

Figure 10. CT, CF, nitrate, and nitrite concentration trends and CF/CT ratio trend over time for well 699-36-70A. Also shown is a correlation plot for normalized concentration data.

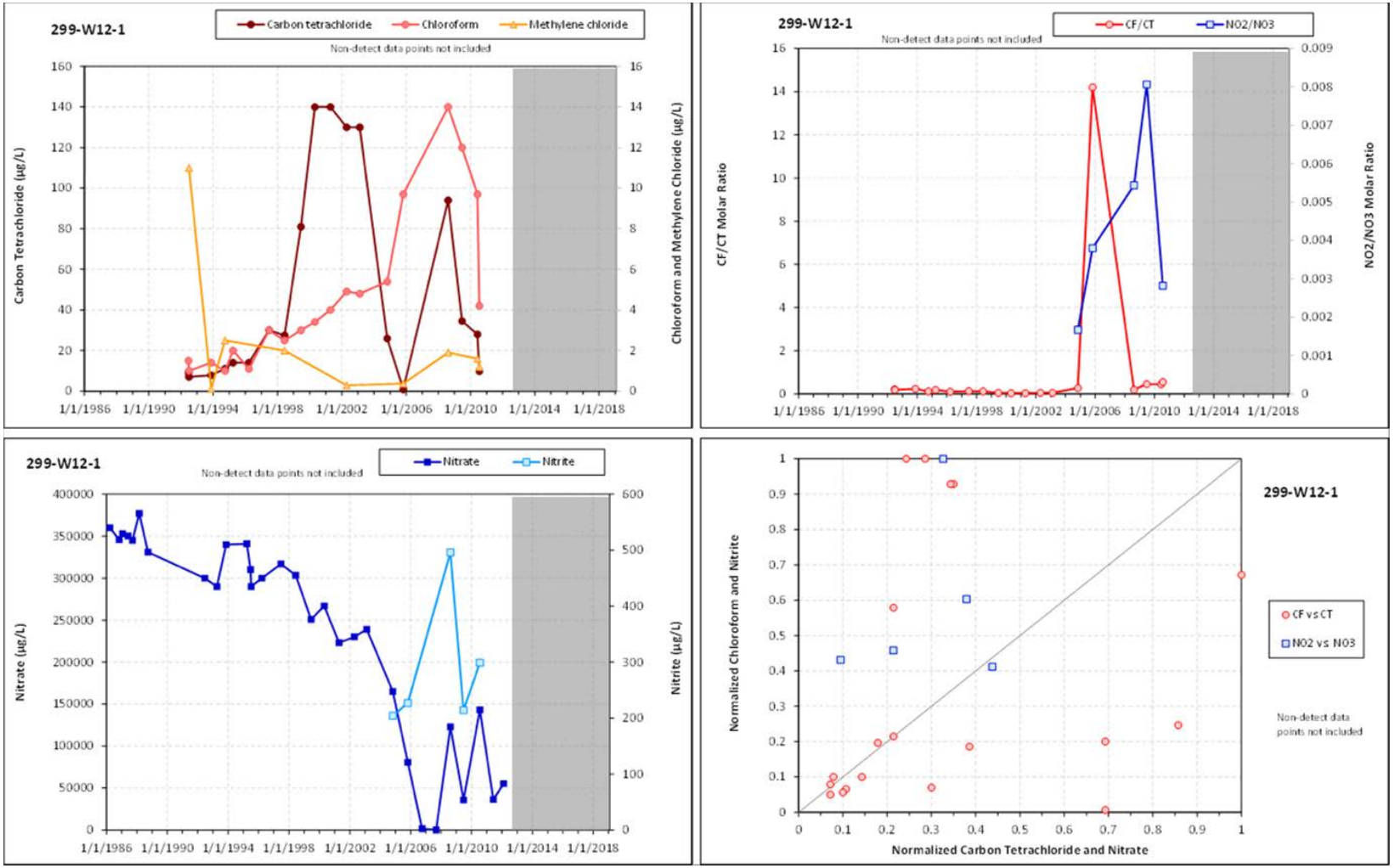

Figure 11. CT, CF, nitrate, and nitrite concentration trends and CF/CT ratio trend over time for well 299-W12-1. Also shown is a correlation plot for normalized concentration data.

3.0 Degradation Mechanisms for CT and Chlorinated Byproducts

In this section, the biological and coupled abiotic-biotic reductive degradation pathways for CT are reviewed. The specific microbiological, physical, and geochemical requirements for each process are identified. Pathways for CT degradation products are also evaluated to provide a basis for interpreting laboratory and field data. Finally, degradation rate values are summarized for CT and chlorinated byproducts. A summary of biotic anaerobic and aerobic degradation pathways for CT and byproducts are provided in Figure 12, including reductive dechlorination (hydrogenolysis) for sequential transformation of CT→CF→DCM→CM→CH_4.

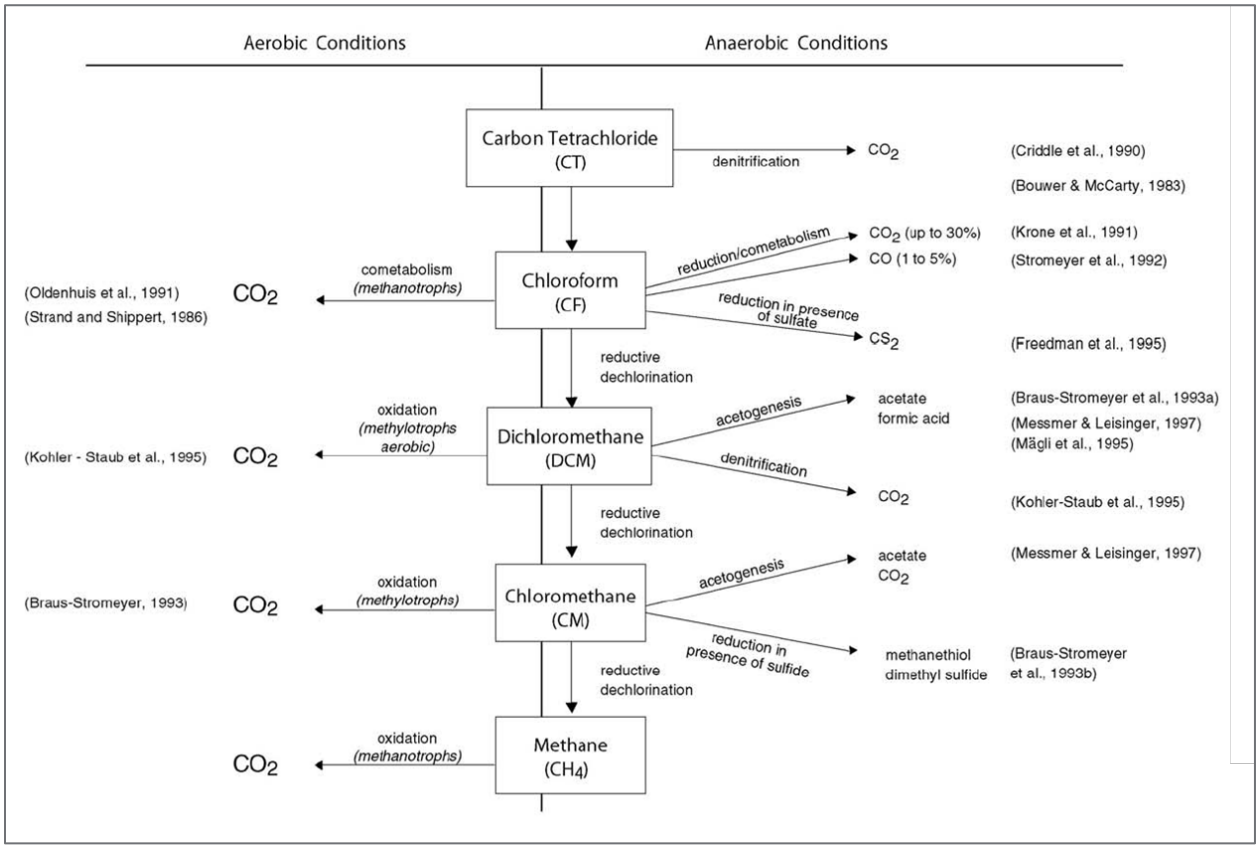

Figure 12. Summary of biological degradation pathways for chlorinated methanes (ESTCP, 2005).

CT can degrade via four different mechanisms: (1) abiotic hydrolysis; (2) biotic hydrogenolysis; (3) a biotic dichlorocarbene pathway; and (4) abiotic degradation by reactive minerals. Abiotic hydrolysis of CT directly leads to CO_2 production, with a half-life of 630 years being experimentally determined for typical Hanford groundwater conditions (Amonette et al. 2012) for this process. Under anaerobic conditions, CT can also degrade via microbially induced reductive dechlorination (hydrogenolysis). As shown in Figure 12, this pathway leads to the production of CF as a persistent intermediate, and reductive dechlorination of CF, in turn, produces DCM. DCM is persistent in anaerobic conditions, but quickly degrades to CO_2 under aerobic conditions. Biotic hydrogenolysis has been demonstrated at Hanford (Truex et al., 1996). CT can also degrade to CO_2 without the production of CF or DCM as intermediate products through a pathway involving production of dichlorocarbene, followed by spontaneous hydrolysis to form formate, which oxidizes to CO_2. This dichlorocarbene pathway was also demonstrated at

Hanford, though it required tightly controlled subsurface conditions (Truex et al., 1996; Hooker et al., 1998; Sherwood et al., 1996). Finally, CT transformation to multiple products (ranging from CF and DCM to relatively less toxic CO, CO_2, formate, and methane) via mineral-mediated abiotic pathways has been reported in the literature and demonstrated for Hanford RLM sediments (G. Wang, personal communication). The sections below provide details of studies for the biotic and abiotic-biotic (reactive mineral) pathways.

3.1 Technical Basis for CT Degradation at Hanford

The 200 West Area CT plume has served as an important test-bed site for a number of R&D programs, including the Volatile Organic Compounds – Arid Integrated Demonstration Program (VOC-ARID ID; 1991-1996) and the Hanford Carbon Tetrachloride Innovative Technology Demonstration Program (1995-2000), whose primary objective was demonstration and comparison of remedial technologies for VOCs and associated contaminants at arid DOE sites (ITRC, 2002). Products of these programs included extensive laboratory treatability studies that demonstrated the innate capacity of Hanford subsurface sediments to degrade CT to CO_2 through mechanisms associated with denitrification in addition to the reductive dechlorination (hydrogenolysis) pathway with CT degrading to CF, DCM, and CM, sequentially. All of these studies, though, supplied acetate as a carbon/energy source to stimulate degradation activity (Brouns et al., 1990; Hooker et al., 1994; Koegler et al., 1989; Last et al., 1991; Last and Rohay, 1991; Niemet and Semprini, 2005; Petersen et al., 1994; Sherwood et al., 1998; Skeen et al., 1992; Truex et al., 1994, 1996, 2001). No estimations of natural biodegradation activity of CT in the Hanford subsurface have been published.

Successful laboratory testing supported the transition to an *in situ* bioremediation field demonstration that was conducted from January 1995 to March 1996 in the 200 West Area of the Central Plateau (Hooker et al., 1998). Briefly, site groundwater conditions were as follows: 2 mg/L CT, 250 mg/L NO_3^-, 55 mg/L SO_4^{2-}, 5 mg/L O_2, pH 7.4, and 19°C. Acetate was injected into two high permeability units (245-255 ft bgs and 286-300 ft bgs) that were hydrologically separated by a low permeability unit. Bio-stimulation resulted in the conversion of CT (~2 kg) to CO_2 coupled to the reduction of NO_3^- to nitrogen gases. Intermittent accumulation of CF was measured as a byproduct, but CF concentrations were controlled (and minimized) by maintaining low NO_3^- concentrations. Acetate injections resulted in significant growth of subsurface microbes; implying that the primary limitation to subsurface degradation activity and growth was organic carbon. The average rate of CT degradation in the Hanford subsurface following bio-stimulation with acetate was 0.85 mg CT/g biomass d^{-1} in the Hanford saturated subsurface (half-life estimation of 68 days). This field demonstration clearly shows that the Hanford subsurface is capable of degrading CT, and CF, when the appropriate environmental conditions are satisfied.

3.2 Biological Degradation of Carbon Tetrachloride (CT)

As a fully halogenated alkane, CT is stable in the environment and resistant to aerobic degradation. The only feasible biological pathway is anaerobic degradation (Figure 12; McCarty and Reinhard, 1993). The predominant biological degradation pathway for CT is anaerobic cometabolic reductive dechlorination (hydrogenolysis), a non-specific process whereby CT is dechlorinated (reduced) to CF (Castro et al., 1985; Krone and Thauer, 1989; Krone et al., 1989a; Picardal et al., 1993; Ruf et al., 1984; Wood et al., 1968). Cometabolism describes a process in which a compound (i.e., CT) that is not used for growth or energy is transformed to another product(s) by microorganisms. Cometabolism of CT has been described for denitrifying, sulfate reducing, methanogenic and acetogenic bacteria, as well as fermenters. These functional groupings of microorganisms are naturally abundant in Hanford subsurface sediments in the 200 West Area and throughout the central plateau (Szecsody et al., 2017). As outlined above, CT degradation has been studied extensively at the Hanford Site. Importantly, cometabolism of CT is not

analogous to the cometabolism of PCE/TCE which utilizes substrate or reaction specific catalytic enzymes to bind and transform the contaminant in its active site. Conversely, CT reactions are not genetically encoded or catalyzed reliably by a specific enzyme, thus gene or protein targeted methods (e.g., enzyme activity probes) cannot be used to measure or infer CT degradation.

Most commonly, CT degradation occurs by anaerobic cometabolism during denitrification, resulting in the formation of CF. The production and accumulation of CF has been studied extensively. Biostimulation studies, including a field demonstration at Hanford, have demonstrated that ORP levels can decrease sharply in response to substrate additions (acetate), permitting the establishment of conditions for anaerobic respiration of NO_3^- and CT. CT degradation activity has been shown to be sensitive to or inhibited by nitrate concentration. This is due to fact that NO_3^- and CT, as highly oxidized compounds, compete as terminal acceptors for cellular electron transfer reactions. Laboratory (Hanford soils; Petersen et al., 1994; Skeen et al., 1994; Franzen et al., 1997; Peyton, 1996) and field studies (Hanford; Hooker et al., 1998; Moffett Field AFB; Semprini et al., 1991) suggest that the maximum sustained CT reduction occurs when NO_3^- levels are low (~100 mg/L) and periodically depleted, ~10 mg/L (Sherwood et al., 1996).

One extensively studied example of CT transformation to CO_2 without any intermediary products is by the denitrifying bacterium, *Pseudomonas stutzeri* KC which actually catalyzes the reaction using a copper containing exometabolite [pyridine-2,6-bis(thiocarboxylate] in response to Fe-limitation. An important distinction of this pathway is that CT biotransformation is activated by low soluble concentrations of iron (as is the case in alkaline pH groundwater) and the reaction rate is completely insensitive to NO_3^- or other competing electron acceptors (Criddle et al., 1990). *P. stutzeri* KC has not been characterized from Hanford sediments, though pseudomonads are highly abundant (Szecsody et al., 2017). Nonetheless, field and laboratory testing at the Hanford Site have shown that CT can be transformed to CO_2 without CF accumulation by the indigenous microorganisms (Truex et al., 1996; Hooker et al., 1998).

Degradation of CT occurs slowly in the natural environment (Semprini et al., 1992) because the availability of organic carbon is generally limited. It is important to note that, for the majority of the above systems and those summarized in Table 4, CT was transformed under anaerobic conditions established and maintained by the supply of an exogenous organic carbon source. Acetate was the preferred substrate for CT degradation studies at Hanford. CT, itself, is not a suitable substrate for microbial growth. Higher rates of natural degradation have been measured in aquifers where CT was co-disposed with other organic constituents (e.g., fuel hydrocarbons; Liang and Grbic-Galic, 1993).

In conclusion, there are two fundamental biotic degradation pathways for CT. One pathway is reductive dechlorination (hydrogenolysis), where CF is produced as an intermediate product that typically accumulates during CT degradation. The other pathway is CT transformation under specific denitrification conditions where CT is degraded to CO_2 and CF is not an intermediate product. Both pathways have been demonstrated in biostimulation studies in the 200W aquifer under anoxic conditions. The pathway leading to production of CF would be catalyzed by a broader group of microorganisms than the pathway without CF production.

3.3 Biological Degradation of Chloroform

Unlike CT, CF can be biologically transformed under aerobic and anaerobic conditions (Figure 12). Anaerobic transformation of CF is similar mechanism to that for CT, however it is not transformed by denitrifying bacteria (Bouwer and McCarty, 1983; Criddle et al., 1990). CF can be degraded by sulfate reducing (Gupta et al., 1996a; Egli et al., 1987), acetogenic (Egli et al., 1990), fermentative (Gali and McCarty, 1989), and methanogenic bacteria (Bagley and Gossett, 1995; Bouwer and McCarty, 1983; Gupta et al., 1996; Mikesell and Boyd, 1990). Aerobically, CF can be cometabolized to CO_2 by a variety

of microorganisms under specific conditions during the degradation of a primary growth substrate (e.g., methane, propane, toluene, and ammonia) via a mono-oxygenase enzyme. Aerobic cometabolism of CF could be monitored and measured from 200 West Area groundwater using molecular tools (i.e., PCR, enzyme probes).

CF production (and possible accumulation) is an important consideration for abiotic and biotic dechlorination of CT and it is likely to mark the rate limiting step for attenuation. CF can be a potent inhibitor of microbial processes responsible for natural degradation of CT (Bouwer and McCarty, 1983ab). Anaerobic and aerobic degradation of CF has been considered to be a cometabolic process (Cappelletti et al., 2012); however, a recent study has discovered *Dehalobacter* populations that are capable of growth linked dechlorination (dehalorespiration) of CF (Grostern et al., 2010). Because CF is a common co-contaminant of industrial solvents (CT, PCE/TCE) it is conceivable that other dehalorespiring microorganisms are also capable of growth linked CF degradation.

Tests in the 200 West Area have shown accumulation of CF under reductive dechlorination (hydrogenolysis) pathway conditions for CT (Truex et al., 1996). Thus, CF is expected to be an indicator for reductive dechlorination (hydrogenolysis) of CT in the 200W aquifer.

Table 4. Biological degradation pathways for chlorinated methanes.

Compound	Product(s)	Conditions	Energy/C	Acceptor	Sustainable	Microbes	Half-life
CT	CO_2	Hydrolysis	-	-	Baseline	-	630 yrs[1]
CT	CF, (DCM, CM)	Anaerobic sequential reductive dechlorination (hydrogenolysis)	OC	NO_3,SO_4, CO_2	Low O_2, reduced micro-sites	DNRB, SRB, Methanogens, Fermenters	3 yrs (Combined Acceptors) 63 – 126 yrs (Sin Acceptor)
CT	CO_2	Aerobic/Anaerobic	OC	NO_3, O_2	Low O_2, reduced micro-sites	*P. stutzeri* KC and other denitrifiers	84 days
CF	DCM	Hydrolysis	-		Baseline	-	3400 yrs[1]
CF	DCM, CO_2, CS_2	Anaerobic Cometabolism	OC	SO4, CO_2	Low O_2, reduced micro-sites	SRB, Acetogens, Fermenters Methanogens (Not DNRB)	0.9 yrs
CF	CO_2	Aerobic Cometabolism	CH_4, propane, toluene, NH_3	O_2	Where co-substrate is available for mono-oxygenase enzyme system	Methylotrophs, Methanotrophs	0.8-17 days
DCM	CM	Hydrolysis	-	-	Baseline	-	704 yrs
DCM	CM, CO_2, acetate, formate	Anaerobic Degradation, Cometabolism	OC	NO_3,SO_4, CO_2	Low O_2, reduced micro-sites	DNRB, Methanogens, Acetogens	15 hrs – 63 days
DCM	CO_2	Aerobic Degradation	DCM	O_2	Highly likely	Methylotrophs, Pseudomonas	7 min – 70 days
CM	CH_4, CO_2, acetate, methanethiol, dimethyl sulfide	Anaerobic Cometabolism; Anaerobic Degradation	CM	CO_2, SO_4	Low O_2, reduced micro-sites	SRB, Acetogens	1.9 hrs
CM	CO_2	Aerobic Cometabolism; Aerobic Degradation	CM	O_2	Highly likely	Methylotrophs	4.3 hrs

[1] Rates generated for Hanford site materials (Amonette et al., 2012; Truex et al., 2001). ND, Not Determined. Half-life calculations were based on published degradation ra
Aronson and Howard, 1997; Biehle et al., 1999; Boopathy, 2002; Cappelletti et al., 2012; Davis and Madsen, 1991; Fathepure et al., 1995; Galli and Leisinger, 1985; Hardy e
1993; Lee et al., 1995; Leisinger et al., 1994; McQuillian et al., 1998; Mechaber et al., 1998; Mehran and Wolf, 1999; Nielsen et al., 1992; Penny et al., 2010; Rugge et al., 19
Beelen and Van Keulen, 1990).

Biological Degradation of Dichloromethane (DCM)

Many microorganisms can couple growth to the complete degradation of dichloromethane under aerobic and anaerobic conditions. Aerobic bacteria are highly effective degraders of DCM (Leisinger and Braus-Stromeyer, 1995; Freedman and Gossett, 1991; Yanghao, 1990); most notable are the methylotrophic bacteria (Leisinger et al., 1994). Anaerobically, DCM is degraded to non-chlorinated products in laboratory systems and groundwater by acetogenic and denitrifying bacteria (Mehran and Wolf, 1999; Mechaber et al., 1998). Because DCM more likely to be mineralized to CO_2 than CM, CM alone cannot be used to reliably inform on the degradation of DCM in the Hanford aquifer. A number of molecular and analytical approaches can quantify in situ DCM degradation activity.

Because DCM is readily degraded under aerobic conditions, it would be expected to have a short half-life in the bulk oxic conditions of the 200W aquifer.

3.4 Biological Degradation of Chloromethane (CM)

Chloromethane can undergo hydrolysis or oxidation to CO_2 under anaerobic (e.g., by acetogenic bacteria; Messmer et al., 1993) and aerobic (e.g., by methylotrophic bacteria; Connell-Hancock et al., 1998; Doronia and Trotsenko, 1997; Doronia et al., 1996; Hartmans et al., 1986) conditions (Keuning et al., 1985; Rasche et al., 1990; Stirling and Dalton, 1979). Because CM is readily degraded as a growth substrate under aerobic conditions, it would be expected to have a relatively short half-life in the bulk oxic conditions of the 200W aquifer.

3.5 Sustainability of Chlorinated Methane Degradation in the Hanford Subsurface

3.5.1 Natural Organic Carbon and Nutrients

TOC contents are typically below 0.5 wt% in Hanford subsurface sediments and groundwater (Newcomer et al., 1995; Truex et al., 2001). Limited information is available regarding the distribution and chemical character of the natural organic matter (NOM) in Hanford groundwater; however, carbon flux would be required to sustain the observed microbial biomass of 10^6 cells/gram of aquifer sediment (Bagwell et al., 2018; Brockman et al., 2004; Qafoku et al., 2018).

Moreover, laboratory and field studies have repeatedly shown microbial biomass to be viable and responsive to environmental conditions for contaminant degradation (Bagwell et al., 2018; Brockman et al., 2004; Qafoku et al., 2018).

A limited scoping study was performed with 200 West Area groundwater and saturated sediments (300-400 ft depth) to characterize the chemical complexity of NOM in the system (Tfaily et al., in preparation). A graphical representation of the chemical complexity of NOM in Hanford subsurface materials is shown in Figure 13. Compounds are color ranked by abundance intensity on a normalized scale from blue (levels decreased) to red (levels increased). Sediment associated OC was found to be predominantly hydrophobic in nature with a strong lipid signature, while the groundwater OC fraction mostly consisted of hydrophilic compounds with a predominant carboxylic-alicyclic molecular signature. These results demonstrate higher than expected chemical complexity of OC between solid and aqueous phases; but there are no quantitative descriptors for various OC compartments and low MW labile carbon cannot be detected by the method deployed here. Organic carbon composition and flux will have an important influence on biotic activity, CT degradation and the sustainability of these processes.

As stated previously, microorganisms in deep Hanford subsurface sediments are present in sufficiently high numbers (> 10^6 cells/gram aquifer sediment) and microbial activity responds quickly (days) to environmental conditions for contaminant degradation without the need for added nitrogen or phosphorous (Bagwell et al., 2018; Brockman et al., 2004; Qafoku et al., 2018). It is unclear what additional factors may specifically limit *in situ* microbial growth and activity, but these results imply that a low level (and possibly intermittently) of basal activity must be occurring for cell maintenance. Nonetheless, the multi-indicator plots in Appendix B suggest that suitable resources are available to sustain *in situ* CT degradation.

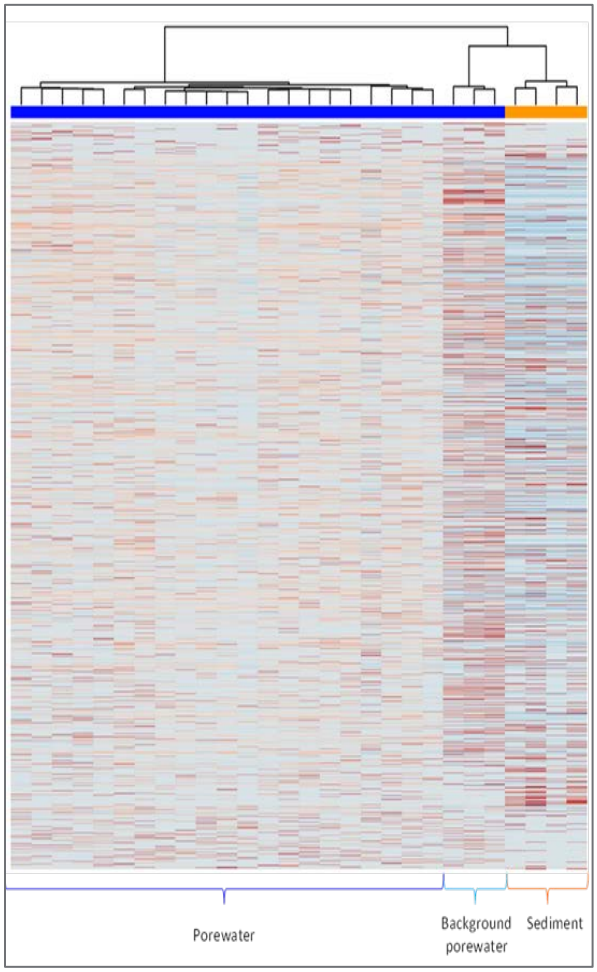

Figure 13. Hierarchical clustering of OC complexity in Hanford sediments and pore water.

3.5.2 Anthropogenic Inputs of Organic Carbon and Nutrients

Liquid waste streams disposed at the site could have provided additional supplies of organic carbon and nutrients to the aquifer; however, the longevity of these resources or potential impacts on CT degradation cannot be ascertained. Organic carbon sources co-disposed with CT included lard oil, TBP, and DBP. TBP and DBP could have also been utilized by *in situ* microbes as a biologically available source of phosphorous (Last et al., 1991). Triethyl phosphate has been used in a similar fashion as a PO_4^{3-}source to stimulate microbial degradation of TCE at an Integrated Demonstration at the Savannah River Site (Brockman et al., 1995).

The biofouling issues that have affected the 200W P&T system conveyance to injection wells, and the injection wells themselves, for treated water have been thoroughly reported (CH2M, 2017; Lee et al., 2017; Thomle et al., 2017). Biofouling is the result of residual organic carbon and nutrients originating from the biological treatment of groundwater in the fluidized bed reactors. Since P&T effluent is providing hydrolytic containment of the CT plume, we know that soluble organic carbon, nutrients, and microbial biomass have been inadvertently supplied to the CT plume and perimeter. Bacterial densities in 200W P&T system treated water have been measured at 10^4-10^6 bacterial cells/mL of effluent. A conservative extrapolation of these values would translate into 2-6 tons of new carbon (biomass) being pumped into the aquifer based on annualized injection well flow rates for the 200W P&T system. The specific impact(s) of P&T on *in situ* activity is not known but these inputs may be having a stimulatory effect on CT degradation by enhancing microbial activity and biomass, and/or contributing to the sustainability of anoxic reduced zones Note, groundwater data from P&T affected monitoring wells was intentionally excluded from the analysis presented here because groundwater conditions and chemistry cannot be reliably interpreted for degradation indicators.

3.6 Abiotic Reductive Dechlorination

Abiotic reductive degradation of CT has been extensively studied. Under anoxic conditions, if appropriate reduced minerals are present, abiotic reductive degradation of can occur and is a potential degradation mechanism in the 200W aquifer under specific conditions. Abiotic reductive dechlorination may include CF production as a potential indicator of the process, although multiple byproducts can be produced. Over time, reduced minerals would need to be regenerated by biological processes to maintain a capacity for CT degradation. Thus, the abiotic pathways depend on continued organic carbon flux and microbial activity, similar to the biotic pathways. For this reason, they are termed abiotic-biotic pathways when referred to as an overall process in this document.

3.6.1 Abiotic Degradation mechanisms for CT by Reactive Iron Minerals

Abiotic reductive dechlorination of CT by reactive iron minerals (e.g., iron sulfides, pyrite and mackinawite, magnetite, marcasite, green rust, and other Fe(II)-bearing clay minerals as well as Fe(II) sorbed to mineral surfaces) has been observed in both laboratory and field studies, and has attracted considerable attention within the remediation research community (Kriegman-King and Reinhard, 1994; Erbs et al., 1999; Assaf-Anid and Lin, 2002; Lee and Batchelor, 2002a; Davis et al., 2003; Kenneke and Webber, 2003; O'Loughlin et al., 2003; Vikesland et al., 2007; USEPA, 2009). He et al. (2015) recently reviewed the various pathways by which reactive iron minerals can degrade CT (Figure 14). Hydrogenolysis is a reductive dechlorination reaction in which mineral surfaces act as electron donors and/or reaction mediators to catalyze CT reduction (Tobiszewski and Namiesnik, 2012). Sequential hydrogenolysis would theoretically result in the systematic dechlorination of CT, forming CF, DCM, CM, and then methane (Holliger et al., 2003).

The hydroxyl radical is a potent oxidant but generally unreactive with polyhalogenated alkanes, like CT. A modified Fenton's reagent (0.5-1.0 M H_2O_2) is necessary to degrade CT, though the degradation mechanism is catalyzed by superoxide anion not the hydroxyl radical (Smith et al., 2004). However, the superoxide anion is unstable in aqueous solutions and thus, is likely to be an insignificant pathway in Hanford groundwater.

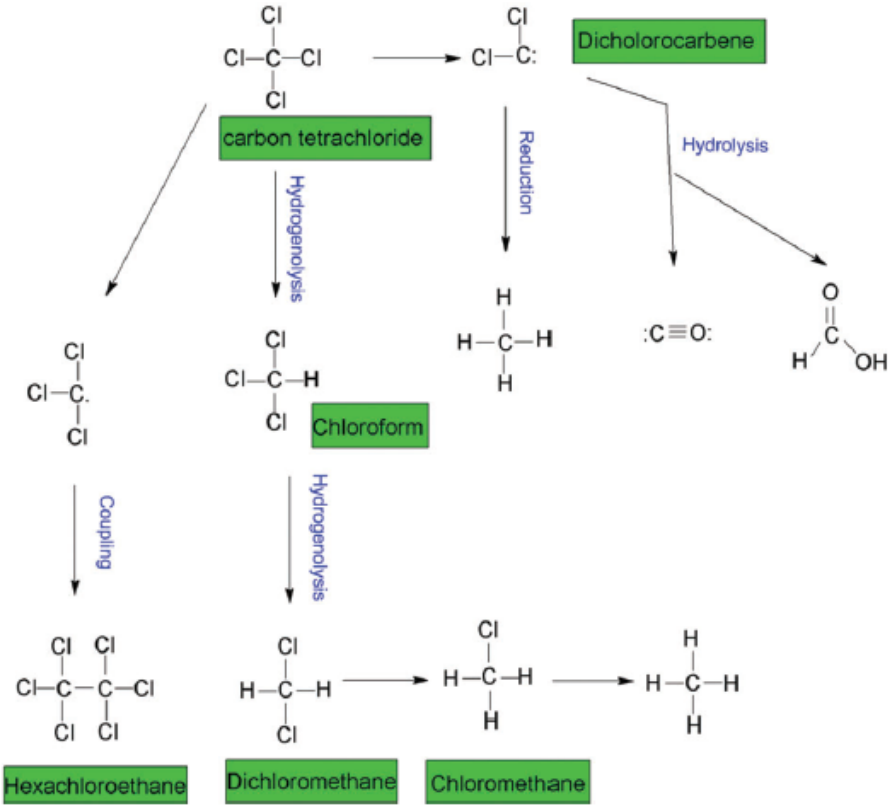

Figure 14. Summary of degradation pathways and products for chlorinated methanes (Egli et al., 1990; Kriegman-King and Reinhard, 1992; Tamara and Butler, 2004) (He et al., 2015)

The CT degradation products from reactive iron minerals can be varied due to the multiple reaction pathways and varied geochemical conditions. CF is usually observed as one daughter product, while other products might depend on different iron minerals (Table 5). Devlin and Muller (1999) and Kenneke and Webber (2003) reported CF as the main daughter products by FeS, followed by minor products such as CO_2, formate, and CS_2. In addition to CF, the final degradation products including CO, CH_4, and formate were also observed in the CT reaction with magnetite (McCormick and Adrianes, 2004; Vikesland et al., 2007). O'Loughlin et al. (2003) observed a variety of intermediates in CT degradation, and the products included CF, DCM, CM, CH_4, acetylene, ethene, ethane, CO, TCE, etc. The non-chlorinated products were frequently observed in the CT degradation by reactive iron minerals (Devlin and Muller, 1999; Kenneke and Webber, 2003; Kriegman-King and Reinhard, 1992; Maithreepala and Doong, 2005; O'Loughlin et al., 2003). For example, Hanoch et al. (2006) conducted CT transformation by bisulfide treated goethite, hematite, magnetite, and kaolinite, where yield was only ~1% CF, together with other likely non-chlorinated products. They also summarized the previous studies of CT reductive dechlorination by FeS and other adsorbed/precipitated Fe(II) minerals, and found a main CF yield range of 0.53-48%. The non-chlorinated products are quite encouraging for site CT attenuation by reactive iron minerals because it indicates that the produced CF (which is much toxic compared to CT) could be further dechlorinated to no toxic chemicals. The availability and form of sulfur in the reductive reaction system could be also important in controlling the final degradation products such as CS_2 (Devlin and Muller, 1999; Kriegman-King and Reinhard, 1992, 1994; Van Eekert et al., 1998).

Table 5. Rate constants and products of abiotic degradation of CT and CF by reactive iron minerals (He et al., 2015) (the half-life calculation in this study is based on the reported rate constants).

Chlorinated Solvents	Mineral Phases	Degradation Product	Conditions	Rate Constant	Reference	Half-life [day]
Chlorinated Methanes						
CCl_4	Mackinawite 1 Mackinawite 2	$CHCl_3$ Chloroform	4 g/L FeS, 13 m^2/g, pH 7.2, 0.6 g/L FeS, 77 m^2/g, pH 7.2,	1.2 ± 0.06 L/m^2/day (3.0 ± 0.22) × 10^{-2} L/m^2/day	Zwank et al. (2005)	0.58 23.1
CCl_4	FeS	$CHCl_3$, possibly CH_4, C_2H_4, C_2H_6	FeS 33 g/L, Tris buffer, pH 7.5	(2.98 ± 0.22) × 10^1/day	Choi et al. (2009)	0.02
CCl_4	FeS	Not monitored	200 g/L FeS, 0.05 M I, pH 6.5	(4.15 ± 0.12) × 10^1/day	Lipczynska-Kochany et al. (1994)	0.02
CCl_4	FeS_2	Not monitored	200 g/L FeS_2, 0.05 M I, pH 6.5	(4.15 ± 0.19) × 10^1/day	Lipczynska-Kochany et al. (1994)	0.02
CCl_4	FeS, fresh FeS, aged	$CHCl_3$, CS_2 $CHCl_3$, CS_2	0.73 g/L FeS 0.73 g/L FeS	1.07/day 1.27/day	Devlin and Muller (1999)	0.65 0.55
CCl_4	FeS	$CHCl_3$, CH_2Cl_2	pH 8, 18 g/L FeS	80% removed in 2.5 hours 9.7 × 10^1/day	Assaf-Anid and Lin (2002)	0.01
CCl_4	FeS, freeze dried	$CHCl_3$	10 g/L FeS, 0.05 m^2/g, pH 8.3, 0.1 M Tris	5.2 ± 0.62 L/m^2/day	Butler and Hayes (2000)	0.13
CCl_4	FeS coating on Iron oxides formed by treating with HS^-	$CHCl_3$	pH 8, 0.1 M tris 0.13 g/L FeS on goethite 0.20 g/L FeS on hematite	0.28 ± 0.14 day 0.22 ± 0.12 day	Hanoch et al. (2006)	2.48 3.15
CCl_4	Pyrite	$CHCl_3$, CO_2, CS_2, formate	pH 6.5, fresh ground pyrite, 14.8 g/L, 0.01 m^2/g, anaerobic conditions	0.16 L/m^2/day	Kriegman-King and Reinhard (1994)	4.33
CCl_4	Pyrite	$CHCl_3$	6 g/L FeS	20% removed in one day 0.22/day	Devlin and Muller (1999)	3.15
CCl_4	Pyrrhotite	$CHCl_3$	6 g/L FeS	60% removed in one day 0.91/day	Devlin and Muller (1999)	0.76
CCl_4	Magnetite			8.9 × 10^{-4} L/m^2/day	McCormick et al. (2002)	779
CCl_4	Green rust(Cl^-)	$CHCl_3$	pH 8	6.23 × 10^{-3} L/m^2/hour	Liang and Butler (2010)	4.63
CCl_4	Green rust (dodecanoate anions)	CF, HCOOH, CO		6.5 × 10^{-2} to 0.47/hour	Ayala-Luis et al. (2012)	0.44-0.06
CCl_4	Magnetite		pH 7.0	4.8 × 10^{-4} L/m^2/day	Danielsen and Hayes (2004)	1444
CCl_4	Magnetite		pH 7.2	1.2 × 10^{-3} L/m^2/day	Zwank et al. (2005)	5.78
CCl_4	Magnetite 9 nm and 80 nm		pH 7.8	2.2 × 10^{-3} L/m^2/day (9 nm) 9.9 × 10^{-4} L/m^2/day (80 nm)	Vikesland et al. (2007)	31.5 700
$CHCl_3$	FeS	Not monitored	pH 7.8, 0.044 g/L, 0.14 m^2/g	6.1 × 10^1 L/m^2/day	Kenneke and Weber (2003)	1.14
$CHCl_3$	FeS coating on iron oxide		pH 8, 0.1M Tris 0.13g/L FeS on goethite 0.20g/L FeS on hematite	(2.23 ± 0.29) x 10^{-3}/day (9.37 ± 0.98) x 10^{-3}/day	Hanoch et al. (2006)	310.8 74.0

USEPA (2009) summarized CT abiotic degradation on different iron-bearing minerals and the potential effects of geochemical condition such as pH. First, for iron sulfide, mackinawite (FeS), pyrrhotite (Fe1-xS), and pyrite (FeS2) are the main iron sulfide phases likely to form in the subsurface environment while the latter two represent the thermodynamically stable phases at shallow aquifer. FeS, a metastable

iron sulfide phases (which can be formed through reductive dissolution of an Fe(III) oxide by S(-II) generated by sulfate reduction bacteria), is the most reactive minerals. There is some evidence suggesting that the abiotic reductive reaction maybe associated with surface-bound Fe(II) and not surface-bound S(-II) (Butler and Hayes, 1998, 1999, 2000). In contrast, electron transfer at the FeS2 surface occurs at sulfur sites because CS2 was detected as the reduction product (Kreigman-King and Reinhard, 1994). The pH effects on CT degradation by iron sulfide have not been well documented, but the sulfide could play an important role in the degradation kinetics, and natural organic matter may influence the distribution of CT degradation products (Hanoch et al., 2006; USEPA, 2009). In addition, the oxidation of both FeS and FeS2 in oxidizing environments could strongly influence their reductive dechlorination abilities and the daughter products (Butler and Hayes, 2001; He et al., 2008). For example, Kreigman-King and Reinhard (1994) showed the dominated degradation products of CO2 or CF under aerobic or anaerobic conditions, respectively. Second, magnetite is a mixed Fe(II)-Fe(III) iron spinel mineral, widely spreading in aquifers as a minor sediment component. Besides the magnetite derived from bedrock weathering, fine-grained authigenic magnetite can be produced by iron-reducing bacteria using Fe(III) (hydr)oxides as the precursor (Mccormick et al., 2004). The degradation of CT on magnetite was mainly through hydrogenolysis, where the degradation rate depends on a number of factors. Vikesland et al. (2007) found that smaller particle size, especially less than ~20 nm, resulted in significantly faster CT degradation. Laboratory experiments also showed that the CT degradation rate on magnetite increased with solution pH (Danielsen and Hayes, 2004; Vikesland et al., 2007; Chio and Lee, 2009). Third, adsorbed Fe(II) on mineral surface, especially on iron oxides such as FeS, magnetite, goethite, lepidocrocite, siderite, and hematite, has been shown dramatic increase of the CT degradation rates (Pecher et al., 2002, Szecsody et al., 2004). The bond to the structural ion makes the sorbed Fe(II) a stronger electro donor, because of the electron density the structural iron is transferred through the bringing oxygen atom to the sorbed Fe(II) (USEPA, 2009). At a fixed pH of 7, the CT degradation rate was directly proportional to the density of Fe (II) sorbed to goethite (Amonette et al., 2000). In general, the reductive degradation rate is proportional to the concentration of sorbed Fe(II) at the mineral surface, which can be determined by chemical extraction or from the measured disappearance of Fe(II) from solutions (USEPA, 2009). Fourth, phyllosilicate clays (such as biotite, smectite, vermiculite, and montmorillonite), another structural iron-bearing minerals often abundant in soil and sediments, also show reductive capacity but with one to three orders of magnitude less than those of other iron sulfides and oxides (USEPA, 2009). Peretyazhko et al. (2012) found the transition from oxic to anoxic zone involved a significant reduction of Fe(III) in phyllosilicates. Fifth, accumulation of Fe(II) through dissolution of another Fe(II)-bearing mineral, siderite (formed in reducing non-sulfidic groundwater system), was also observed (Peretyazhko et al. 2012). Siderite could also contribute to CT degradation, although little work has been carried out on evaluating its reactivity. Finally, green rust (mixed valance Fe(II)/Fe(III) layered hydroxides) has been found in reducing soils. Laboratory experiments showed increased CT degradation rates on green rusts with increasing solution pH (pH 4.45-11.16) (USEPA, 2009).

3.6.2 Abiotic Degradation Rate and Half-life for CT by Reactive Iron Minerals

Hanoch et al. (2006) and He et al. (2015) reviewed the CT reductive degradation rates by common reactive iron minerals including FeS, FeS_2, pyrrhotite, magnetite, and green rust at near neutral pH conditions. The CT degradation rate constant (k) and the daughter products reported in the literature are compiled in Table 5. In addition, two experimental abiotic degradation of CF by FeS are also listed in Table 5. No information is available on the abiotic degradation rates of DCM by FeS and FeS_2, or other iron-bearing minerals. The kinetics of abiotic degradation of CT are generally well described as first-order reactions, and either first-order degradation rate constants or surface-area-normalized first-order rate constants are usually reported. The surface-area-normalized rate constant is calculated by dividing the first-order rate constant by the surface area of the mineral per unit volume (m^2/L) in the system, which may provide a better comparison of rate constants for different minerals in different systems since the CT

degradation occurs on the mineral surfaces. Based on the reported first-order rate constant, the half-life (days) of the CT degradation is calculated using the equation of $t_{1/2} = \ln(2)/k$ for each experiment and the results are added in Table 5. It should be noted that, in Table 5, both first-order rate constants and surface-area-normalized first-order rate constants were used for the half-life calculation, depending on how the rate constant is reported in the literatures. Although direct comparison between the different experiments in Table 5 is difficult, the data still illustrates that the CT degradation on FeS was the fastest among all the tested minerals. The rate of CT degradation on FeS_2 was slower than on FeS, but still faster than the other reactive iron minerals such as magnetite and green rusts. Ayala-Luis et al. (2012) reported a normalized rate constant order of Fe(0) > green rust > Fe(II) sorbed goethite > magnetite for CT degradation by iron minerals. Meanwhile, USEPA (2009) summarized that FeS was the most reactive mineral; magnetite was approximately tenfold less reactive than FeS, and sulfate green rust was about tenfold less reactive than magnetite. Laboratory evidence suggests that the more thermodynamically stable phases (FeS_2 and magnetite) support comparatively slower reduction rates than metastable phases, such as FeS (USEPA, 2009).

In terms of the half-life, Table 5 shows that the half-life of the CT abiotic reduction was of 0.02-3.5 days for FeS (except for the "Mackinawite 2" sample); 3.15 and 4.33 days for two FeS_2 samples; 0.06-4.63 days for green rust; and 5.78-1444 days for magnetite. In the case of CF, a half-life of 1.14 days on FeS, and ~74-311 days on FeS-coated hematite and goethite were obtained. Overall, theses laboratory experiments with pure iron minerals showed pretty fast CT abiotic degradation process. Their potential application to field CT neutral attenuation might be supported by field studies. Three field studies (Table 6) have demonstrated the effectiveness of abiotic degradation of CT with reactive iron minerals, in which a half-life of 1.34 days was obtained based on the reported rate constant of 0.36×10^{-3} min/m^2 with aquifer material (Kenneke and Webber, 2003); and both CF and CS_2 (degradation products) were detected in an industrial site or in a (surficial) aquifers (Davis et al., 2003; Devlin and Muller, 1999).

Table 6. Field studies that demonstrated abiotic CT degradation (He et al., 2015) (the half-life calculation in this study is based on the reported rate constants).

Chlorinated Solvents	Systems	Minerals	Mechanisms and Identification	Rate Constants	References	Half-life
CCl_4	Industrial site, infilled estuarine environment	Pyrite	CF to CS_2 ratio=2.4:1 Low molecular organic acid Excess inorganic Cl^-	n/a	Davis et al. (2003)	
CCl_4 and 14 halo-genated methane	Sediment and aquifer material	Sorbed Fe(II)	Fe(II) extraction	0.36×10^{-3} min/m^2	Kenneke and Weber (2003)	1.34 day
CCl_4	Surficial sand aquifer	FeS	CF to CS_2 ratio 2:1 Column study	n/a	Devlin and Muller (1999)	

3.6.3 Reactive Iron Minerals in Sediments at Hanford 200 Area

Reactive iron minerals are Fe(II)-bearing solid phases that usually form under anoxic conditions and are commonly observed in subsurface environments. In order to predict the potential for abiotic degradation of CT in the 200 West Area, it is necessary to understand the geology and mineralogy of the enclosing sediments, especially the iron and sulfur-rich minerals. In general, Hanford, Ringold, and Cold Creek formation sediments in the 200W aquifer contain a mixture of mafic (i.e., sediments derived from basalt) and granitic minerals, with mafic minerals (pyroxenes, amphiboles) and clay minerals containing significant Fe and Mn phases. The mineralogy of the Hanford sediments has been previously studied (Table 7), and a variety of Fe(II)-bearing minerals have been reported having the potential for contaminants remediation via surface-mediated reduction by electron transfer from Fe(II)-bearing

minerals (Baer et al., 2010; El Aamrani et al., 2007; Missana et al., 2003; Powell et al., 2004; Kendelewicz et al., 2000; Martinez et al., 2006; Scott et al., 2005; Fredrickson et al., 2004). Pearce et al. (2014) summarized the sediments recovered from the boreholes drilled at several locations mainly across the 200 area on the Central Plateau, and listed the details on the geology and the mineralogy of the samples (Table 8). The sediment data shows similar in composition and invariably contained a magnetic, Fe-rich mineral fraction consisting of magnetite, titanomagnetite, ilmenite, Fe(II)/Fe(III) phyllosilicates, and Fe(III) oxides, as well as carbonates, pyroxenes and feldspars.

Table 7. Summary of Hanford mineralogy (Szecsody et al., 2017; Xie et al., 2003).

Mineral	Formula	Both Fm (% wt)	Hanford Fm (% wt)	Ringold Fm (% wt)
Quartz	SiO_2	37.7 ± 12.4	38.4 ± 12.8	37.03 ± 12.4
Microcline	$KAlSi_3O_8$	17.0 ± 6.7	15.3 ± 4.4	18.7 ± 8.0
Plagioclase	$NaAlSi_3O_8$-$CaAl_2Si_2O_8$	18.7 ± 7.7	22.2 ± 7.2	15.5 ± 6.8
Pyroxenes	$(Ca,Mg,Fe)Si_2O_6$	3.03 ± 5.99	5.01 ± 7.83	1.14 ± 2.52
Calcite	$CaCO_3$	4.97 ± 7.19	1.91 ± 1.71	0.68 ± 0.92
Magnetite	Fe_3O_4	5.09 ± 4.37	4.46 ± 4.12	5.68 ± 4.63
Amphiboles	$Ca_2(Mg, Fe, Al)_5 (Al, Si)_8O_{22}(OH)_2$	5.55 ± 5.97	5.46 ± 5.67	5.64 ± 6.40
Apatite	$Ca_{10}(PO_4)_6(OH)_2$	0.60 ± 1.04	0.52 ± 0.92	0.67 ± 1.16
Mica[(a)]	$(K, Na,Ca)(Al, Mg, Fe)_2$-$_3(Si,Al)_4O_{10}(O, F, OH)_2$	2.07 ± 4.47	2.46 ± 3.74	1.71 ± 5.15
Ilmenite	$FeTiO_3$	2.51 ± 2.66	1.28 ± 1.51	3.67 ± 3.00
Epidote	$\{Ca_2\}\{Al_2Fe^{3+}\}[O\|OH\|SiO_4\|Si_2O_7]$	1.65 ± 2.98	1.78 ± 3.75	1.52 ± 2.14

(a) Muscovite, biotite, phlogopite, lepidolite, clintonite, illite, phengite

Table 8. Analyses of sediments from the Hanford Site (Pearce et al., 2014)

Sample Site	Geology	Mineralogy	References
Environmental Restoration Disposal Facility (ERDF)	Interstratified fine,| medium and course sands of the Hanford formation (Ice Age flood deposits) of Pleistocene age (15–20 K years old). Occasional finer layers of silty sand ranging to sandy silt slackwater deposits	Feldspar, quartz, 0.5 wt.% magnetite	Pearce et al.
200 East Area: Trench 94 Subpit (218-E-12B Burial Ground) – silty, fine sand (SF)	Silty, fine sand from 12.2 m below ground surface (bgs). 3 m above bedrock	Feldspar, quartz, 1 wt.% magnetite	Pearce et al.
200 East Area: Trench 94 Subpit (218-E-12B Burial Ground) – pebbly sand (SC)	Pebbly sand from 12.2 m bgs. 3 m above bedrock	Feldspar, quartz, 0.1 wt.% magnetite	Pearce et al.
200 West Area: Trench Z-9 (Plutonium Finishing Plant Complex)	Sandy silt from 29 m bgs	Quartz, magnetite, ilmenite, Clay: kaolinite, illite Feldspar: orthoclase Ilmenite Mica: biotite, muscovite	Ames (1974)
200 West Area: Borehole 299-W22–50 (South East corner of S-SX Tank Farm)	Fine-grained silty sediments (<2 mm) of the Hanford formation from 66–72 m bgs, just above water table	43.0 wt.% quartz, 30.0 wt.% plagioclase, 7.4 wt.% orthoclase, 4.5 wt.% mica, 2.0 wt.% amphibole, 1.0 wt.% chlorite, 0.1 wt.% magnetite	Baer et al. (2010) and McKinley et al. (2007)
300 Area: 55 m borehole (South Processing Pond)	Pliocene-age Ringold formation at 51.5–51.8 m bgs consisting of fine-grained deposits. Basalt bedrock exists below Ringold Formation at ~58 m bgs	Quartz, cristobalite, feldspar, calcite, hematite, magnetite; traces of smectite	Peretyazhko et al. (2012)

Truex et al. (2017) and Szecsody et al. (2017) conducted iron extractions on sediments collected from Hanford, Ringold, and Cool Creek formations at Central Plateau to characterize the potential for contaminant redox reactions in the Hanford sediments (Table 9 and Table 10). They found that the sediments contained a total of 14 to 44 mg/g extractable iron, based on a 3-week 5M HCl extraction. The results show that, in general, the amorphous and crystalline ferric iron oxide phase concentrations were small (available for microbial iron reduction), whereas the majority of ferrous iron was likely in pyroxene and amphibole phases. Ferrous phases accounted for ~25% to 50% of the total iron, including minor ferrous in carbonates/sulfides. They concluded that, although all of these sediments are from the vadose zone, some abiotic reduction can occur under water-saturated conditions (Szecsody et al., 2014).

Table 9. Ferrous and ferric iron phases in sediments based on liquid extractions (Truex et al., 2017)

Sample Name	Sample Location	ads. Fe^{II} (mg/g)	$Fe^{II}CO_3$, FeS (mg/g)	Other Fe^{II} (mg/g)	am. Fe^{III} (mg/g)	crys. Fe^{III} (mg/g)	Other Fe^{III} (mg/g)	Total Fe^{II+III} (mg/g)
C9507-B35434	T19 14C (CCUz)	< 1.20E-3	0.316	5.25	0.0195	0.549	13.8	19.4
C9507-B35443	T19 16C (CCUc)	< 1.20E-3	< 1.20E-3	7.24	< 1.20E-3	0.061	6.90	14.1
C9507-B35461	T19 138' (Ringold)	< 1.20E-3	3.92	5.50	0.1852	0.327	19.2	28.6
C9510-B361N1	T25 14C (H2/CCU)	< 1.20E-3	< 1.20E-3	9.57	0.0086	0.286	13.8	23.4
C9512-B36177	S-9 8C (H1/2)	< 1.20E-3	0.991	4.18	0.0414	0.228	11.1	16.3
C9512-B361F3	S-9 20C (H2)	< 1.20E-3	1.22	4.98	0.0382	0.640	14.6	20.8
C9512-B361F3	S-9 20C (H2)	< 1.20E-3	1.22	4.80	0.0351	0.632	13.9	19.9

ads. = adsorbed, am. = amorphous, crys. = crystalline

Table 10. Ferrous and ferric iron phases in sediments based on liquid extractions (Szecsody et al., 2017).

Borehole Depth (ft)	HEIS #	ads. Fe^{II} (mg/g)	$Fe^{II}CO_3$, FeS (mg/g)	Other Fe^{II} (mg/g)	am. Fe^{III} (mg/g)	crys. Fe^{III} (mg/g)	Other Fe^{III} (mg/g)	Total Fe^{II+III} (mg/g)
C9552 104.2-105.2	B34H37	< 2.50E-3	2.01	15.08	1.91E-02	5.70E-03	17.07	17.09
C9552 134.1-135.1	B34H55	< 2.50E-3	1.69	16.68	1.96E-02	4.65E-03	18.36	18.38
C9552 194.2-195.2	B34H79	< 2.50E-3	2.84	19.23	3.68E-02	< 2.50E-3	22.05	22.07
C9487 58.2 - 59.2	B34W66	< 2.50E-3	2.31	15.80	3.55E-03	9.20E-02	18.05	18.11
C9487 134.1-135.1	B34WB2	< 2.50E-3	1.89	16.61	1.97E-02	4.64E-03	18.48	18.50
C9487 230.0-231.0	B354L8	< 2.50E-3	1.92	16.51	1.86E-02	8.17E-02	18.41	18.43
C9488 219.3 – 220.3	B355L3	< 2.50E-3	2.07	16.87	3.70E-03	1.22E-01	18.93	18.95
C9488 219.3 – 220.3	B355L3	< 2.50E-3	2.28	18.17	3.43E-03	1.37E-01	20.43	20.45

In efforts to investigate the potential of Fe-bearing minerals on Tc(VII) reduction at Hanford site, detailed Fe-bearing mineral characterization on both Hanford formation and Ringold formation sediment samples had been conducted previously. For Hanford formations sediments, Baer et al. (2010) and Pearce et al. (2014) isolated the magnetic Fe(II)/Fe(III)-bearing mineral from sediments collected from the oxic zone during drilling of an uncontaminated borehole located near the 200 West Area. They investigated the structure and chemical composition of the sediment-derived iron oxides to assess their potential for electron transfer reaction to contaminants (Tc(VII)) at the oxide-solution interfaces. Both the X-ray diffraction (XRD) and scanning electron microscopy (SEM) and compositions determined energy dispersive spectroscopy (EDS) analyses indicates that the isolated highly magnetic sediment fraction contains predominantly bulk magnetite particles. However, the mineral surface analyses using X-ray photoelectron spectroscopy (XPS) and X-ray magnetic circular dichroism (XMCD) indicated that a likely incomplete thin layer coating of aluminosilicate (1-2 nm), or a oxidized Fe(III) mineral film such as goethite might inhibit or reduce the redox reaction extent between the contaminants with magnetite. They observed that the structural Fe at the mineral-solution interface is highly responsive to the aqueous environment, where, if surface initially oxidized, could be reduced to electron donating Fe(II) by transition of the aqueous environment from oxidizing to reducing. In principle, this structural Fe(II) was

then capable of catalyzing the reduction of contaminant in the groundwater by heterogeneous electron transfer at the mineral–solution interface. In the case of Ringold formation sediments, Peretyazhko et al (2012) characterized the mineralogically heterogeneous, Fe(II)-bearing sediments during investigating Tc(VII) reduction at Hanford site. Six intact Ringold formation fine-grained sediment cores in a semi-confined aquifer were collected at sequential depth from a 55 m borehole within 300 Area (Table 11). The upper most sample was located immediately above the oxic/anoxic transition zone, and the other five deeper samples were collected from the anoxic zone. Table 11 shows the observed Fe(II) mineral species, characterized by the chemical extractions (Table 12) , X-ray diffraction, electron microscopy, and Mössbauer spectroscopy, that included Fe(II)-phyllosilicates, FeS_2, magnetite and siderite. They found that the iron mineral suite was complex, and no direct correlation of iron mineral properties to sample depth or lithology was observed. All the samples collected in the anoxic zone contained reduced Fe(II)-rich phyllosilicates (illite, smectite, etc.). Pyrite, siderite, and Fe(III)/Fe(II) (oxy)hydroxides (goethite, hematite and magnetite) were prevalent in different depth. The extraction results (Table 12) also suggested that the transition from oxic to anoxic layers involved a significant reduction of Fe(III) in phyllosilicates, and leading to accumulation of Fe(II) and a complete disappearance of easily-reducible, poorly-crystalline Fe(III) (hydr)oxides. Their results showed that Tc(VII) reduction occurred on all anoxic samples.

Table 11. Fe speciation in sediment suspensions (Peretyazhko et al., 2012)

Sample	Fe_{tot} mM	Pyrite[a] mM	Siderite[b] mM	Magnetite[b] mM	Fe(II)-phyllosilicate[b] mM	Fe(III)-phyllosilicate[b] mM	Fe(II)/Fe(III) (oxyhydr)oxides[b] mM
18.0–18.3 m	44.42	nd[c]	nd	nd	7.11	37.31	nd
18.3–18.6 m	6.18	0.394	nd	nd	2.41	3.43	nd
30.8–31.1 m	1.29	0.003	0.39	0.15	0.22	0.39	nd
39.0–39.3 m	8.40	0.014			2.35		
47.2–47.5 m	6.59	0.062	nd	nd	1.84	1.52	2.70
51.5–51.8 m	3.55	0.004	0.21	0.89	0.50	0.57	1.14

[a] calculated from $S_{pyritic}$ data (Table 3),
[b] calculated from Mössbauer fitting results,
[c] not detected.

Table 12. Extracted Fe in sediments (< 0.5 mm fraction. Errors are standard deviations of three replicates) (Peretyazhko et al., 2012)

Sample	Fe_{tot} µmol/g	Fe(II) $_{HCl}$[a] µmol/g	Fe_c[b] µmol/g	Fe_{ca}[c] µmol/g	Fe_{dcb}[d] µmol/g
18.0–18.3 m	671	9.4 ± 0.4	4.1 ± 0.3	22.0 ± 1.0	139.5 ± 2.2
18.3–18.6 m	679	85.1 ± 0.5	11.4 ± 0.6	20.8 ± 1.1	126.9 ± 3.4
30.8–31.1 m	862	370.9 ± 7.0	100.2 ± 5.8	118.6 ± 16.3	249.0 ± 9.1
39.0–39.3 m	1000	72.7 ± 1.9	16.3 ± 1.4	21.5 ± 1.6	158.7 ± 2.1
47.2–47.5 m	766	70.1 ± 2.0	17.6 ± 0.4	16.6 ± 1.1	94.7 ± 7.3
51.5–51.8 m	1420	243.4 ± 15.6	189.2 ± 0.3	156.9 ± 12.4	232.4 ± 5.7

[a] 1 h 0.5 M HCl extractable Fe(II);
[b] citrate extractable Fe;
[c] citrate-ascorbate extractable Fe;
[d] dithionite-citrate-bicarbonate extractable Fe.

3.6.4 Abiotic Degradation of CT in Ringold Formation Sediments – Screening Test

An unpublished screening test of abiotic CT degradation was conducted for four Ringold formation samples collected from 200 West Area: fresh core samples of mud (113 m bgs) and sand (108 m bgs)

from 699-43-69, and archived samples of gravel (90 m bgs) and sand (84 m bgs) from 299-W15-43 (G. Wang, personal communication). Because these results are unpublished and were a preliminary screening effort, they are informational only as a potential indicator that some sediment conditions in the 200W aquifer could have conditions suitable for abiotic reductive dechlorination processes. No significant degradation was observed for sand (108 m bgs) and gravel (90 m bgs) samples in a solution with 5 µg/L CT for an experiment duration of 150 h. This is consistent with the observation of low to non-detectable sorbed Fe (II) in samples from the same unit. However, degradation was observed in the fresh mud samples at an initial aqueous concentration of 5 µg/L (Figure 15). The CT half-lives determined were 32, 144, and 48 days for the top (mud-1), middle (mud-2), and lower sections (mud-3) of the core, respectively. The corresponding rate constants are of ~0.0002-0.0009 h^{-1}. These previous screening results imply an uneven distribution of either surface-sorbed Fe (II) and/or reactive iron minerals in the sediments.

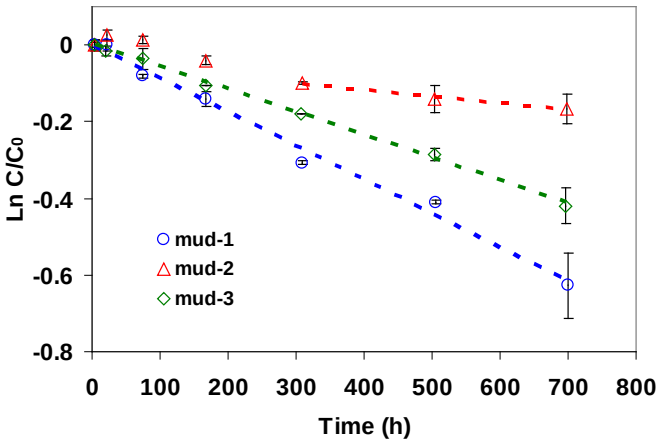

Figure 15. CT degradation in fresh mud observed using batch experiments. All data plotted are control vial-corrected. Similar Fe (II) contents were extracted in mud-1 and mud-3, whereas the value in mud-2 was near the detection limit (Wang, G. personal communication).

3.7 Radiolysis of CT in Hanford Sediments

Organic contaminants, including chlorinated methanes, can be effectively degraded upon exposure to ionizing radiation. CT and CF, though, are much more resistant to radiolytic decomposition than TCE; requiring an exposure of 200 and 400 kR, respectively, to decrease the concentration by 50% in groundwater or soil vapor (Matthews et al., 1993). Radiolytic decomposition of CT is expected to be an insignificant pathway for the 200W aquifer.

4.0 Data Analysis and Interpretation

The prior sections describe the biotic and abiotic reductive degradation mechanisms for CT, as well as chlorinated byproducts, along with normalized reaction rates for each mechanism based on published values from controlled laboratory studies, and field trials. In addition to abiotic hydrolysis, CT can degrade via three other mechanisms: (1) biotic hydrogenolysis, where CF accumulates as an intermediate byproduct; (2) a biotic dichlorocarbene pathway to CO_2, with no measureable intermediate byproducts; and (3) abiotic degradation by reactive minerals, where CF and a range of other compounds may be intermediate byproducts. Published reaction rate data are for conditions where biostimulation amendments have been added or reactive minerals are present; thus, this information is only useful in assessing relative rates of CT and byproduct degradation, not for absolute rates of natural attenuation in the 200W aquifer. Previous field trials have demonstrated that the Hanford subsurface microbial populations can degrade CT to CF (hydrogenolysis) and CO_2 (dichlorocarbene pathway) during respiratory nitrate reduction (denitrification) when a labile organic carbon substrate is available. The coincident presence of CF with CT in the aquifer near the disposal areas is another indicator that reductive dechlorination (hydrogenolysis) occurred historically when CT was co-disposed with organic carbon wastes. The literature review provided unequivocal information that, under the appropriate conditions, biotic and abiotic-biotic reductive degradation can occur in the 200W aquifer.

CT degradation mechanisms were used to identify indicators of degradation activity. 200 West Area groundwater data and the relative significance of measured trends in groundwater chemistry were evaluated, taking into account the effect of P&T activities on monitoring well data. Examination of available groundwater data throughout the plume over the period from 1986 to the present provides evidence that biotic CT degradation has taken place and continues to occur in the 200W aquifer. Briefly, the multiple lines of evidence for continuing in situ biotic CT degradation are as follows.

- CF concentration trends are an indicator of CT degradation by reductive dechlorination. CF can only be derived by the anaerobic degradation of CT in anoxic, reduced zones within the aquifer. At monitoring wells, concentrations of CT and CF are affected by aquifer heterogeneity, plume migration, adsorption, and degradation. However, based on a relative rate analysis for CT and CF, increasing CF concentrations and an increasing CF/CT ratio are indicators for CT degradation that can be used in conjunction with the above indicators. Because CF is stable in Hanford groundwater, the interpretation of CF data must be made cautiously. The widespread presence of CF in the aquifer is an indication that reductive dechlorination (hydrogenolysis) occurred in the past, which was likely driven in large part by the co-disposal of organic waste at the primary CT disposal areas. For monitoring data away from the source area, CF trends in the groundwater data are more indicative of recent degradation activity.
- Anaerobic reductive dechlorination (hydrogenolysis) of CT in the 200 West groundwater is indicated by the detection of DCM across a wide spatial area and into recent time. DCM only originates from the degradation of CT (and CF) occurring in anoxic/reduced zones by reductive dechlorination. DCM is a reliable indicator of more recent degradation activity because DCM is quickly metabolized to CO_2 in oxic groundwater (which is the condition in the bulk 200W aquifer). Thus, detection of DCM in groundwater indicates biotic degradation in anoxic/reduced zones that must be recent and within proximity to the wells where DCM is detected (i.e., not from historical degradation near a source zone with co-disposed organic waste).
- The detection, and in certain cases the accumulation, of nitrite is clear evidence of microbially catalyzed nitrate reduction to nitrite. Nitrite is evidence of incomplete nitrate reduction (as the first step in the pathway). There is ample evidence in the literature (including site-specific data) that shows nitrate degradation is positively correlated with anaerobic degradation of CT. Nitrite is a reliable indicator of recent denitrification activity in anoxic/reduced zones because nitrite is highly

unstable in oxic groundwater and will quickly oxidize back to nitrate. Thus the detection of nitrite in a monitoring well is evidence of denitrification that is recent and within close proximity to the wells where it is detected. Note that the nitrite detection limit is high because of the high nitrate concentrations in many wells. Therefore, it may be that nitrite is more ubiquitous at low concentrations, but detection is masked by the high detection limits.

Mechanisms and pathways for CT/CF degradation are well established in the literature. There is a wealth of site-specific data (experimental, field, and monitoring) that supports biotic degradation of CT and conditions suitable for abiotic-biotic reductive degradation in the 200W aquifer. The analysis of 200 West Area groundwater data revealed numerous well locations distributed throughout the aquifer where multiple indicators of local anoxic/reduced conditions and CT degradation pathway products (DCM) coincide. The analysis was restricted to well locations that have not been influenced by any P&T operations in the 200 West Area. More than three decades of groundwater data reveals a pattern of persistent *in situ* CT degradation activity. The sustainability of biotic and coupled biotic-abiotic processes depends on anoxic, reduced conditions and the supply of organic carbon. An organic carbon energy source is required to fuel microbiological pathways, and the metabolism of organic carbon generates anoxic, reduced conditions that propagate anaerobic degradation and sustain reducing power for abiotic processes. Organic carbon is the single most important driver (or rate limiting factor) of CT degradation in the 200W aquifer. Indicators of recent anoxic activity demonstrate that there is an organic carbon flux into anoxic zones that supports continued denitrification and CT degradation.

The oxic conditions of the bulk aquifer are not conducive to biotic degradation of CT or CF. DCM and CM degradation would be expected within high permeability flow paths where oxic conditions dominate. The conceptual model of CT degradation in the 200W aquifer is based on CT and CF degradation occurring in anoxic, reduced silt or clay lenses, possibly the RLM unit, which will comprise only a portion of the total aquifer volume. There are adequate indicators that these zones exist and that CT and CF degradation is currently occurring. However, for remediation purposes, a bulk aquifer degradation rate is needed to evaluate the overall impact that biotic and abiotic degradation pathways are having on the CT plume. CT concentrations/mass and CT degradation in anoxic silt zones may also be of interest for the remedy because CT in these silt zones may be a continuing CT source for adjacent higher permeability sediments as those permeable materials become cleaner due to P&T operations.

Based on the aquifer setting and geochemical conditions required for CT transformation, degradation will be constrained to silt lenses or features in the bulk aquifer where anoxic conditions can be sustained. Monitoring wells are screened within high permeability regions and do not measure these zones directly. Therefore, we must interpret the data as a groundwater sample taken from an overwhelmingly oxic aquifer with comparatively small contributions (and indicators) originating from anoxic zones.. Degradation products from the anoxic zones would 1) be diluted when measured at monitoring wells and 2) potentially be affected by the bulk oxic conditions, if the products can be transformed aerobically. Similarly, rates of degradation in a silt zone represent only a portion of the total aquifer volume and CT mass. Thus, a degradation rate assigned to a silt zone would need to be scaled, resulting in a slower degradation rate for the bulk aquifer.

Reductive dechlorination (hydrogenolysis) is a coupled rate process for CT→CF→DCM→CM that requires anaerobic conditions to proceed. Microcosm tests consistently show CF accumulation as an intermediate of reductive dechlorination. Figure 6 shows the predicted CT and CF responses for a range of reductive dechlorination half-lives and initial concentrations appropriate for the 200 West Area plume. Note, that these are simulated batch conditions (first-order kinetics) and can only be used for relative analysis of trends, not prediction of actual concentrations or processes in the field.

Briefly, a base CF concentration of 10 µg/L was used in the rate-estimation plots (Figure 6) because most wells have CF concentrations in this range. CT concentrations, however, range from 10 to several thousand µg/L. When the CT concentration is high (~100 µg/L and higher), even a moderate rate of CT reductive dechlorination (hydrogenolysis) will cause the CF concentration to increase when the CF degradation rate is similar to or even faster than the CT rate. The only exception to this result is if the CF degradation rate were very high (e.g., a half-life of less than 50 years). Thus, at locations where CT is in the 100-1000 µg/L range and the degradation rate of CT is at a half-life between 100 and 400 years, CF concentrations would be expected to increase over time with a noticeable increase in a 10- to 20-year period. At groundwater monitoring wells, CT and CF concentrations are affected by changing geochemical conditions, plume migration, and a variable degradation rate. Thus, the strongest indicator for potential CT degradation would be if CF concentrations are increasing and the CF/CT ratio is increasing. Both metrics imply that CF is being produced as an accumulating byproduct of reductive dechlorination. At locations where CT is dilute (10s of µg/L), the CF concentration increase over a 10- to 20-year period would be comparatively quite small and potentially a stable trend, even when reductive dechlorination of CT is occurring at a consistent rate. There are 16 groundwater well locations in the studied area of the 200W aquifer where DCM, nitrite, and CF-based indicators (Table 2), and visual inspection of trends (Appendix B), offer convincing evidence of reductive dechlorination (hydrogenolysis).

In the absence of site-specific laboratory rate data, rough interpretation of the potential CT degradation rate can be made for the reductive dechlorination (hydrogenolysis) pathway based on the CF concentration data. From the rate estimate evaluation (Figure 6), it is unlikely that the bulk aquifer CT half-life from biotic degradation of CT to CF is less than 100 years. If that were the case, CF concentrations in area of CT concentration above 100 µg/L would be increasing. However, the bulk aquifer CT half-life from biotic degradation of CT to CF could be 400 years, and potentially somewhat faster, and it would still be consistent with the available site data.

The above rate assessment uses reductive dechlorination (hydrogenolysis) of CT to CF as the primary degradation pathway. However, abiotic degradation pathways and another biotic degradation pathway could also be active *in situ* but do not result in the accumulation of CF. Thus, potential contributions of these pathways to the overall CT degradation rate are not captured by the CF-based rate or presence of DCM. Pervasive indicators of anoxic, reduced geochemical conditions (the same indicators that were used for reductive dechlorination; 58 monitoring wells) demonstrate that conditions conducive to these other pathways exist. The biotic pathway for CT degradation without accumulation of CF requires a specific condition in the Hanford subsurface (Truex et al., 1996; Hooker et al., 1998; Sherwood et al., 1996) that may be less likely than conditions conducive to the pathway leading to accumulation of CF. Abiotic pathways depend on the presence of appropriate surface-phase minerals in a reduced form. These surface phases would be possible in the portion of the aquifer with anoxic conditions. Given the more specialized conditions needed for these alternative CT degradation mechanisms it is assumed that their contribution to the overall CT degradation rate would be equal to or less than the contribution of the CT to CF pathway. Thus, additional pathway contributions would not result in an overall CT degradation half-life less than 100 years if we estimate the half-life of the CT to CF degradation pathway to be 400 years. Collectively, though, the biotic and abiotic-biotic mechanisms could result in a half-life less than 400 years. Additional effort would be required to define a more specific half-life value between 100 and 400 years. The need for additional laboratory testing would depend on the impact that a more specific degradation rate estimate could have on remedy decisions for the CT in the Ringold Unit E (Rwie) and Ringold Unit A (Rwia) formations of the 200W aquifer. In particular, because the transport velocity is slower in the Rwia formation, a half-life greater than 100 years may still be of significance for attenuating the Rwia CT plume.

If laboratory tests were conducted, the focus would be on quantifying CT and CF degradation processes and rates in low permeability zones where anoxic conditions would most likely exist in the aquifer. Scaling degradation rates derived from specific zones to the full aquifer would take into consideration 1) the percent volume of the aquifer occupied by anoxic, reduced silt zones and possibly RLM and 2) the mass of CT in these zones relative to the mass in the remainder of the aquifer. Anoxic silt zones would be a subset of the silt-dominated zones in the aquifer because they need to have properties that shield the inner portion of the silt zone from the bulk oxic groundwater conditions.

A preliminary examination of borehole logs for a subset of wells in the 200W aquifer was conducted to evaluate the presence and extent of silt zones (Appendix C). The evaluation included two separate analyses (Figure C.2 in Appendix C): (1) calculating the aggregate silt fraction below the top of Rwie across the total depth (below Rwie) for each well; and (2) calculating the aggregate silt fractions for Rwie and Rwia separately for a subset of wells for which the top of the Rwia was identified. The second analysis defined Rwie as starting from the top of Rwie to the top of Rwia, and the section of the Rwia evaluated extended from the top of Rwia until the total depth of each well. The results of these analyses, summarized in Table 13, indicated a total of about 51% of wells with some level of silt content below the top of Rwie. The analysis conducted separately for Rwie and Rwia showed about 43% of the wells with silt content for Rwie and 20% of the wells for Rwia. Even though a smaller percentage of wells showed any silt content for Rwia, the average silt content for this formation was about 45% of the evaluated thickness compared to 8.4% for Rwie.

Table 13. Results of the silt analysis conducted for the 200W aquifer.

Silt Analysis for the 200W Aquifer	Number of Wells Analyzed	Number of Wells with Silt Units	Average Silt Content
Aggregate silt fraction below the top of Rwie across the total depth for each well	115	59	5.7%
Aggregate silt fraction below the top of Rwie and above the Rwia*	96	42	8.4%
Aggregate silt fraction below the top of Rwia for the total depth of each well**	96	19	45%

* Average thickness of Rwie for the analyzed wells was 239 ft.
** Average thickness of the section of Rwia for the analyzed wells was 49 ft. The information for the full thickness of Rwia was not available.

In summary, analysis of historical groundwater data for the 200 West Area provides strong evidence that CT degradation has occurred, and continues to occur, in the 200W aquifer. The detection of multiple indicators of degradation confirms the presence of local anoxic activity, identifies the principle CT degradation pathway, and the repeated detection of short-lived degradation products (i.e., DCM, NO_2^-) demonstrates the clear potential for sustained CT attenuation in the 200W aquifer. A relative rate assessment indicates that CT degradation to CF is occurring in the aquifer at a CT degradation half-life of greater than 100 years. There are several CT degradation pathways that cannot be included in this type of analysis because they do not form byproducts that can be readily measured. Their combined contribution to an overall CT degradation rate was conservatively assumed to be equal to or less than the rate estimate for the degradation pathway to CF. Based on this assumption, these additional pathways would not result in a CT degradation half-life of less than 100 years. The best estimate of a collective CT biotic and abiotic-biotic degradation half-life for the 200W Area plume is between 100 and 400 years.

If additional quantification of CT degradation processes and rates is sought, laboratory testing to support this effort could be conducted as described in the next section. The rates gathered from laboratory testing

would need to be scaled to estimate a bulk biotic/reductive CT degradation rate based on an estimate of anoxic zones.

5.0 Path Forward

Laboratory testing could be peformed to explicitely measure CT and CF degradation mechanisms and rates by focusing on low permeability zones where anoxic and reducing conditions would be established, and sustained, in the aquifer. Compound specific isotope analysis (CSIA) is the recommended analytical technique to measure the ratios of isotopes for direct, unambiguous evidence for contaminant attenuation (physical, biotic, abiotic), to identify principle attenuation mechanism(s), and allow for specific quantification of CT and CF transformation rates *in situ* and from specific laboratory investigations. This approach is based on the principle of kinetic isotope fractionation which simply means that individual attenuation process produce specific and diagnostic shifts in isotope ratios of parent and degradation products. Thus, isotope fractionation can not only be used to calculate degradation rates, but also provide clear discrimination of process mechanisms responsible for CT and CF degradation. We propose utilizing two dimensional compound specific isotope analysis (2D-CSIA) of $^{13}C/^{12}C$ and $^{37}C/^{35}Cl$ for improved sensitivity and resolution. Briefly, as CT and CF are degraded, the parent compound becomes enriched in heavy isotopes ($\delta^{13}C$ and $\delta^{37}Cl$) over time. Per the 2D-CSIA approach, $\delta^{37}Cl$ vs $\delta^{13}C$ plots reveal compound specific isotopic enrichment relative to its initital (or referenced) isotopic composition. This delta value measures the reaction rate and the slope of the line is characteristic of the specific attenuation mechanism(s) that are active. 2D-CSIA results have been used to aid in identifying and distinguishing active biotic and abiotic chloroform degradation (Rodríguez-Fernández et al. 2015).

CSIA involves the determination of stable isotope delta values (isotopic signatures) for individual compounds (CT and CF) for quantitative measure of degradation rates and mechanisms. We proposed applying 2D-CSIA to 1) calculate compound specific *in situ* degradation rates based on the natural abundance of stable C and Cl isotopes from groundwater samples, as well as 2) to calculate compound specific degradation rates from laboratory studies that specifically quantify the reactivity of geological formations or conditions in the 200W Area aquifer.

Isotopic analysis of CT and CF from groundwater samples can be used to identify plume areas where degradation is occurring or suspected based on prior analysis of groundwater data and degradation indicators. Additionally, this analysis can determine if the same or different combination(s) of degradation processes are involved in CT and CF degradation. The analysis provided in this report assumes that sequential, reductive dechlorination (hydrogenolysis) is the predominant degradation pathway in the 200W Area aquifer. Analysis of natural isotopic ratios of CT and CF from source areas and the distal plume will yield signature enrichment factors for each compound *in situ* that are diagnostic of the abiotic and biotic degradation pathway(s) attenuating CT and CF in the aquifer. Moreover, supporting laboratory investigations can explicitly measure degradation rates of individual pathways, selected well locations or aquifer formations, or provide accurate rate measurments that cannot be practically measured *in situ* because the processes are occurring slowly, episodically, and are heterogeneous in their distribution throughout the bulk aquifer.

CSIA will be used to calculate first order degradation rate constants and the extent of CT and CF degradation to generate isotopic enrichment factors from aquifer materials and laboratory samples. Physical attenuation forces do not produce an isotopic fractionation pattern; thus the processes are easily distinguished from reactive processes. The CSIA method provides improved mechanistic resolution and quantitation. Further, this approach avoids many of the challenges and limitations articulated in this report for interpreting concentration data to infer *in situ* degradation mechanisms and potential rates.

Anaerobic Biodegradation: Under anaerobic conditions, cometabolic degradation of CT and CF is catalyzed by nitrate-reducers (CT→CF only), methanogens, acetogens, fermenters, sulfate-reducers, and iron-reducers has been widely demonstrated. Isotopic enrichment factors associated with biotic degradation of CT and CF will need to be measured. Two fundamental degradation pathways for CT

have been demonstrated at Hanford in prior treatability studies. CSIA approach will be used to quantify reductive dechlorination (hydrogenolysis), and direct metabolism of CT and CF to CO_2 under denitrifying conditions where detectable indicators are not produced. Chloroform can serve as a growth supporting electron acceptor by some *Dehalobacter* and *Desulfitobacterium* spp. (Grostern et al. 2010; Tang and Edwards 2013). Reductive dechlorination of chloroform to dichloromethane by *Dehalobacter*-containing cultures results in significant carbon isotope fractionation (ε = -27.5‰) that can be referenced to monitor chloroform biodegradation (Chan et al. 2012). In addition to CSIA, quantitative PCR (qPCR) can be used to quantify chloroform reductase genes and *Dehalobacter* DCM strains as a supporting line of evidence in assessing chloroform and dichloromethane biodegradation.

Abiotic Degradation: Abiotic transformations with iron containing minerals including iron oxides and iron sulfides may play a significant role in natural attenuation of CT and CF (McCormick et al. 2002; Zwank et al. 2005). For iron (hydr)oxides (magnetite, goethite, hematite, and lepidocrocite) and siderite ($FeCO_3$), carbon isotope enrichment factors during abiotic degradation of CT are in the range of -29 ± 3‰ (Zwank et al. 2005). Although lower, carbon isotope fractionation during abiotic degradation of CT by FeS (ε=-15.9‰) was also significant. Zero valent iron (ZVI) mediated degradation of carbon tetrachloride also results in significant carbon isotope fractionation (VanStone et al. 2008). These reference values will provide basis for monitoring abiotic transformation of CT and CF.

6.0 References

Adam G, H Duncan. 2001. Development of a Sensitive and Rapid Method for the Measurement of Total Microbial Activity Using Fluorescein Diacetate (FDA) in a Range of Soils. Soil Biology and Biochemistry 33: 943–51.

Ames L.L. 1974. Characterization of Acitnide Bearing Soils: Top Sixty Centimeters of 216-Z-9 Enclosed Trench. Pacific Norwest National Laboratory, Richland, Washington.

Amonette, J.E., D.J. Workman, D.W. Kennedy, J.S. Fruchter, and Y.A. Gorby. 2000. Dechlorination of carbon tetrachloride by Fe(II) associated with goethite. *Environmental Science & Technology* 34: 4606-4613.

Amonette JE, PM Jeffers, O Qafoku, CK Russell, DR Humphrys, TW Wietsma, MJ Truex. 2012. Abiotic degradation rates for carbon tetrachloride and chloroform: Final report. PNNL-22062.

Amonette JE, PM Jeffers, O Qafoku, CK Russell, TW Wietsma, MJ Truex. 2010. Abiotic degradation rates for carbon tetrachloride and chloroform: Progress in FY2009. PNNL-19142.

Aronson D, PH Howard. 1997. Anaerobic biodegradation of organic chemicals in groundwater — A summary of field and laboratory studies: Final report prepared for the American petroleum Institute by Environmental Science Center, Syracuse Research Corporation, North Syracuse, N.Y., 262 p.

Assaf-Anid, N., and K.Y. Lin. 2002. Carbon tetrachloride reduction by Fe^{2+}, S^{2-}, and FeS with vitamin B12 as organic amendment. *Journal of Environmental Engineering* 128: 94–99.

Ayala-Luis, K.B., N.G. Cooper, C.B. Koch, and H.C. Hansen. 2012. Efficient dechlorination of carbon tetrachloride by hydrophobic green rust intercalated with dodecanoate anions. *Environmental Science & Technology* 46: 3390–3397.

Baer D.R., Grosz A.E., Ilton E.S., Krupka K.M., Liu J., Penn R.L. and Pepin A. 2010. Separation, characterization and initial reaction studies of magnetite particles from Hanford sediments. *Physics and Chemistry of the Earth* 35, 233–241.

Bagwell CE, AR Lawter, KJ Cantrell, CF Brown. 2018. Evaluation of central plateau remediation alternatives: interim status report. PNNL-28055.

Balkwill DL, EM Murphy, DM Fair, DB Ringelberg, DC White. 1998. Microbial communities in high and low recharge environments: implications for microbial transport in the vadose zone. Microb. Ecol. 35:156-171

Boopathy R. 2002. Anaerobic biotransformation of carbon tetrachloride under various electron acceptor conditions. Bioresource Technol. 84:69-73

Bouwer EJ, PL McCarty. 1983a. Transformations of 1- and 2-Carbon Halogenated Aliphatic Organic Compounds under Methanogenic Conditions. Appl. Environ. Microbiol. 45:1286-94.

Bouwer EJ, PL McCarty. 1983b. Transformations of Halogenated Organic Compounds underDenitrification Conditions. Appl. Environ. Microbiol. 45:1295-9.

Brockman FJ, TL Kieft, JK Fredrickson, BN Bjornstad, SW Li, W Spangenburg, PE Long. 1992. Microbiology of vadose zone paleosols in southcentral Washington state. Microb. Ecol. 23:279-301.

Brockman FJ, JS Selker, ML Rockhold. 2004. Integrated field, laboratory, and modeling studies to determine the effects of linked microbial and physical spatial heterogeneity on engineered vadose zone bioremediation. PNNL-14535.

Brockman FJ, W Payne, DJ Workman, A Soong, S Manley, TC Hazen. 1995. Effect of gaseous nitrogen and phosphorous injection on in situ bioremediation of a trichloroethylene-contaminated site. J. Haz. Materials. 41:287-298.

Brouns TM, SS Koegler, WO Heath, JK Fredrickson, HD Stensel, DL Johnstone, and TL Donaldson. 1990. Development of a biological treatment system for Hanford groundwater remediation. FY 1989 Status Report, PNL-7290.

Butler, E.C. and K.F. Hayes. 1998. Effects of solution composition and pH on the reductive dechlorination of hexachloroethane by iron sulfide. *Environmental Science & Technology* 32: 1276-1284.

Butler, E.C., and K.F. Hayes. 1999. Kinetics of the transformation of trichloroethylene and tetrachloroethylene by iron sulfide. *Environmental Science & Technology* 33: 2021–2027.

Butler, E.C., and K.F. Hayes. 2000. Kinetics of the transformation of halogenated aliphatic compounds by iron sulfide. *Environmental Science & Technology* 34: 422–429.

Butler, E.C., and K.F. Hayes. 2001 Factors influencing rates and products in the transformation of trichloroethylene by iron sulfide and iron metal. *Environmental Science & Technology* 35: 3884–3891.

Cappelletti M, D Frascari, D Zannoni, S Fedi. 2012. Microbial degradation of chloroform. Applied Microbiology and Biotechnology 96:1395-1409.

Castro CE, RS Wade, NO Belser. 1985. Biodehalogenation: reactions of cytochrome P-450 with polyhalomethanes. Biochemistry 24:204-10.

Chan, C.C.H., S.O.C. Mundle, T. Eckert, X. Liang, S. Tang, G. Lacrampe-Couloume, E.A. Edwards, and B. Sherwood Lollar. 2012. Large Carbon Isotope Fractionation during Biodegradation of Chloroform by Dehalobacter Cultures. *Environmental Science & Technology* 46 no. 18: 10154-10160.

Choi, K., and W. Lee. 2009. Reductive dechlorination of carbon tetrachloride in acidic soil manipulated with iron(II) and bisulfide ion. *Journal of Hazardous Materials* 172: 623–630.

CH2M. 2017. Nature of injection well foulant and recommendations to limit injection well fouling at 200 West Pump & Treat. SGW-61398, Rev 0.0, CH2M Plateau Remediation Company, Richland, WA

CH2M. 2018 200 West Pump and Treat 4th Quarter 2017 Briefing. SGW-61781-VA, Rev 0.0, CH2M Plateau Remediation Company, Richland WA

CHPRC. 2012. *200-ZP-1 Interim Pump and Treat System Summary Performance Report for Calendar 2012*. DOE/RL-2012-36, Rev. 0, CH2MHill Plateau Remediation Company, Richland, Washington.

CP-47631, 2016, *Model Package Report: Central Plateau Groundwater Model Version, 6.3.3*, Rev. 3, CH2M HILL Plateau Remediation Company, Richland, Washington. Available at:http://pdw.hanford.gov/arpir/index.cfm/viewDoc?accession=0069098H.

Danielsen, K., and K.F. Hayes. 2004. pH dependence of carbon tetrachloride reductive dechlorination by magnetite. *Environmental Science & Technology* 38: 4745–4752.

Davis, A., G.G. Fennemore, C. Peck, C.R. Walker, J. McIlwraith, and S. Thomas. 2003. Degradation of carbon tetrachloride in a reducing groundwater environment: implications for natural attenuation. *Applied Geochemistry* 18: 503–525.

Davis, A., G.G. Fennemore, C. Peck, C.R. Walker, J. McIlwraith, and S. Thomas. 2003. Degradation of carbon tetrachloride in a reducing groundwater environment: implications for natural attenuation. *Applied Geochemistry* 18: 503–525.

Devlin, J.F., and D. Muller. 1999. Field and laboratory studies of carbon tetrachloride transformation in a sandy aquifer under sulfate reducing conditions. *Environmental Science & Technology* 33: 1021–1027.

DOE. 2009. *200 West Area 200-ZP-1 Pump and Treat Remedial Design/Remedial Action Work Plan*. DOE/RL-2008-78, Rev. 0, Reissue, U.S. Department of Energy, Richland Operations Office, Richland, Washington.

DOE. 2011. Annual Status Report (Fiscal Year 2010): Composite Analysis of Low-Level Waste Disposal in the Central Plateau at the Hanford Site. DOE/RL-2010-105, Rev. 0, U.S. Department of Energy, Richland Operations Office, Richland, Washington.

DOE. 2012a. *Record of Decision for Interim Remedial Action Hanford 200 Area Superfund Site 200-UP-1 Operable Unit*. 12-AMRP-0171, U.S. Department of Energy, Richland Operations Office, Richland, Washington.

DOE. 2012b. *Calendar Year 2011 Annual Summary Report for the 200-ZP-1 and 200-UP-1 Operable Unit Pump-and-Treat Operations*. DOE/RL-2012-03, Rev. 0, U.S. Department of Energy, Richland Operations Office, Richland, Washington.

DOE. 2018a. *Hanford Site Groundwater Monitoring Report for 2017*. DOE/RL-2017-66, Rev. 0, U.S. Department of Energy, Richland Operations Office, Richland, Washington.

DOE. 2018b. *Calendar Year 2017 Annual Summary Report for Pump-and-Treat Operations in the Hanford Central Plateau Operable Units*. DOE/RL-2017-68, Rev. 0, U.S. Department of Energy, Richland Operations Office, Richland, Washington.

Davis JW and SS Madsen. 1991. The Biodegradation of Methylene Chloride In Soils. Environmental Toxicology and Chemistry 10:463-474.

Dybas MJ, GM Tatara, CS Criddle. 1995. Localization and characterization of the carbon tetrachloride transforming activity of Pseudomonas sp. strain KC. Appl. Environ. Microbiol. 61:758-62.

Dybas MF, M Barcelona, S Bezbordnikov, S Davics, L Forney, H Heuer, O Kawka, T Mayotte, L Sepulveda-Torres, K Smalla, M Sneathen, J Tiedje, T Voice, DC Wiggert, ME Witt, CS Criddle. 1998. Pilot-scale evaluation of bioaugmentation for in-situ remediation of a carbon tetrachloride contaminated aquifer. Environ. Sci. Technol. 32:3598-3611.

Egli C, S Stromeyer, AM Cook, T Leisinger. 1990. Transformation of tetra- and trichloromethane to CO2 by anaerobic bacteria is a non-enzymatic process. FEMS Microbiology Letters 68:207-212.

Egli C, T Tschan, R Scholtz, AM Cook, T Leisinger. 1988. Transformation of tetrachloromethane to dichloromethane and carbon dioxide by Acetobacterium woodii. Appl Environ Microbiol 54:2819-24.

El Aamrani S., J. Gimenez, M. Rovira, F. Seco, M. Grive, J. Bruno, L. Duro, J. de Pablo. 2007. A spectroscopic study of uranium (VI) interaction with magnetite. *Applied Surface Science*. 253: 8794-8797.

Elsner M., R.P. Schwarzenbach, and S.B. Haderlein. 2004. Reactivity of Fe(II)-bearing minerals toward reductive transformation of organic contaminants. *Environmental Science & Technology 38*, 799-807.

EPA. 1995. Superfund record of decision : Hanford 200-Area (USDOE) OU 200-ZP-1, Benton County, WA. EPA/ROD/R10-95/114, U.S. Envrironmental Protection Agency, Region 10, Seattle, Washington.

EPA. 2008 Record of Decision Hanford 200 Area 200-ZP-1 Superfund Site Benton County, Washington. HANFORD-200-ZP-1-ROD, U.S. Envrironmental Protection Agency, Region 10, Seattle, Washington.

Erbs, M., H.C.B. Hansen, and C.E. Olsen. 1999. Reductive dechlorination of carbon tetrachloride using iron(II) iron(III) hydroxide sulfate (green rust). *Environmental Science & Technology* 33: 307–311.

ESTCP. 2005. *Bioaugmentation for Remediation of Chlorinated Solvents: Technology Development, Status, and Research Needs*. DoD Environmental Security Technology Certification Program.

Evans JC, RW Bryce, DJ Bates, ML Kemner. 1990. *Hanford site groundwater surveillance for 1989*. PNL-7396.

Fathepure BZ, GA Youngers, DL Richter, and CE Downs. 1995. In Situ Bioremediation of Chlorinated Hydrocarbons under Field Aerobic-Anaerobic Environments. Bioremediation of Chlorinated Solvents, pp. 169-186.

Franzen MEL, JN Petersen, TP Clement, BS Hooker, RS Skeen. 1997. Pulsing of multiple nutrients as a strategy to achieve biologically active zones during in situ carbon tetrachloride remediation. Computational Geosciences 1:271-88.

Fredrickson J.K., J.M. Zachara, D.W. Kennedy, R.K. Kukkadapu, J.P. McKinley, S.M. Heald, C. Liu, A.E. Plymale. 2004. Reduction of TcO4- by sediment-associated biogenic Fe(II). *Geochimica et Cosmochimica Acta*. 68: 3171-3187.

Fredrickson JK, SW Li, FJ Brockman, DL Haldeman, PS Amy, DL Balkwill. 1995. Time-dependent changes in viable numbers and activities of aerobic heterotrophic bacteria in subsurface sediments. J Microbiol Methods 21:253-265.

Gälli R, T Leisinger. 1985. Specialized bacterial strains for the removal of dichloromethane from industrial waste. Conservation Recycling 8:91-100.

Grostern A, M Duhamel, S Dworatzek, EA Edwards. 2010. Chloroform respiration to dichloromethane by a Dehalobacter population. Environmental Microbiology 12:1053-60.

Hanoch, R.J., H. Shao, and E.C. Butler. 2006. Transformation of carbon tetrachloride by bisulfide treated goethite, hematite, magnetite, and kaolinite. *Chemosphere* 63: 323–334.

Hardy L, E Moeri, and MC Salvador. 1999. Rapid Intrinsic Degradation of Chlorinated Solvents at a Manufacturing Site in Brazil. Natural Attenuation of Chlorinated Solvents, Petroleum Hydrocarbons, and Other Organic Compounds. Fifth International In Situ and Onsite Bioremediation Symposium, pp. 19-28.

Hartman, M.J., L.E. Morasch, and W.D. Webber. 2000. *Hanford Site Groundwater Monitoring for Fiscal Year 1999*. PNNL-13116, Pacific Northwest National Laboratory, Richland, Washington.

Hartman, M.J., L.E. Morasch, and W.D. Webber. 2006. *Hanford Site Groundwater Monitoring for Fiscal Year 2005*. PNNL-15670, Pacific Northwest National Laboratory, Richland, Washington.

He, Y.T., J.T. Wilson, and R.T. Wilkin. 2008. Transformation of reactive iron minerals in a permeable reactive barrier (biowall) used to treat TCE in groundwater. *Environmental Science & Technology* 42: 6690–6696.

He, Y.T., J.T. Wilson, C. Su, and R.T. Wilkin. 2015. Review of Abiotic degradation of chlorinated solvents by reactive iron minerals in aquifer. *Groundwater Monitoring&Remediation*. 35: 57-75.

Holliger, C., C. Regeard, and G. Diekert. 2003, Dehalogenation by anaerobic bacteria. In *dehalogenation: Microbial Processes and Environmental Applications*, ed. M.M. Häggblom and I.D. Bossert, 115–157. Boston: Kluwer Academic Publishers.

Hooker BS, R Skeen, and J Petersen. 1994. Biological destruction of CCI4: II. Kinetic modeling. Biotechnology and Bioengineering. 44. 211 - 218.

Hooker B, RS Skeen, MJ Truex, DB Anderson. 1998. In situ bioremediation of carbon tetrachloride: Field test results. Bioremediation J 1:181-93.

Innovative Treatment Remediation Demonstration Program. 2000. Literature Review: “Natural Attenuation Mechanisms and Rates for Chloromethane Subsurface Contamination at Hanford,” Hanford Carbon Tetrachloride Project. http://hanford-site.pnl.gov/groundwater/reports/PNNL_13560.pdf.

Interstate Technology and Regulatory Council. 2002. “A Systematic Approach to In Situ Bioremediation in Groundwater Including Decision Trees for In Situ Bioremediation of Nitrates, Carbon Tetrachloride, and Perchlorate,” http://www.itrcweb.org/common/ content.asp?en=TA301724&sea=Yes&set=Both&sca=Yes&sct=Long.

Kendelewicz T., P. Liu, C.S. Doyle, and G.E. Brown. 2000. Spectroscopic study of the reaction of aqueous Cr(VI) with Fe_3O_4 (111) surfaces. *Surface Science* 469: 144-163.

Kenneke, J.F. and E.J. Webber. 2003. Reductive dehalogenation of halomethanes in iron- and sulfate-reducing sediments, 1. Reactivity pattern analysis. *Environmental Science & Technology* 37: 713–720.

Kieft TL, PS Amy, FJ Brockman, JK Fredrickson, BN Bjornstad, LL Rosacker. 1993. Microbial abundance and activities in relation to water potential in the vadose zones of arid and semiarid sites.

Koegler SS, TM Brouns, W Heath, and RJ Hicks. 1989. Biodenitrification of Hanford groundwater and process effluents: FY 1988 status report. PNL-6917.

Kriegman-King, M.R., and M. Reinhard. 1992. Transformation of carbon tetrachloride in the presence of sulfide, biotite, and vermiculite. *Environmental Science & Technology* 26: 2198–2206.

Kriegman-King, M.R., and M. Reinhard. 1994. Transformation of carbon tetrachloride by pyrite in aqueous solution. *Environmental Science and Technology* 28: 692–700.

Krone UE, RK Thauer. 1989. Reductive dehalogenation of chlorinated C1-hydrocarbons mediated by corrinoids. Biochemistry 28:4908-4914.

Krone UE, K Laufer, RK Thauer, HP Hogenkamp. 1989a. Coenzyme F430 as a possible catalyst for the reductive dehalogenation of chlorinated C1 hydrocarbons in methanogenic bacteria. Biochemistry 28:10061-5.

Kuder, T., B.M. van Breukelen, M. Vanderford, and P. Philp. 2013. 3D-CSIA: Carbon, Chlorine, and Hydrogen Isotope Fractionation in Transformation of TCE to Ethene by a Dehalococcoides Culture. *Environmental Science & Technology* 47 no. 17: 9668-9677.

Last GV, RJ Lenhard, BN Bjornstad, JC Evans, KR Roberson, FA Spane, JE Amonette, ML Rockhold. 1991. Characteristics of the volatile compounds – Arid Integrated Demonstration Site. PNL-7866.

Last GV and VJ Rohay. 1991. Carbon tetrachloride contamination, 200 West Area, Hanford Site: arid site integrated demonstration for remediation of volatile organic compounds. PNL-SA-19564.

Lee BD, JW Morad, DL Saunders, KC Johnson. 2017. Letterr Report: Analysis of injection well samples for biofouling constituents. PNNL-27082.

Lee CH, TA Lewis A Paszczynski, RL Crawford. 1999. Identification of an extracellular catalyst of carbon tetrachloride dehalogenation from Pseudomonas stutzeri strain KC as pyridine-2,6-bis(thiocarboxylate). Biochem Biophys Res Comm. 261:562-6

Lee MD, PF Mazierski, RJ Buchanan Jr, DE Ellis, and LS Sehayek. 1995. Intrinsic In Situ Anaerobic Biodegradation of Chlorinated Solvents at an Industrial Landfill. Intrinsic Bioremediation, pp. 205-222.

Lee, W., and B. Batchelor. 2002a. Abiotic reductive dechlorination of chlorinated ethylenes by iron-bearing soil minerals. 1. Pyrite and magnetite. *Environmental Science &Technology* 36: 5147–5154.

Leisinger T, R Bader, R Hermann, M Schmid-Appert, S Vuilleumier. 1994. Microbes, enzymes and genes involved in dichloromethane utilization. Biodegradation 5:237-48.

Liang LN and D Grbic-Galic. 1993. Biotransformation of Chlorinated Aliphatic Solvents in the Presence of Aromatic Compounds under Methanogenic Conditions. Environmental Toxicology and Chemistry. 12:1377-1393.

Liang, X., and E.C. Butler. 2010. Effect of natural organic matter model compounds on the transformation of carbon tetrachloride by chloride green rust. *Water Research* 44: 2125–2132

Lipczynska-Kochany, E., S. Harms, and N. Nadarajah. 1994. Degradation of carbon tetrachloride in the presence of iron and sulphur containing compounds. *Chemosphere* 29: 1477–1489.

Mabey W, T Mill. 1978. Critical review of hydrolysis of organic compounds in water under environmental conditions. J. Phys. Chem. Ref. Data 7:383-415.

Maithreepala, R.A., and R.A. Doong. 2005. Enhanced de chlorination of chlorinated methanes and ethenes by chloride green rust in the presence of copper. *Environmental Science & Technology* 39: 4082–4090.

Matthews SM, AJ Boegel, RA Caufield, MC Jovanovich, JA Loftis. 1993. Radiolytic decomposition of environmental contaminants using an electron accelerator. UCRL-JC-113510.

McCarty PL, Reinhard M. 1993. Biological and chemical transformations of halogenated aliphatic compounds in aquatic and terrestrial environments. In: The Biogeochemistry of Global Change: Radiative Trace Gases. Oremland,RS (ed). Chapman & Hall: New York, NY. pp. 839-852.

McCarty PL, L Semprini. 1994. Ground water treatment for chlorinated solvents. In: JE Matthews (ed) Handbook of Bioremediation. Lewis Publishers, London pp. 87-116.

McCormick, M.L., E.J. Bouwer, and P. Adriaens. 2002. Carbon Tetrachloride Transformation in a Model Iron-Reducing Culture: Relative Kinetics of Biotic and Abiotic Reactions. *Environmental Science & Technology* 36 no. 3: 403-410.

McCormick, M.L., and P. Adriaens. 2004. Carbon tetrachloride transformation on the surface of nanoscale biogenic magnetite particles. *Environmental Science & Technology* 38: 1045–1053.

McKinley J. P., J.M. Zachara, J. Wan, D.E. McCready, and S.M. Heald. 2007. Geochemical controls on contaminant uranium in vadose Hanford formation sediments at the 200 Area and 300 Area, Hanford Site, Washington. *Vadose Zone Journal*. 6, 1004–1017.

McQuillan DM, BH Faris, and BH Swanson. 1998. Intrinsic Cometabolism of Carbon Tetrachloride with Gasoline: Regulatory Site-Closure. Natural Attenuation: Chlorinated and Recalcitrant Compounds, the First International Conference on Remediation of Chlorinated and Recalcitrant Compounds, pp. 263-268.

Mechaber RA, BY Su, and E Cox. 1998. Intrinsic Bioremediation of Chlorinated and Non-Chlorinated VOCS at a RCRA Landfill. Natural Attenuation: Chlorinated and Recalcitrant Compounds, the First International Conference on Remediation of Chlorinated and Recalcitrant Compounds, pp. 275-280.

Mehran M and JL Wolf Jr. 1999. Natural Attenuation of Methylene Chloride in Ground Water. Natural Attenuation of Chlorinated Solvents, Petroleum Hydrocarbons, and Other Organic Compounds. Fifth International In Situ and Onsite Bioremediation Symposium, pp. 13-18.

Missana T., C. Maffiotte, M. Garcia-Gutierrez. 2003. Surface reactions kinetics between nanocrystalline magnetite and uranyl. *Journal of Colloid and Interface Science*. 261: 154-160.

Moir JWB, NJ Wood. 2001. Nitrate and nitrite transport in bacteria. CMLS Cellular and Molecular Life Sciences 58:215-224.

Nielsen PH, PE Holm, and TH Christensen. 1992. A Field Method for Determination of Groundwater and Groundwater-Sediment Associated Potentials for Degradation of Xenobiotic Organic Compounds. Chemosphere. 25(4):449-462.

Niemet MR, L Semprini. 2005. Column studies of anaerobic carbon tetrachloride biotransformation with Hanford aquifer material. Groundwater Monitoring & Remediation 25:82-82.

Nikolausz, M., I. Nijenhuis, K. Ziller, H.-H. Richnow, and M. Kästner. 2006. Stable carbon isotope fractionation during degradation of dichloromethane by methylotrophic bacteria. *Environmental Microbiology* 8 no. 1: 156-164.

O'Loughlin, E.J., K.M. Kemner, and D.R. Burris. 2003. Effects of Ag, Au and Cu on the reductive dechlorination of carbon tetrachloride by green rust. *Environmental Science & Technology* 37: 2905–2912.

Passeport E, R Landis, G Lacrampe-Couloume, EJ Lutz, EE Mack, K West, S Morgan, BS Lollar. 2016. Sediment monitoring natural recovery evidenced by compound specific isotopic analysis and high-resolution pore water sampling. *Environ Sci & Technol* 50:12197-204

Passeport E, R Landis, SOC Mundle, K Chu, EE Mack, E Lutz, BS Lollar. 2014. Diffusion sampler for compound specific carbon isotope analysis of dissolved hydrocarbon contaminants. *Environ. Sci & Technol* 48:9582-90

Pearce, C.I., J. Liu, D.R. Baer, O. Qafoku, S.M. Heald, E. Arenholz, A.E. Grosz, J.P. McKinley, C.T. Resch, M.E. Bowden, M.H. Engelhard, and K.M. Rosso. 2014. "Characterization of Natural Titanomagnetites ($Fe_{3-x}Ti_xO_4$) for Studying Heterogeneous Electron Transfer to Tc(VII) in the Hanford Subsurface." *Geochimica et Cosmochimica Acta*, 128:114-127.

Pecher, K., S.B. Haderlein and R.P. Schwarzenbach. 2002. Reduction of polyhalogenated methanes by surface-bound Fe(II) in aqueous suspensions of iron oxides. *Environmental Science & Technology* 36: 1734-1741.

Penny C, S Vuilleumier, F Bringel. 2010. Microbial degradation of tetrachloromethane: mechanisms and perspectives for bioremediation. FEMS Microbiol. Rev. 74:257-75.

Peretyazhko T.S., J.M. Zachara, R.K. Kukkadapu, S.M. Heald., I.V. Kutnyakov, C.T. Resch, B.W. Arey, C.M. Wang, L. Kovarik, J.L. Phillips, and D.A. Moore. 2012. Pertechnetate (TcO_4^-) reduction by reactive ferrous iron forms in naturally anoxic, redox transition zone sediments from the Hanford Site, USA. *Geochimica et Cosmochimica Acta* 92, 48–66.

Petersen JN, RS Skeen, KM Amos, BS Hooker. 1994. Biological destruction of CCl4: I. Experimental design and data. Biotechnology & Bioengineering 43:521-8

Petrovskis EA, TM Vogel, P Adriaens. 1994. Effects of electron acceptors and donors on transformation of tetrachloromethane by Shewanella putrefaciens MR-1. FEMS Microbiol Lett 121:357-63.

Peyton B. 1996. Improved biomass distribution using pulsed injections of electron donor and acceptor. Wat. Res. 30:756-58.

Phanikumar MS, DW Hyndman, DC Wiggert, MJ Dybas, ME Witts, CS Criddle. 2002. Simulation of microbial transport and carbon tetrachloride biodegradation in intermittently-fed aquifer columns. Water Resources Research doi:10.1029/2001WR000289

Picardal FW, RG Arnold, H Couch, AM Little, ME Smith. 1993. Involvement of cytochromes in the anaerobic biotransformation of tetrachloromethane by Shewanella putrefaciens 200. Appl Environ Microbiol 59:3763-70.

Powell, B. A., R.A. Fjeld, D.I. Kaplan, J.T. Coates, S.M. Serkiz. 2004. $Pu(V)O_2^+$ interactions with synthetic magnetite (Fe_3O_4). *Environmental Science & Technology 38*, 6016-6024.

Powell B.A., R.A. Fjeld, D.I. Kaplan, J.T. Coates, and S.M. Serkiz. 2005. $Pu(V)O_2^+$ adsorption and reduction by synthetic hematite and goethite. *Environmental Science & Technology 39*, 2107-2114.

Qafoku NP, C Bagwell, AR Lawter, MJ Truex, JE Szecsody, O Qafoku, L Kovarik, L Zhong, A Mitroshkov, V Freedman. 2018. Conceptual model of subsurface processes for iodine at the Hanford site. PNNL-28053; DVZ-RPT-0004 Rev 1.0

Riley RG, DS Sklarew, CF Brown, PM Gent, JE Szecsody, AV Mitroshkov, CJ Thompson. 2005. Carbon tetrachloride and chloroform partition coefficients derived from aqueous desorption of contaminated Hanford sediments. PNNL-15239.

Rodríguez-Fernández, D., M. Rosell, C. Domènech, C. Torrentó, J. Palau, and A. Soler. 2015. C and Cl-CSIA for Elucidating Chlorinated Methanes Biotic and Abiotic Degradation at a Polluted Bedrock Aquifer. *Procedia Earth and Planetary Science* 13: 120-123.

Ruf HH, H Ahr, W Nastainczyk, V Ulrich, D Mansuy, JP Battioni, R Montiel-Montoya, A Trautwein. 1984. Formation of a Ferric Carbanion Complex from Halothane and Cytochrome P-450: Electron Spin Resonance, Electronic Spectra, and Model Complexes. Biochemistry 23: 5300-5306.

Rügge K, PL Bjerg, TH Christensen. 1995. Distribution of organic compounds from municipal solid waste in the groundwater downgradient of a landfill (Grindsted, Denmark). Environ. Sci. Technol. 29:1395-1400.

Schullehner J, L Stayner, B Hansen. 2017. Nitrate, nitrite, and ammonium variability in drinking water distribution systems. International Journal of Environmental Research and Public Health. 14:276, doi:10.3390/ijerph14030276

Scott T. B., G.C. Allen, P.J. Heard, and M.G. Randell. 2003. Reduction of U(VI) to U(IV) on the surface of magnetite. *Geochimica et Cosmochimica Acta* 69: 5639–5646.

Semprini L, GD Hopkins, DB Janssen, M Lang, PV Roberts, PL McCarty. 1991. In-situ biotransformation of carbon tetrachloride under anoxic conditions. EPA/600/2-90/060. Environmental Protection Agency, Ada, OK.

Semprini L, GD Hopkins, PL McCarty, PV Roberts. 1992. In situ transformation of carbon tetrachloride and other halogenated compounds resulting from biostimulation under anoxic conditions. Environ. Sci. Technol. 26: 2454-2461.

Sherwood JL, J Petersen, RS Skeen. 1998. Biodegradation of 1,1,1-trichloroethane by a carbon tetrachloride-degrading denitrifying consortium. Biotechnology and Bioengineering. 59:393-99.

Sherwood JL, JN Petersen, RS Skeen, NB Valentine. 1996. Effects on nitrate and acetate availability on chloroform production during carbon tetrachloride destruction. Biotechnology & Bioengineering 51:551-7.

Skeen RS, KM Amos, JN Petersen. 1994. Influence of nitrate concentration on carbon tetrachloride transformation by a denitrifying microbial consortium. Wat. Res. 28:2433-38

Skeen RS, KR Roberson, DJ Workman, JN Petersen, M Shouche. 1992. In situ bioremediation of Hanford groundwater. PNNL-SA-20550

Smith RA, AL Teel, RJ Watts. 2004. Identification of the reactive oxygen species responsible for carbon tetrachloride degradation in modified Fenton's systems. Environ. Sci. Technol. 38:5465-69.

Streile GP et al., 1991. Intermediate-scale subsurface transport of co-contaminants, PNL Annual Report for 1990 to the DOE Office of Energy Research – Part 2: Environmental Sciences. PNL-7600.

Swanson LC, VJ Rohay, JM Faurote. 1999. Hydrogeologic conceptual model for the carbon tetrachloride and uranium/technetium plumes in the 200 West Area: 1994 through 1999 Update. BHI-01311, Bechtel Hanford, Inc, Richland WA.

Szecsody, J.E., J.S. Fruchter, M.D. Williams, V.R. Vermeul, and D. Sklarew. 2004. In situ chemical reduction of aquifer sediments: enhancement of reactive iron phases and TCE dechlorination. *Environmental Science & Technology* 38: 4656–4663.

Szecsody J.E., D Jansik, J.P. McKinley, and N. Hess. 2014. "Influence of alkaline waste on technetium mobility in Hanford formation sediments." *Journal of Environmental Radioactivity* 135:147-160.

Szecsody JE, MJ Truex, BD Lee, CE Strickland, JJ Moran, MM Snyder, CT Resch, AR Lawter, L Zhong, BN Gartman, DL Saunders, SR Baum II Leavy, JA Horner, BD Williams, BB Christiansen, EM McElroy, MK Nims, RE Clayton, D Appriou. 2017. Geochemical, microbial, and physical characterization of 200-DV-1 operable unit B-complex cores from boreholes C9552, C9487, and C9488 on the Hanford site central plateau. PNNL-26266.

Tamara M.L., E.C. Butler. 2004. Effects of Iron Purity and Groundwater Characteristics on Rates and Products in the Degradation of Carbon Tetrachloride by Iron Metal. Environmental Science & Technology 38:1866–1876. doi: 10.1021/es0305508.

Tang, S., and E.A. Edwards. 2013. Identification of Dehalobacter reductive dehalogenases that catalyse dechlorination of chloroform, 1,1,1-trichloroethane and 1,1-dichloroethane. *Philosophical Transactions of the Royal Society B: Biological Sciences* 368 no. 1616.

Tfaily MM, JE Kyle, RK Chu, JG Toyoda, EH Denis, DL Saunders, EA Cordova, MJ Truex, JE Szecsody B Lee, NP Qafoku. (In Prep) Organic matter composition of sediment and pore water at Hanford: Implications for iodine (and other contaminants) speciation and mobility.

Thomle JN, BD Lee, GL Dai, MJ Truex. 2017. 200 West Pump & Treat facility biofouling assessment. PNNL-26783 Rev 0.0

Tobiszewski, M., and J. Namiesnik. 2012. Abiotic degradation of chlorinated ethanes and ethenes in water. *Environmental Science Pollution Research* 19: 1994–2006.

Truex MJ, BS Hooker, and DB Anderson. 1996. Accelerated in situ bioremediation of groundwater. Innovative Technology Summary Report. PNNL-11313.

Truex MJ, CD Johnson, DR Newcomer, LA Doremus, BS Hooker, BM Peyton, RS Skeen, A Chilakapati. 1994. Deploying in situ bioremediation at the Hanford site. PNL-SA-24280

Truex MJ, CJ Murray, CR Cole, RJ Cameron, MD Johnson, RS Skeen, CD Johnson. 2001. Assessment of carbon tetrachloride groundwater transport in support of the Hanford carbon tetrachloride innovative technology demonstration program. PNNL-13560

Truex MJ, CJ Newell, BB Looney, K Vangelas. 2006. Scenarios Evaluation Tool for Chlorinated Solvent Monitored Natural Attenuation. WSRC-STI-2006-00096, Washington Savannah River Company, Aiken, SC, USA.

Truex MJ, D Johnson, DC Newcomer, L Doremus, BS Hooker, B Peyton, RS Skeen, and A Chilakapati. 1994. Deploying in situ bioremediation at the Hanford Site. PNL-SA-24280

Truex M.J., J.E. Szecsody, N. Qafoku, C.E. Strickland, J.J. Moran, B.D. Lee, and M. Snyder. 2017. *Contaminant attenuation and transport characterization of 200-DV-1 operable unit sediment samples*. PNNL-26208, RPT-DVZ-AFRI-037. Pacific Northwest National Laboratory, Richland, WA.

USEPA. 2009. Identification and characterization methods f or reactive minerals responsible for natural attenuation of chlorinated organic compounds in ground water, EPA600-R09/115.

Van Beelen P and F Van Keulen. 1990. The Kinetics of the Degradation of Chloroform and Benzene in Anaerobic Sediment from the River Rhine. Hydrobiol. Bull. 24(1):13-21.

van Eekert M.H.A, T.J. Schroder, A.J.M. Stams, G. Schraa, and J.A. Field. 1998. Degradation and fate of carbon tetrachloride in unadapted methanogenic granular sludge. *Applied Environmental Microbiology* 64: 2350–2356.

VanStone, N., M. Elsner, G. Lacrampe-Couloume, S. Mabury, and B. Sherwood Lollar. 2008. Potential for Identifying Abiotic Chloroalkane Degradation Mechanisms using Carbon Isotopic Fractionation. *Environmental Science & Technology* 42 no. 1: 126-132.

Vikesland, P.J., A.M. Heathcock, R.L. Rebodos, and K.E. Makus. 2007. Particle size and aggregation effects on magnetite reactivity toward carbon tetrachloride. *Environmental Science & Technology* 41: 5277–5283.

WHC. 1994. *Groundwater Maps of the Hanford Site, June 1993*. WHC-EP-0394-7, Westinghouse Hanford Company, Richland, Washington.

WHC. 1996. *Groundwater Maps of the Hanford Site, June 1995*. WHC-EP-0394-11, Westinghouse Hanford Company, Richland, Washington.

Wood JM, FS Kennedy, RS Wolfe. 1968. The reaction of multihalogenated hydrocarbons with free and bound reduced vitamin B_{12}. Biochemistry 7:1707-1713.

Xie Y, C. Murray, G. Last, and R. Mackley. 2003. *Mineralogical and Bulk-Rock Geochemical Signatures of Ringold and Hanford Formation Sediments*. PNNL-14202, Pacific Northwest National Laboratory, Richland, Washington.

Xu C, DI Kaplan, S Zhang, M Athon, Y-F Ho, H-P Li, CM Yeager, KA Schwehr, R Grandbois, D Wellman, PH Santschi. 2015. Radioiodine sorption/desorption and speciation transformation by subsurface sediments from the Hanford Site. J Environ Radio 139:43-55.

Zwank, L., M. Elsner, A. Aeberhard, R.P. Schwarzenbach, and S.B. Haderlein. 2005. Carbon Isotope Fractionation in the Reductive Dehalogenation of Carbon Tetrachloride at Iron (Hydr)Oxide and Iron Sulfide Minerals. *Environmental Science & Technology* 39 no. 15: 5634-5641.

Appendix A – Synopsis of Pump-and-Treat Systems in the 200 West Area

There are three regimes that are relevant to the recent history of groundwater flow in the vicinity of the 200 West Area: 1) the time period prior to active groundwater remediation, 2) the time period for the Interim Remedial Action (IRA), and 3) the present time period for the remedial action specified in the final Record of Decision (ROD). Summary descriptions of each of these regimes are provided in the following sub-sections. Additional details on the wells used for pump-and-treat (P&T) and timeframes for pumping can be found in the cited reports and related documents. The information described in this Appendix provides the basis for identifying zones potentially impacted by P&T, and thus which wells outside those zones may be suitable for analyzing groundwater chemistry data.

A.1 Time Period Prior to P&T

Prior to operation of 200 West Area IRA P&T systems in 1994, groundwater flow in the 200 West Area was a function of the natural gradient plus the influence of artificial recharge stemming from historical practices. Figure A.1 depicts the water table hydraulic head contours for June 1993. Groundwater flow across the broader area was generally towards the east, though the geology of the area resulted in northerly flow near the northern portion of the 200 West Area. The unconfined aquifer in most of the 200 West Area is underlain by the Ringold Lower Mud (RLM) unit, which, where present, acts as a locally confining unit. However, this unit is absent in the northeastern portion of the 200 West Area, so the unconfined aquifer extends to the top of the basalt in that vicinity. The outcrop of Gable Butte basalt also constrains groundwater flow north of the 200 West Area. Additionally, the water table mound in the vicinity of the Plutonium Finishing Plant (PFP; also referred to as Z Plant) impacted the directions of the groundwater gradient in the southern and central portions of the 200 West Area.

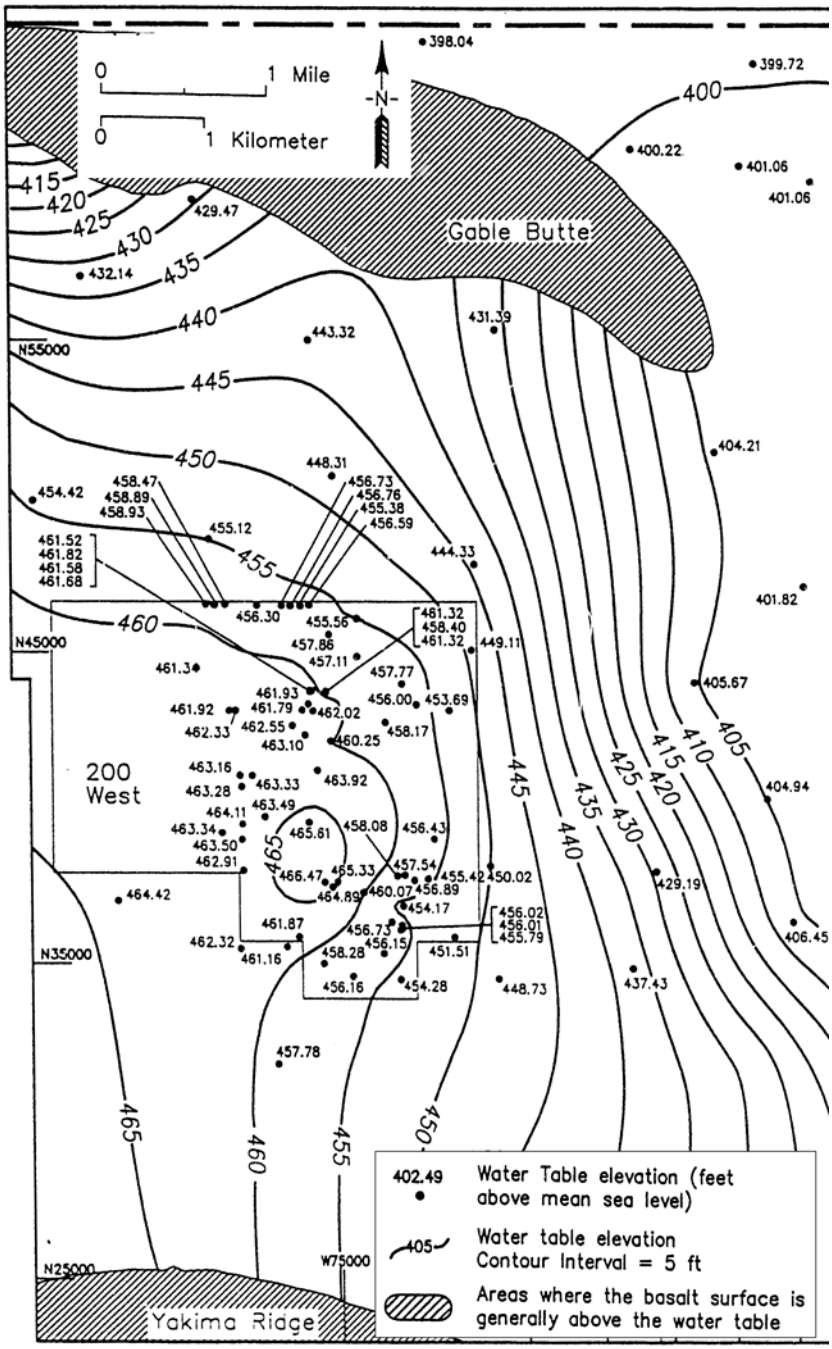

Figure A.1. June 1993 water level contours for the unconfined aquifer (adapted from WHC, 1994).

A.2 Interim P&T Period

In the mid-1990s, P&T was implemented as an IRA, sometimes referred to as an Interim Remedial Measure (IRM), for the 200-ZP-1 and 200-UP-1 OUs. Later, beginning in 2007, another IRA P&T system was operated for Waste Management Area (WMA) T. The 200-ZP-1 OU IRA P&T system was the largest, both in terms of spatial extent and flow rates, and thus had the largest impact on hydraulic conditions in the unconfined aquifer. The 200-UP-1 OU and WMA T IRA P&T systems operated with only a few wells at much lower total flow rates. The nature of these IRA P&T systems and the wells

involved are described below. For the 200-ZP-1 OU IRA P&T system, the impact of extraction and injection on water table elevations is also discussed.

A.2.1 200-ZP-1 OU IRA P&T System

The 200-ZP-1 OU IRA P&T system was operated for the purpose of minimizing further migration of carbon tetrachloride, chloroform, and TCE in the 200 West Area groundwater away from the vicinity of the 216-Z cribs/trenches and the PFP, in accordance with the 1995 200-ZP-1 OU ROD (EPA, 1995). The 200-ZP-1 OU IRA P&T system started in March 1994 [Hartman et al., 2006; HANFORD-200-ZP-1-ROD, 2008; DOE/RL-2008-78, 2009; DOE/RL-2010-105, 2011], though some references cite a 1996 start year [Hartman et al., 2006; ROD 200-UP-1, 2012; DOE/RL-2012-03, 2012; DOE/RL-2012-36, 2012].

The 200-ZP-1 OU IRA P&T system initially consisted of wells in the vicinity of the Plutonium Finishing Plant (PFP), but was later expanded northwards as new characterization information became available. By July 2005 (Figure A.2), existing wells 299-W15-765, 299-W15-40, 299-W15-43, and 299-W15-44 had been converted to extraction wells and made operational, adding to wells 299-W15-45 and 299-W15-47 brought online in fiscal year (FY) 2004 and the other wells in the system: 299-W15-34, 299-W15-35, 299-W15-32, 299-W15-36, 299-W15-29, 299-W18-36, and 299-W18-37 (with the latter three wells being injection wells). The 200-ZP-1 OU IRA P&T system was further expanded by adding additional extraction wells between FY 2005 and FY 2008, having 14 extraction wells and 5 injection wells in FY 2008 (Figure A.3) [DOE/RL-2008-78, 2009]. In 2012, at the end of operations for the 200-ZP-1 OU IRA P&T system (deactivated in May 2012), 14 extraction wells were part of the system (Figure A.4). However, four extraction wells were offline due to low water levels (299-W15-6, 299-W15-36, 299-W15-40, and 299-W15-765) and well 299-W15-47 was offline due to a failed pump [DOE/RL-2012-36, 2012]. Most of the extraction wells (except 299-W15-225) had screen lengths between 10.7 and 18.2 meters and thus did not penetrate the full aquifer.

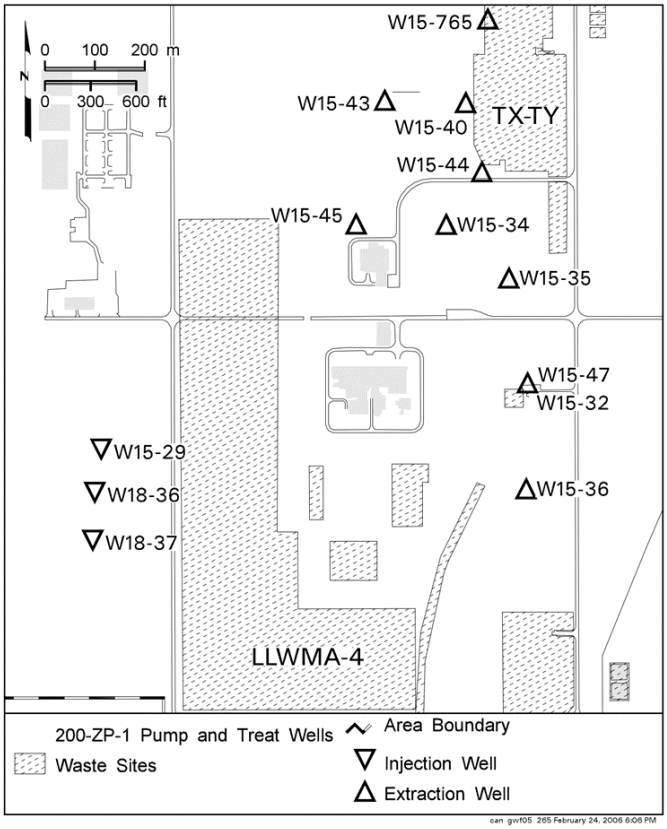

Figure A.2. 200-ZP-1 OU IRA P&T system, as of FY 2005 (Hartman et al., 2006).

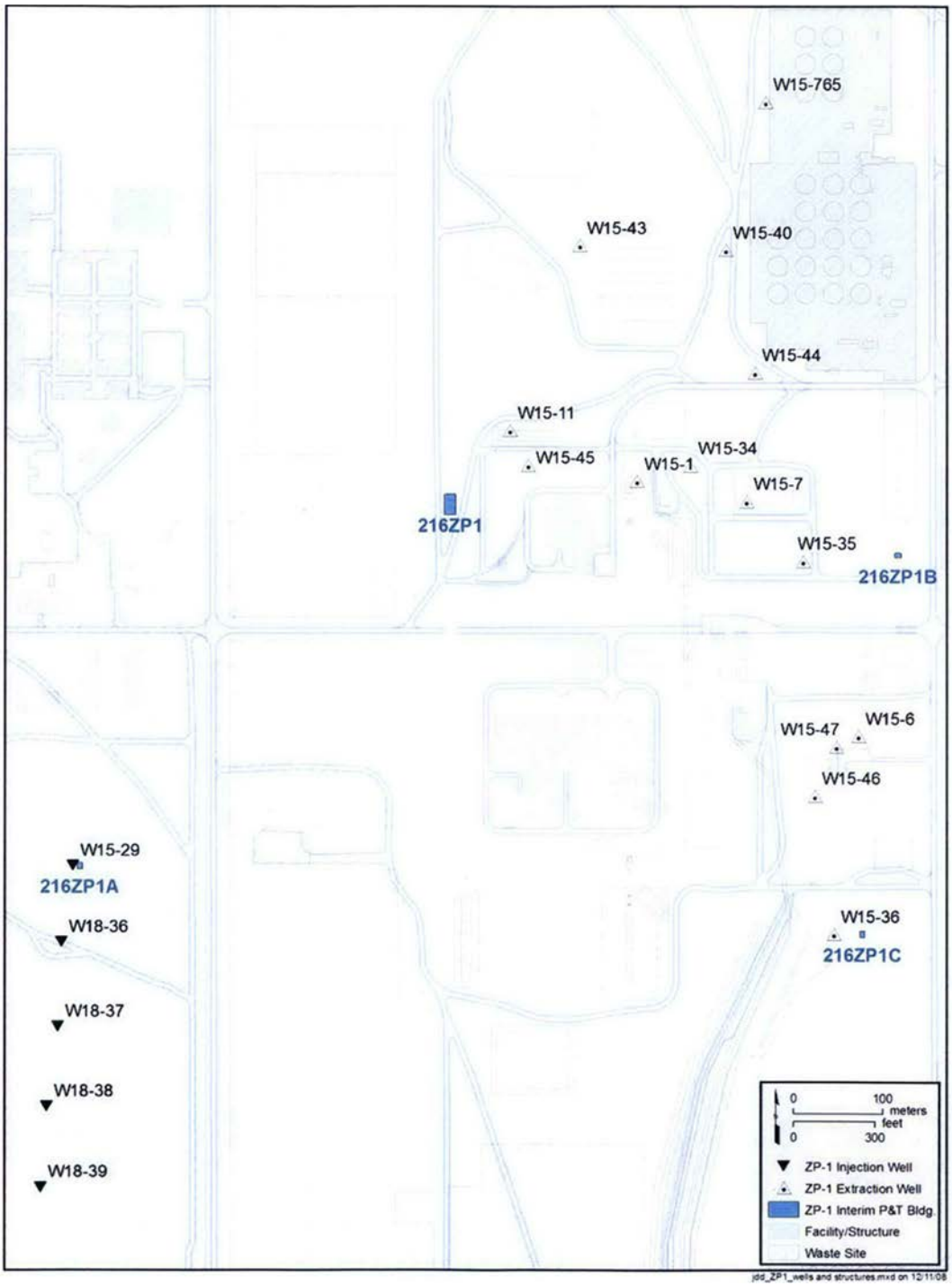

Figure A.3. 200-ZP-1 OU IRA P&T system, as of FY 2008 [DOE/RL-2008-78, 2009].

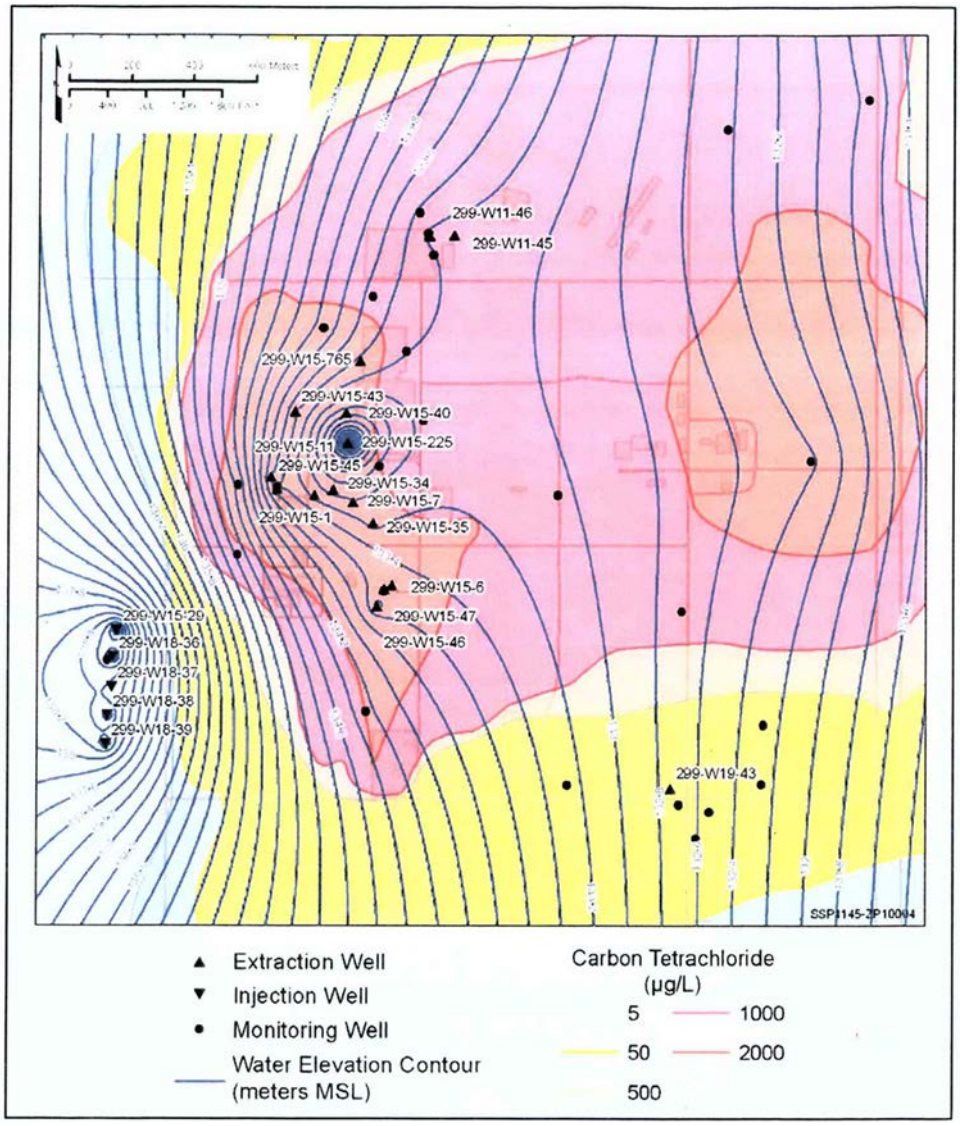

Figure A.4. 200-ZP-1 OU IRA P&T system, as of 2012, and water table elevation contours [DOE/RL-2012-03, 2012].

The 200-ZP-1 OU IRA P&T system influenced groundwater flow directions nominally in the central portion of the 200 West Area. But this area (and the ability to pump from some wells) was also subject to changes as the water table mound created by historical artificial recharge slowly dissipated. June 1995 water table contours (Figure A.5) lack details that could reflect the influence of pumping, but are broadly consistent with the 1993 contours (Figure A.1) and show a groundwater mound in the 200 West Area and east and northerly flow directions. Water level contours for 1999 (Figure A.6), 2005 (Figure A.7), and 2012 (Figure A.4) show more details of the impact of the 200-ZP-1 OU IRA P&T system (and the smaller influences of the 200-UP-1 OU and WMA T IRA P&T systems) on water level contours and flow directions.

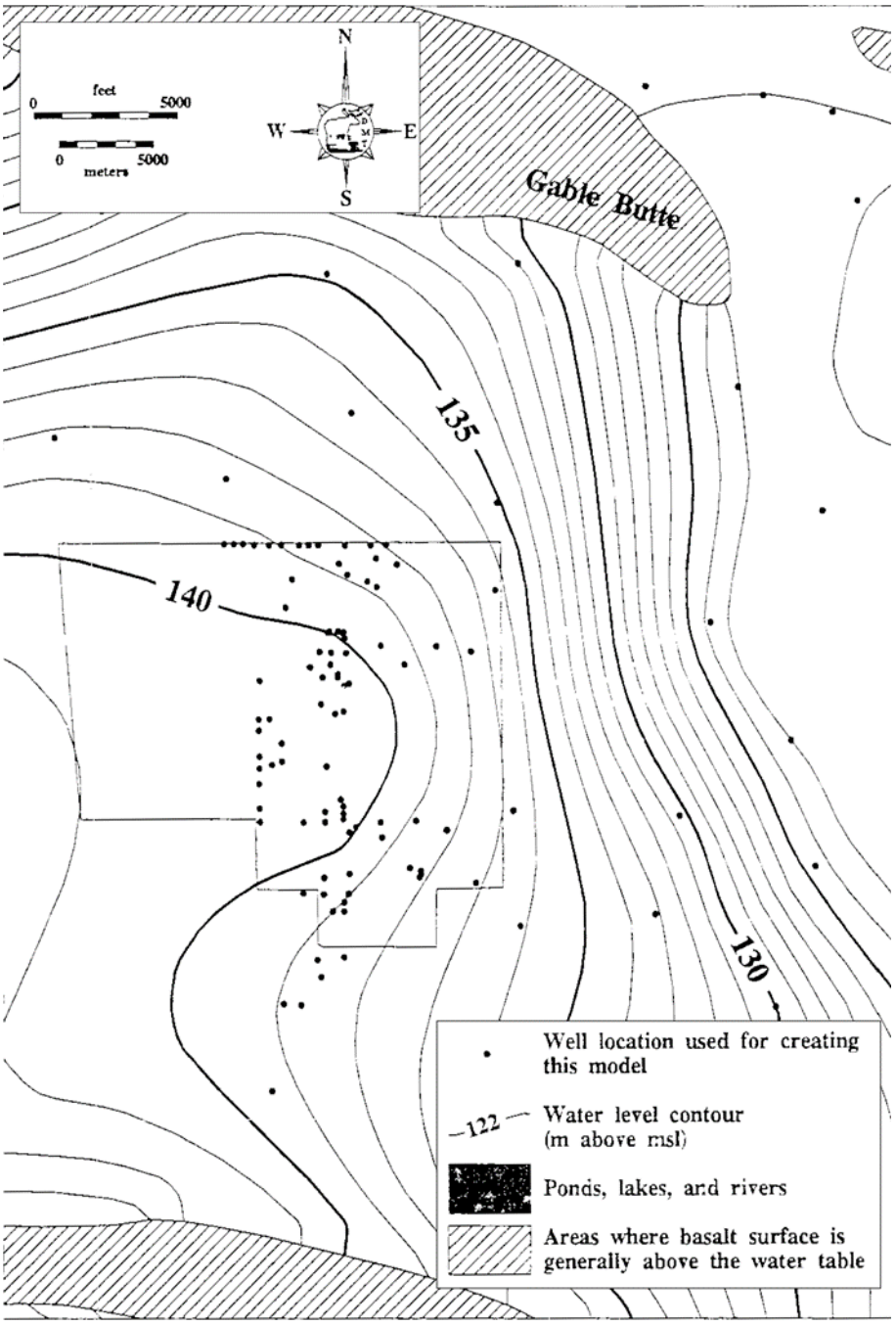

Figure A.5. June 1995 water level contours for the unconfined aquifer (adapted from WHC, 1996).

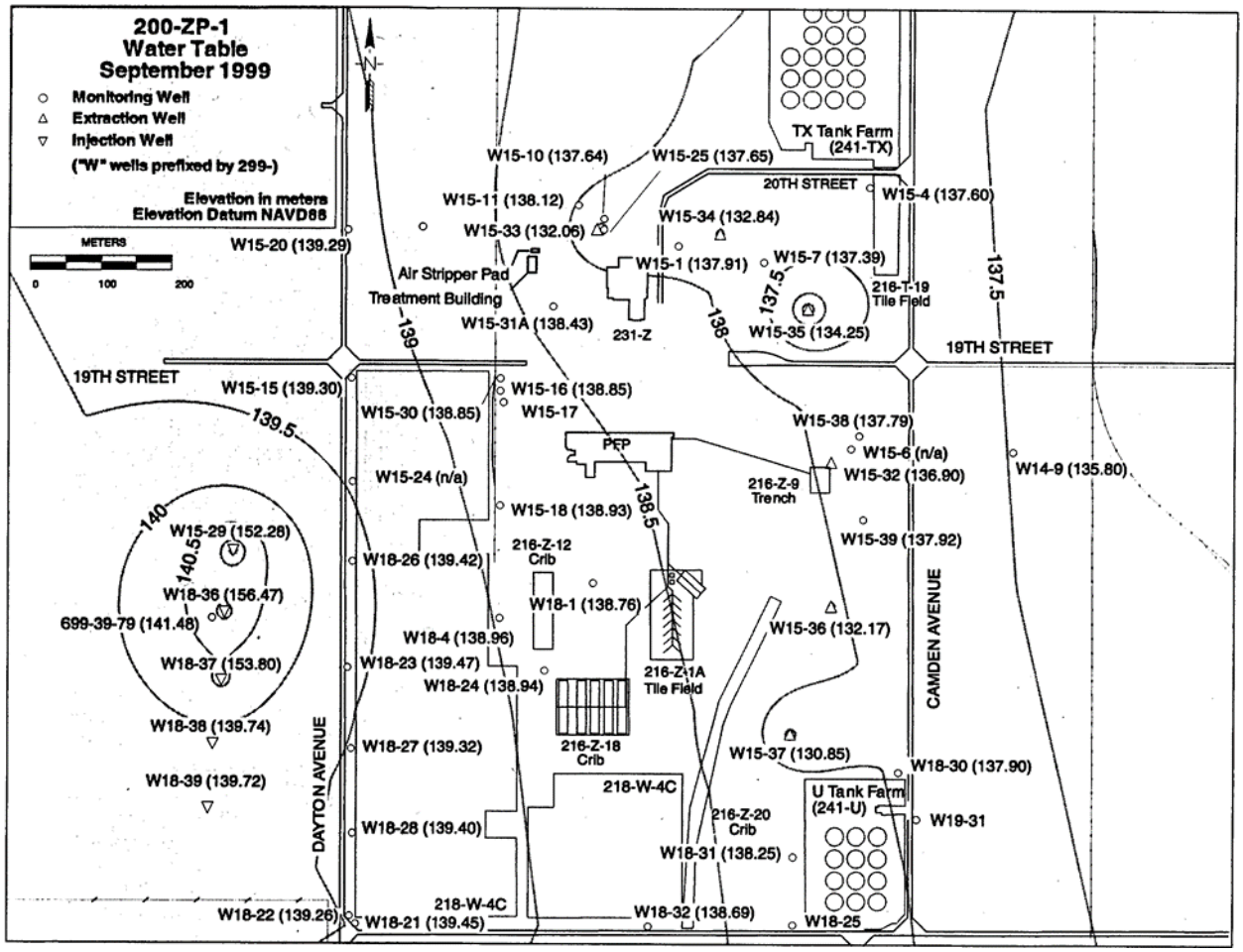

Figure A.6. September 1999 water level contours for the unconfined aquifer (Hartman et al., 2000).

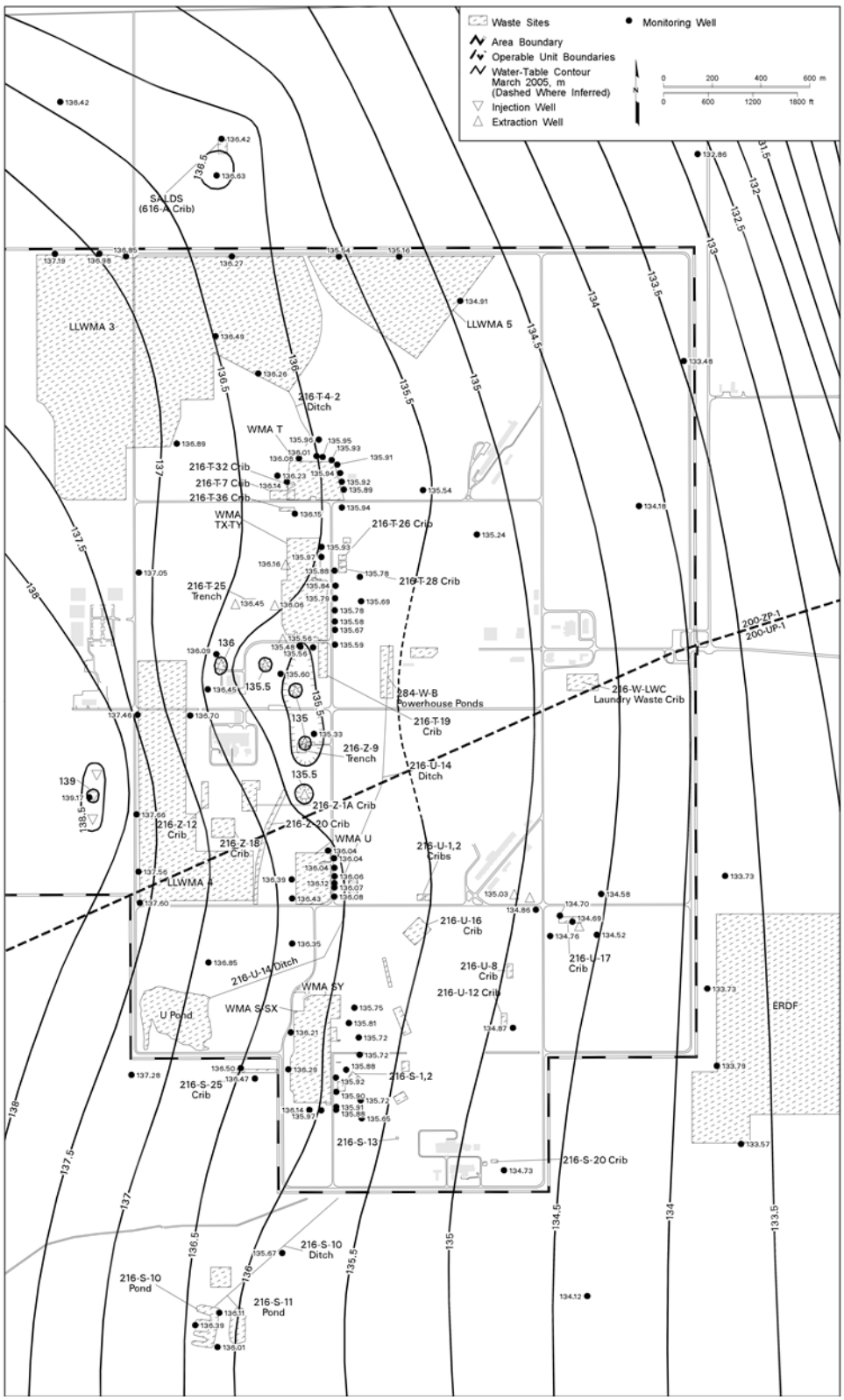

Figure A.7. March 2005 water level contours for the unconfined aquifer (Hartman et al., 2006).

The *200 West Area 200-ZP-1 Pump-and-Treat Remedial Design/Remedial Action Work Plan* [DOE/RL-2008-78, 2009] provides the following description of the 200 West Area groundwater flow as of 2008, when preparations were underway to implement the 2008 200-ZP-1 ROD [HANFORD-200-ZP-1-ROD].

The depth to the water table in the 200 West Area varies from about 50 m (164 ft) in the southwest corner near the former 216-U-10 Pond to >100 m (328 ft) in the north. The groundwater flow is primarily to the east, except in the northern portion of the 200 West Area where the flow is to the east-northeast. Groundwater flow is locally influenced by the 200-ZP-1 OU interim remedial measure (IRM) pump-and-treat system and permitted effluent discharges at the State-Approved Land Disposal Site. The groundwater flow rates typically range from 0.0001 to 0.5 m/day (0.00033 to 1.64 ft/day) across the 200-ZP- 1 OU. However, the water table continues to decline at a rate of approximately 0.21 m/yr (0.69 ft/yr) because the large influx of artificial recharge has ceased.

A.2.2 200-UP-1 OU IRA P&T System

The 200-UP-1 OU IRA P&T system was a smaller system designed to address technetium-99 and uranium contamination in groundwater resulting from historical disposal practices at the 216-U-1/2 Cribs, though secondary contaminants CT and nitrate were also treated. The system started operating in 1994 [DOE/RL-2010-105, 2011; DOE/RL-2012-03, 2012]) and ceased operations in March 2011 [DOE/RL-2012-03, 2012], though there were intermittent extended down times for specific testing, maintenance, and equipment failures.

The 200-UP-1 OU IRA P&T system, located adjacent to the 216-U-17 Crib, consisted of one to three extraction wells, which changed over time, and one or zero injection wells (early on, an injection well was used, but water was later sent to the Effluent Treatment Facility for treatment). Initially, wells 299-W19-24 and 299-W19-23 were used for extraction, and well 299-W19-25 was used for injection. In 1997, well 299-W19-39 was used for extraction and well 299-W19-36 for injection. In the early 2000s through 2011, wells 299-W19-36 and 299-W19-43 were also used for extraction (Figure A.8). Total extraction flow rates appear to have been around 189 L/min (50 gpm) or less over the duration of system operations.

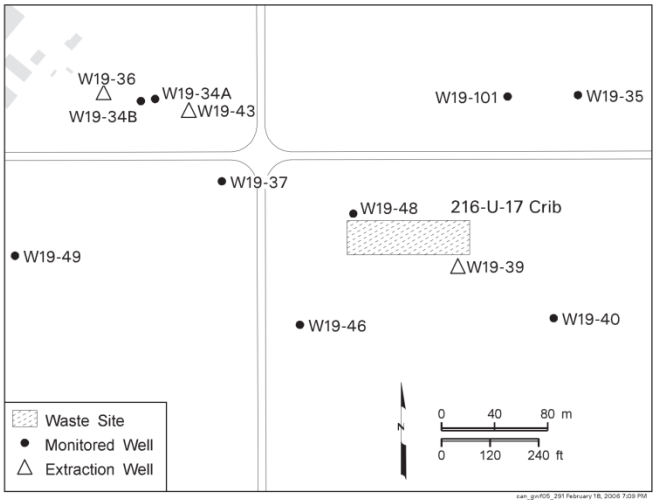

Figure A.8. 200-UP-1 OU IRA P&T system, as of 2005 (Hartman et al., 2006).

A.2.3 WMA T IRA P&T System

Starting in 2007 and continuing into 2012, an IRA P&T system was operated to treat technetium-99 contamination in groundwater to the east of and within WMA T [DOE/RL-2010-105, 2011]. This IRA P&T system consisted of two extraction wells (299-W11-45 and 299-W11-46, shown in Figure A.9), with extracted water sent to ETF for treatment/disposal. The system appears to have pumped at total flow rates that varied over time, but which were generally less than 189 L/min (50 gpm).

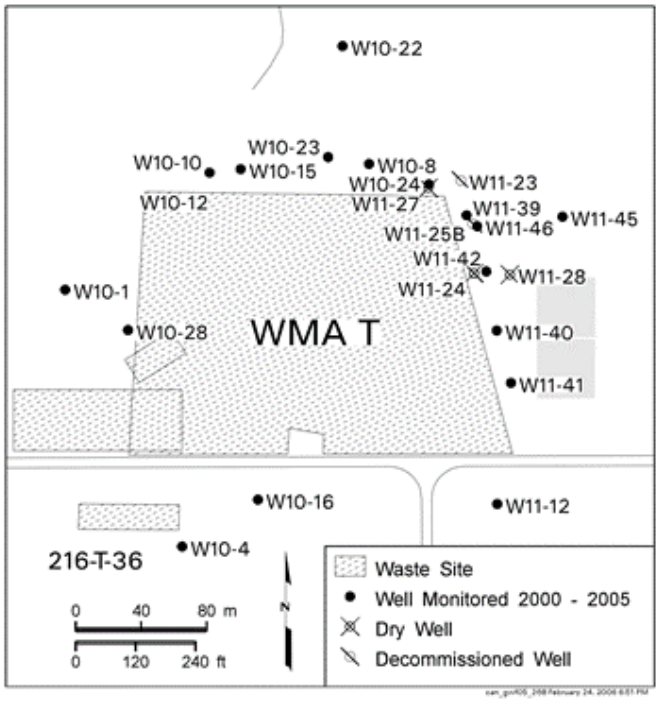

Figure A.9. Wells near WMA T (Hartman et al., 2006). Wells 299-W11-45 and 299-W11-46 were used in a small IRA P&T system starting in 2007.

A.3 Current P&T System

The 200 West Groundwater Treatment Facility (200W P&T system) began operations in July 2012 to replace previous IRA P&T systems as part of the remedies specified in the 2008 ROD for the 200-ZP-1 OU [HANFORD-200-ZP-1-ROD, 2008] and the 2012 ROD for the 200-UP-1 OU [HANFORD-200-UP-1-ROD, 2012]. The 200W P&T system (Figure A.10) is remediating the 200 West Area CT plume and also treats comingled contaminants such as hexavalent chromium, iodine-129, nitrate, technetium-99, trichloroethene, and tritium [DOE/RL-2017-68]. The objective of the remediation is to achieve 95% removal of CT over a projected 25-year operational life for the facility (2012-2037). The 200W P&T system receives groundwater from 26 extraction wells in the 200 West Area CT groundwater plume (plus 6 wells located in the 200 East Area). Treated groundwater is injected into 29 wells around the perimeter of the 200 West Area CT groundwater plume at a target flow rate of 150 gpm to achieve hydraulic flow path control for the CT plume and for the Iodine-129 plume to the southeast of the 200 West Area.

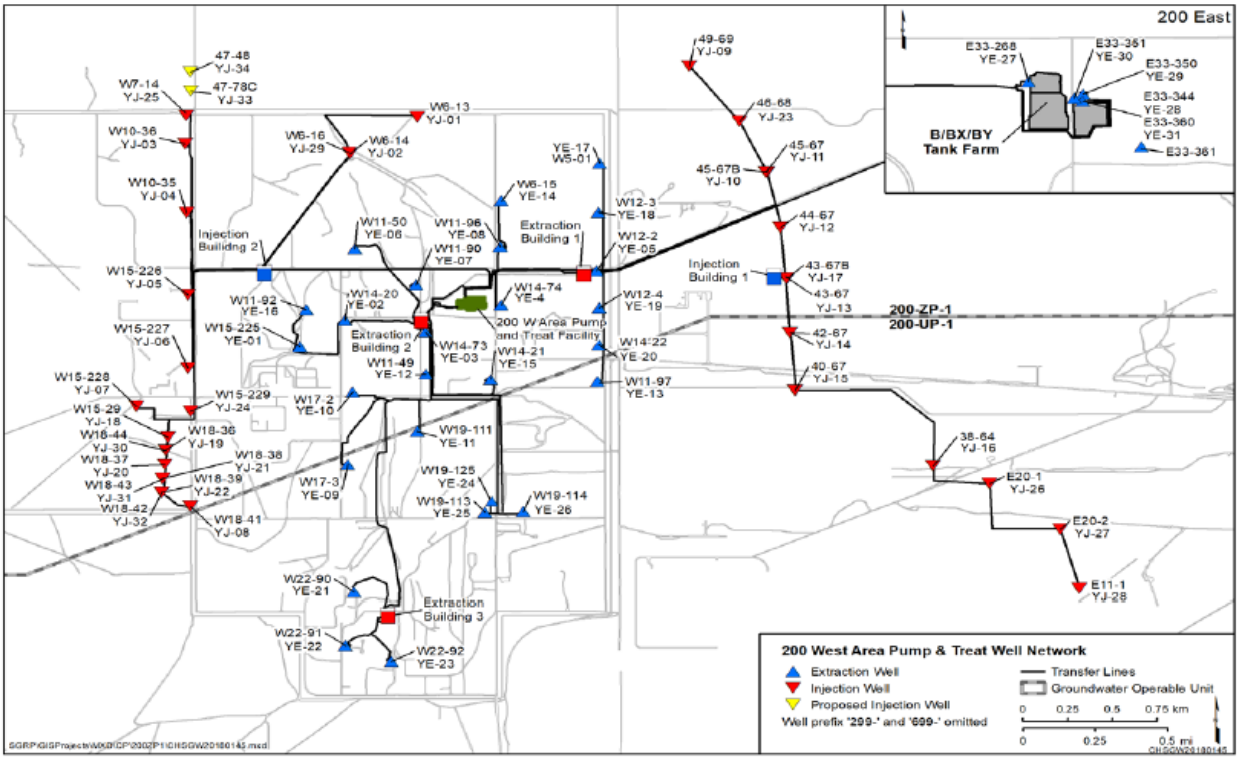

Figure A.10. 200 West Area Pump-and-Treat network (DOE/RL-2017-68, 2018)

Figure A.11depicts water level contours for the unconfined aquifer for June 2012 (prior to startup of the 200W P&T system) and for December 2017 (when the 200W P&T system was operating). The latter time shows the impact of the P&T wells on groundwater hydraulics. A numerical model has been used to investigate that impact on groundwater hydraulics in terms of how the groundwater moves. Figure A.12 shows the predicted zone of influence and contours for the magnitude of groundwater dilution in 2020, based on injection of clean water under the current pumping scheme. Particle tracking was conducted with the numerical model to show the forward path taken by water when injected (Figure A.13) and the path where groundwater was drawn from when extracted (Figure A.14). Locations outside of these zones of influence are expected to be less disturbed.

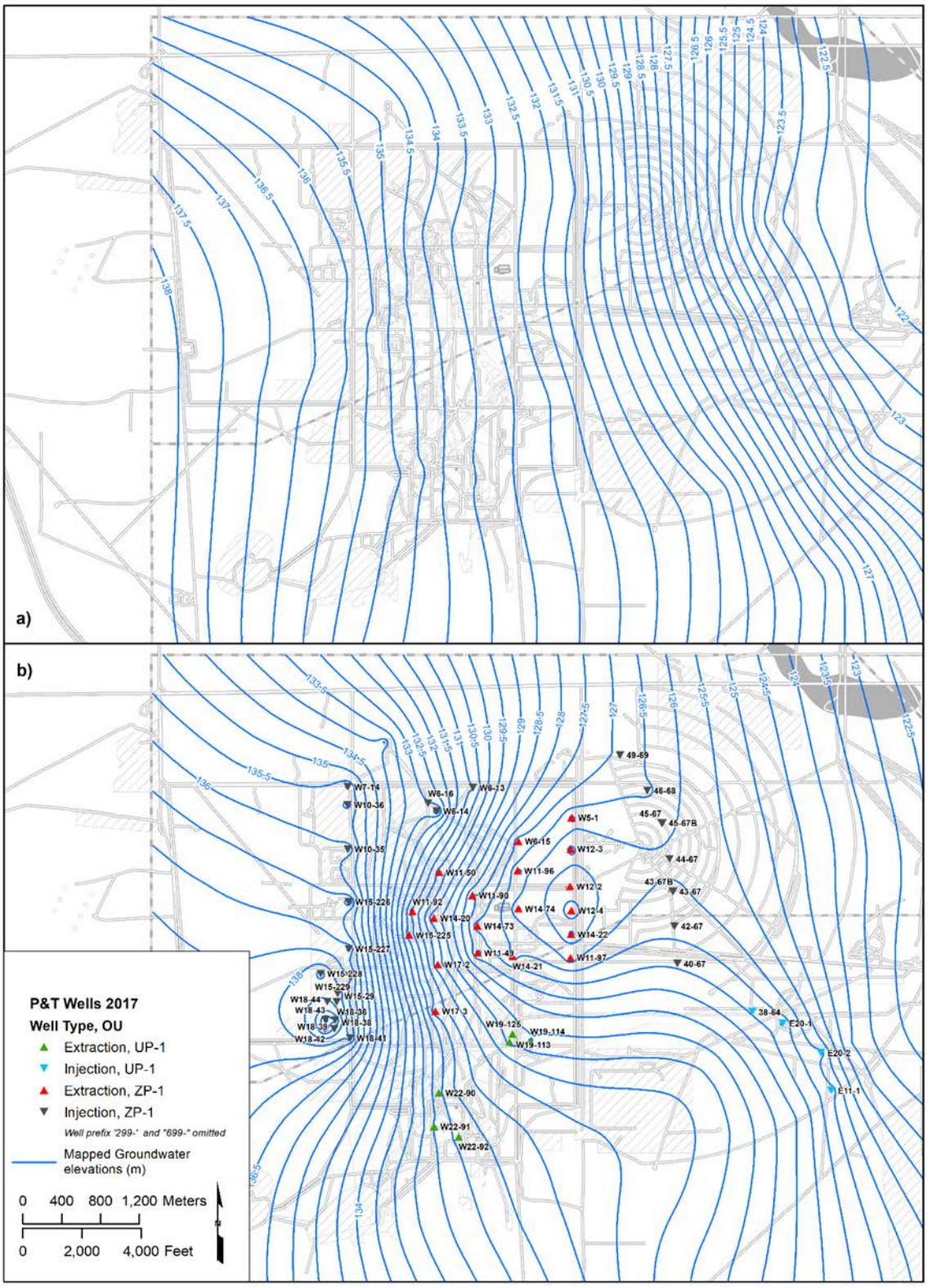

Figure A.11. Water level contours for the unconfined aquifer (above the RLM) for (a) June 2012 and (b) December 2017 [DOE/RL-2017-68, 2018]

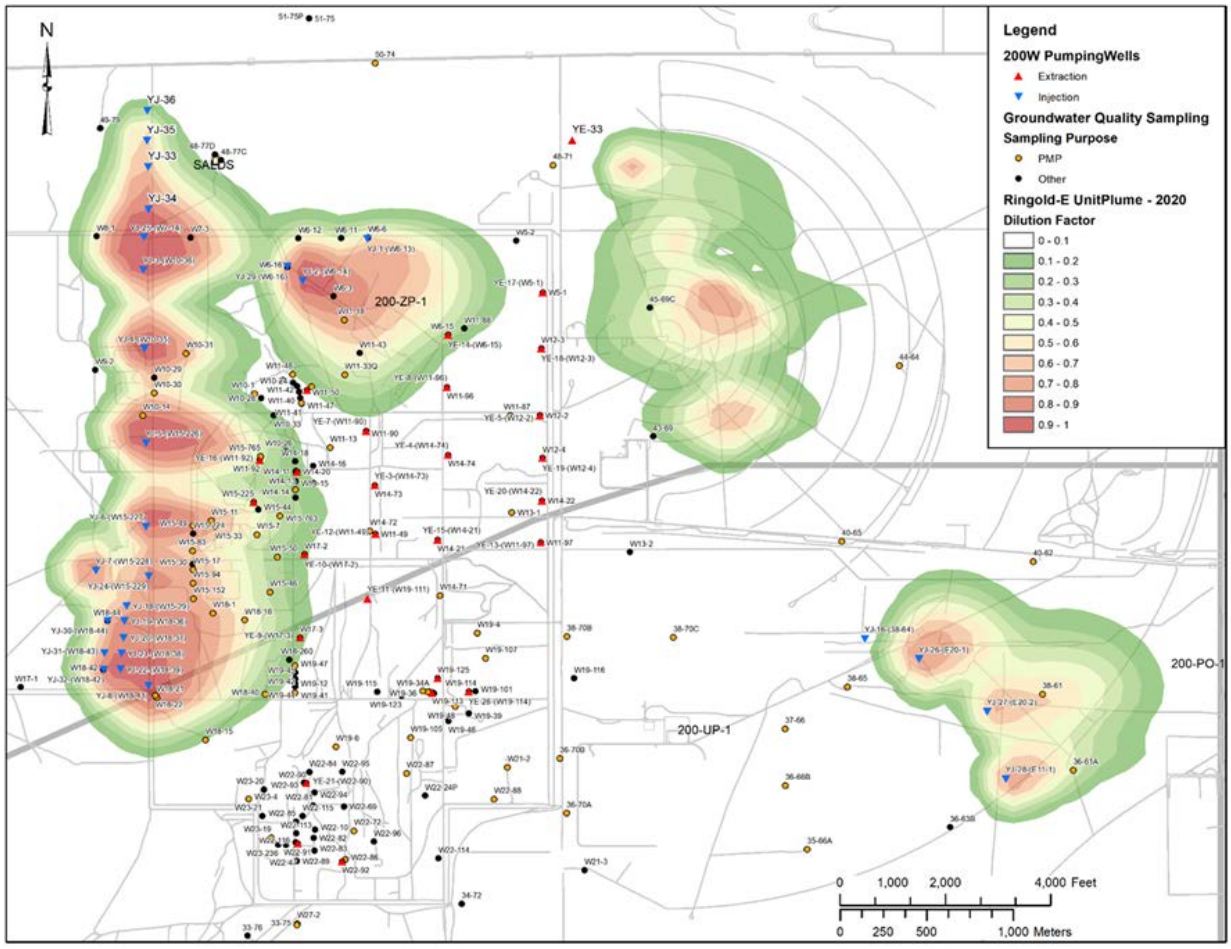

Figure A.12. Numerical model results showing dilution of groundwater in the unconfined aquifer Ringold E unit (above the RLM) in 2020. Adapted from information provided by the site contractor modeling team for particle tracking results and dilution zone calculations that were derived from simulations using the Central Plateau Groundwater Model (CP-47631))

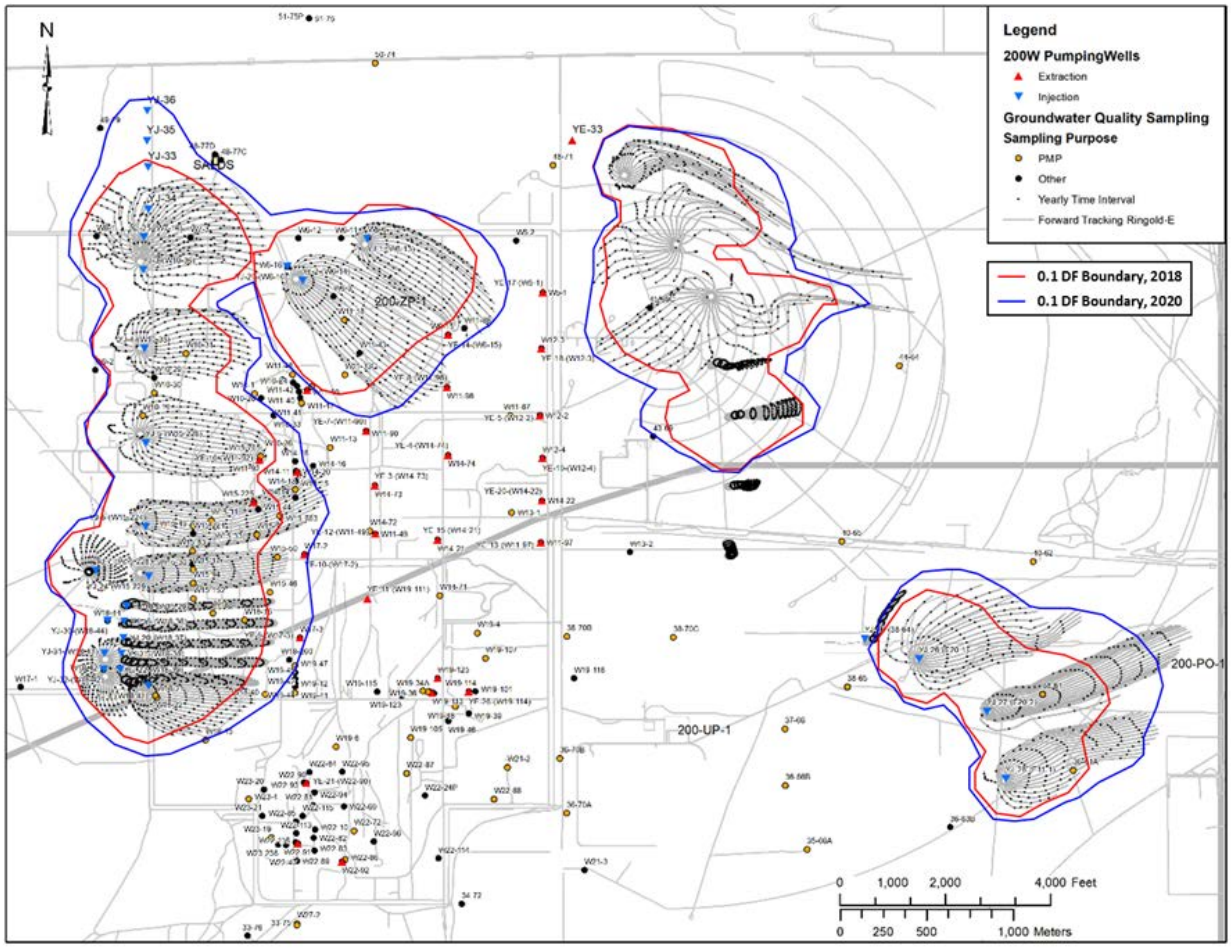

Figure A.13. Numerical model results showing flow paths (forward particle tracking) of injected water from June 2012 to October 2022. Overlain on the pathlines are the outer boundaries of the groundwater 10% dilution factor for 2018 results (red) and 2020 results (blue; Figure A.12) for groundwater in the unconfined aquifer Ringold E unit (above the RLM).(Adapted from information provided by the site contractor modeling team for particle tracking results and dilution zone calculations that were derived from simulations using the Central Plateau Groundwater Model (CP-47631))

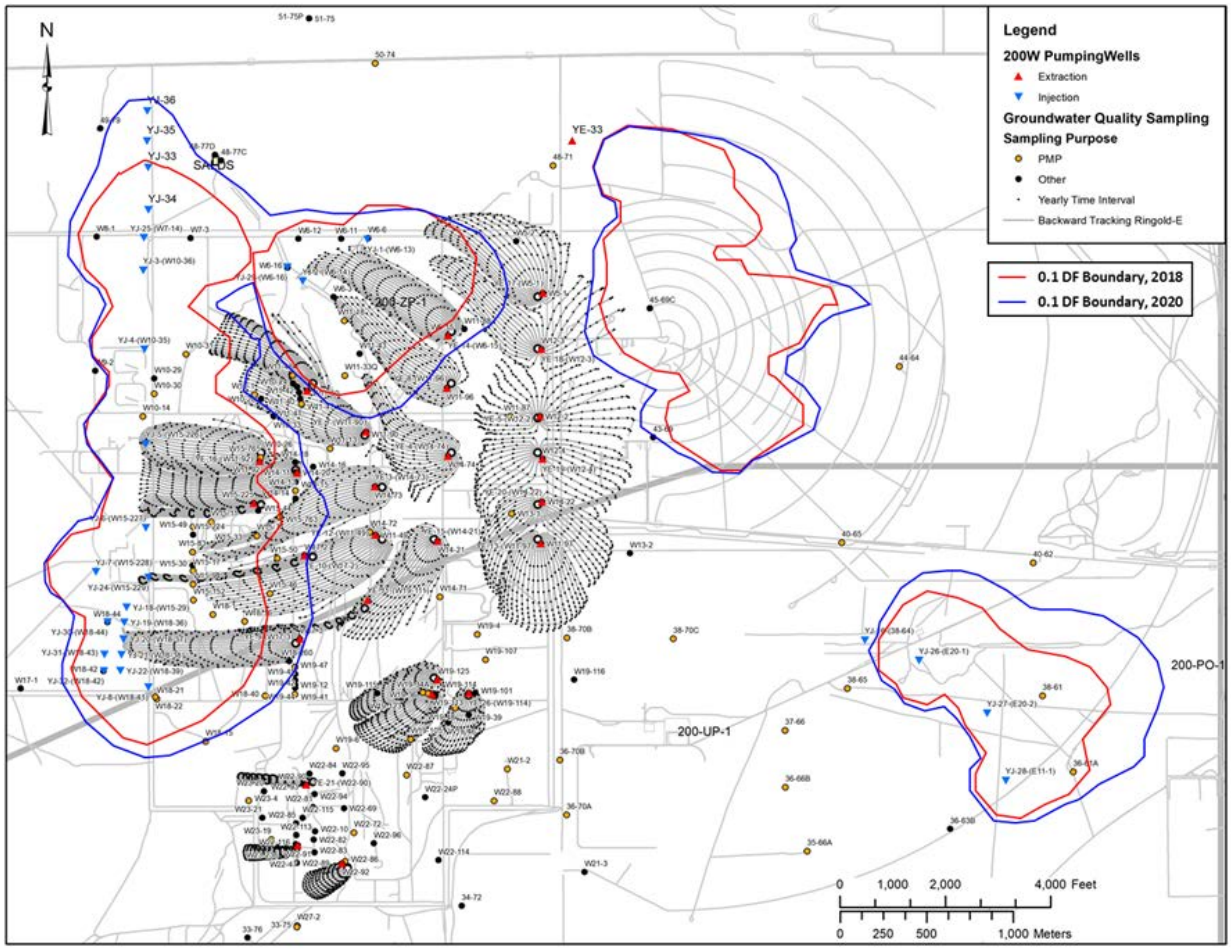

Figure A.14. Numerical model results showing flow paths (backwards particle tracking) of extracted water from June 2012 to October 2022. Overlain on the pathlines are the outer boundaries of the groundwater 10% dilution factor for 2018 results (red) and 2020 results (blue; Figure A.12) for groundwater in the unconfined aquifer Ringold E unit (above the RLM). (Adapted from information provided by the site contractor modeling team for particle tracking results and dilution zone calculations that were derived from simulations using the Central Plateau Groundwater Model (CP-47631))

Appendix B – Data and Plots

B.1 Additional Data Tables for Attenuation Indicators

The tables presented below list attenuation indicator information (CF, DCM, and nitrate detections, CF/CT slope) for wells where only DCM or only nitrate were detected (Table B.1) or where neither DCM nor nitrate were detected (Table B.2).

Table B.1. Detection and CF/CT slope indicator data for the North (shaded) and South (unshaded) well groups for three time periods, from January 1986 through (A) February 1994, (B) June 2012, and (C) January 2019, where either DCM or nitrite (but not both) were detected during the relevant time frames for the specified well group.

	Number of Detections of …			Percent of All Samples …						
	CF	DCM	Nitrite	CF		DCM		Nitrite		CF/CT
Well	AB C	AB C	AB C	A B C		A B C		A B C		Slope
299-W10-30	0 37	0 0 0	0 1 1	--	50.0 63.6	--	0.00.0	--	11.1 5.9	1.1 E-05
299-W10-31	0 712	0 0 0	0 1 1	--	87.5 92.3	--	0.00.0	--	9.15.6	1.6 E-05
299-W11-33Q	0 17	0 0 0	0 1 1	--	100.0 100.0	--	0.00.0	--	100.0 14.3	
299-W11-88	0 28	0 0 0	0 5 6	--	16.7 40.0	--	0.00.0	--	41.7 30.0	
699-45-69A	1 1519	0 1 1	0 0 1	20.0	78.9 82.6	0.0	5.64.5	0.0	0.04.5	-1.2 E-03
699-45-69C	0 37	0 0 0	0 1 2	--	33.3 43.8	--	0.00.0	--	11.1 12.5	-1.3 E-05
299-W11-34P	0 77	0 0 0	0 1 1	--	100.0 100.0	--	0.00.0	--	9.19.1	-9.9 E-06
299-W10-13	5 2020	3 6 6	0 0 0	23.8	51.3 51.3	14.3	15.4 15.4	0.0	0.00.0	-2.7 E-06
299-W10-21	2 3737	1 6 6	0 0 0	100.0	97.4 97.4	50.0	15.8 15.8	0.0	0.00.0	6.7 E-06
299-W10-22	0 2222	0 4 4	0 0 0	--	100.0 100.0	--	18.2 18.2	--	0.00.0	9.3 E-06
299-W10-28	0 33	0 0 0	0 3 6	--	100.0 100.0	--	0.00.0	--	7.912.2	-4.0 E-05
299-W10-9	7 88	1 1 1	0 0 0	100.0	100.0 100.0	14.3	12.5 12.5	0.0	0.00.0	5.4 E-08
299-W11-14	4 1414	1 4 4	0 0 0	66.7	77.8 77.8	16.7	22.2 22.2	0.0	0.00.0	2.6 E-07
299-W11-20	0 11	0 1 1	0 0 0	--	100.0 100.0	--	100.0 100.0	--	-- --	
299-W11-3	2 2323	1 4 4	0 0 0	100.0	95.8 95.8	50.0	16.7 16.7	0.0	0.00.0	1.9 E-06
299-W11-31	2 55	1 2 2	0 0 0	40.0	62.5 62.5	20.0	25.0 25.0	0.0	0.00.0	-2.7 E-06
299-W11-6	2 2525	0 3 3	0 0 0	100.0	96.2 96.2	0.0	11.5 11.5	0.0	0.00.0	-9.7 E-07
299-W11-7	3 1818	0 5 5	0 0 0	100.0	90.0 90.0	0.0	25.0 25.0	0.0	0.00.0	1.7 E-08
299-W6-10	3 1515	3 3 3	0 0 0	60.0	88.2 88.2	60.0	17.6 17.6	0.0	0.00.0	-5.0 E-06
299-W6-12	2 66	1 3 3	0 0 0	40.0	66.7 66.7	20.0	33.3 33.3	0.0	0.00.0	-6.1 E-05
299-W6-14	0 11	0 1 1	0 0 0	--	100.0 100.0	--	100.0 100.0	--	-- --	
299-W6-2	11 2323	6 1010	0 0 0	45.8	60.5 60.5	25.0	26.3 26.3	0.0	0.00.0	3.3 E-07
299-W6-8	1 44	1 1 1	0 0 0	12.5	36.4 36.4	12.5	9.19.1	0.0	0.00.0	1.6 E-04
299-W6-9	3 66	2 2 2	0 0 0	60.0	75.0 75.0	40.0	25.0 25.0	0.0	0.00.0	-1.7 E-06
299-W7-1	4 2323	5 1010	0 0 0	21.1	60.5 60.5	26.3	26.3 26.3	0.0	0.00.0	-7.0 E-06
299-W7-10	4 1717	3 6 6	0 0 0	36.4	70.8 70.8	27.3	25.0 25.0	0.0	0.00.0	1.3 E-04
299-W7-11	6 1919	1 5 5	0 0 0	60.0	73.1 73.1	10.0	19.2 19.2	0.0	0.00.0	1.1 E-04
299-W7-12	3 2828	3 1212	0 0 0	33.3	80.0 80.0	33.3	34.3 34.3	0.0	0.00.0	-1.0 E-04
299-W7-5	9 2929	3 1212	0 0 0	47.4	70.7 70.7	15.8	29.3 29.3	0.0	0.00.0	3.0 E-05
299-W7-6	2 1111	4 1010	0 0 0	11.1	33.3 33.3	22.2	30.3 30.3	0.0	0.00.0	-1.2 E-04

Well	Number of Detections of … CF AB C	DCM AB C	Nitrite AB C	Percent of All Samples … CF A B C	DCM A B C	Nitrite A B C	CF/CT Slope
299-W7-7	4 2424	4 1111	0 0 0	26.7 68.6 68.6	26.7 31.4 31.4	0.0 0.00.0	-2.4 E-05
299-W7-8	8 1616	5 9 9	0 0 0	61.5 57.1 57.1	38.5 32.1 32.1	0.0 0.00.0	2.3 E-04
299-W8-1	3 3434	3 1414	0 0 0	15.0 48.6 48.6	15.0 20.0 20.0	0.0 0.00.0	4.9 E-05
299-W9-1	2 1111	3 8 8	0 0 0	11.8 36.7 36.7	17.6 26.7 26.7	0.0 0.00.0	2.3 E-04
699-40-65	0 1219	0 0 0	0 1 2	-- 50.0 61.3	-- 0.00.0	-- 4.87.1	-1.6 E-04
699-44-64	0 612	1 1 1	0 0 1	0.0 50.0 60.0	20.0 8.35.0	0.0 0.03.6	-8.3 E-05
299-W22-87	0 511	0 0 0	0 3 4	-- 25.0 40.7	-- 0.00.0	-- 15.0 17.4	-5.6 E-06
299-W13-2P	0 02	0 0 0	0 0 1	-- --100.0	-- -- 0.0	-- --50.0	
299-W13-2Q	0 02	0 0 0	0 0 1	-- --100.0	-- -- 0.0	-- --50.0	
299-W22-95	0 07	0 0 0	0 0 1	-- --100.0	-- -- 0.0	-- -- 5.0	-5.4 E-05
299-W14-10	0 00	0 0 0	1 1 1	0.0 0.00.0	0.0 0.00.0	50.0 33.3 33.3	
299-W19-14	0 55	0 2 2	0 0 0	-- 100.0 100.0	-- 40.0 40.0	-- 0.00.0	7.9 E-06
299-W19-15	2 99	0 1 1	0 0 0	18.2 50.0 50.0	0.0 5.65.6	0.0 0.00.0	-3.5 E-06
299-W19-17	0 11	0 0 0	0 1 1	-- 100.0 100.0	-- 0.00.0	0.0 16.7 16.7	
299-W21-1	0 33	0 1 1	0 0 0	-- 75.0 75.0	-- 25.0 25.0	0.0 0.00.0	9.4 E-04
299-W22-22	3 66	1 1 1	0 0 0	33.3 46.2 46.2	11.1 7.77.7	0.0 0.00.0	-1.4 E-04
299-W22-26	0 1313	0 0 0	0 4 6	0.0 59.1 59.1	0.0 0.00.0	-- 12.9 18.2	-8.0 E-05
299-W22-40	7 1212	2 2 2	0 0 0	58.3 70.6 70.6	16.7 11.8 11.8	0.0 0.00.0	-1.3 E-04
299-W22-41	5 88	2 2 2	0 0 0	50.0 61.5 61.5	20.0 15.4 15.4	0.0 0.00.0	-1.7 E-04
299-W22-42	7 1414	2 4 4	0 0 0	70.0 77.8 77.8	20.0 22.2 22.2	0.0 0.00.0	-5.8 E-05
299-W22-43	5 1919	1 5 5	0 0 0	45.5 73.1 73.1	9.1 19.2 19.2	0.0 0.00.0	-8.7 E-05
299-W23-13	1 66	1 1 1	0 0 0	50.0 75.0 75.0	50.0 12.5 12.5	0.0 0.00.0	-1.3 E-04
299-W23-20	0 11	0 0 0	0 1 2	-- 100.0 100.0	-- 0.00.0	-- 2.53.9	
699-36-67	0 2424	0 1414	0 0 0	-- 77.4 77.4	-- 45.2 45.2	-- 0.00.0	-3.4 E-05
699-36-70B	0 3139	0 0 0	0 2126	-- 91.2 92.9	-- 0.00.0	-- 75.0 72.2	-1.4 E-04
699-37-68	0 2323	0 1414	0 0 0	-- 85.2 85.2	-- 51.9 51.9	-- 0.00.0	-9.4 E-05
699-38-70	10 2727	1 3 3	0 0 0	50.0 69.2 69.2	5.3 7.97.9	0.0 0.00.0	5.1 E-06
299-W19-115	0 01	0 0 0	0 0 3	-- --100.0	-- -- 0.0	-- -- 0.0	

Table B.2. Detection and CF/CT slope indicator data for the North (shaded) and South (unshaded) well groups for three time periods, from January 1986 through (A) February 1994, (B) June 2012, and (C) January 2019, where neither DCM nor nitrite were detected during the relevant time frames for the specified well group.

Well	Number of Detections of …			Percent of All Samples …									CF/CT Slope
	CF			DCM			Nitrite			CF			DCM			Nitrite			
	A	B	C	A	B	C	A	B	C	A	B	C	A	B	C	A	B	C	
299-W11-87	0	12	21	0	0	0	0	0	1	--	100.0	100.0	--	0.0	0.0	--	0.0	4.8	-1.7 E-06
299-W10-12	0	3	3	0	0	0	0	0	0	--	100.0	100.0	--	0.0	0.0	--	0.0	0.0	
299-W10-15	4	10	10	0	0	0	0	0	0	100.0	100.0	100.0	0.0	0.0	0.0	0.0	0.0	0.0	-1.5 E-06
299-W10-29	0	3	3	0	0	0	0	0	0	--	60.0	60.0	--	0.0	0.0	--	0.0	0.0	-4.9 E-06
299-W11-86	0	3	3	0	0	0	0	0	0	--	100.0	100.0	--	--	--	--	--	--	6.9 E-03
299-W6-1	1	4	4	0	0	0	0	0	0	50.0	80.0	80.0	0.0	0.0	0.0	0.0	0.0	0.0	6.3 E-06
299-W19-104	0	2	2	0	0	0	0	0	0	--	100.0	100.0	--	--	--	--	--	--	
299-W19-13	1	3	3	0	0	0	0	0	0	11.1	27.3	27.3	0.0	0.0	0.0	0.0	0.0	0.0	3.5 E-05
299-W22-23	2	3	3	0	0	0	0	0	0	66.7	50.0	50.0	0.0	0.0	0.0	0.0	0.0	0.0	
299-W22-7	0	0	0	0	0	0	0	0	0	--	0.0	0.0	--	0.0	0.0	--	--	--	
299-W23-16	0	0	0	0	0	0	0	0	0	0.0	0.0	0.0	0.0	0.0	0.0	0.0	0.0	0.0	
299-W23-17	0	0	0	0	0	0	0	0	0	0.0	0.0	0.0	0.0	0.0	0.0	0.0	0.0	0.0	
699-39-68	0	0	1	0	0	0	0	0	0	--	--	100.0	--	--	0.0	--	--	0.0	

B.2 Multi-Indicator Plots for Southern Well Group

Multi-indicator plots for groundwater data from selected well locations in the southern grouping of wells (85 wells total, 62 with CT detections) in the 200 West Area. Data from the southern grouping of wells is most relevant up through current 200 West P&T system operations.

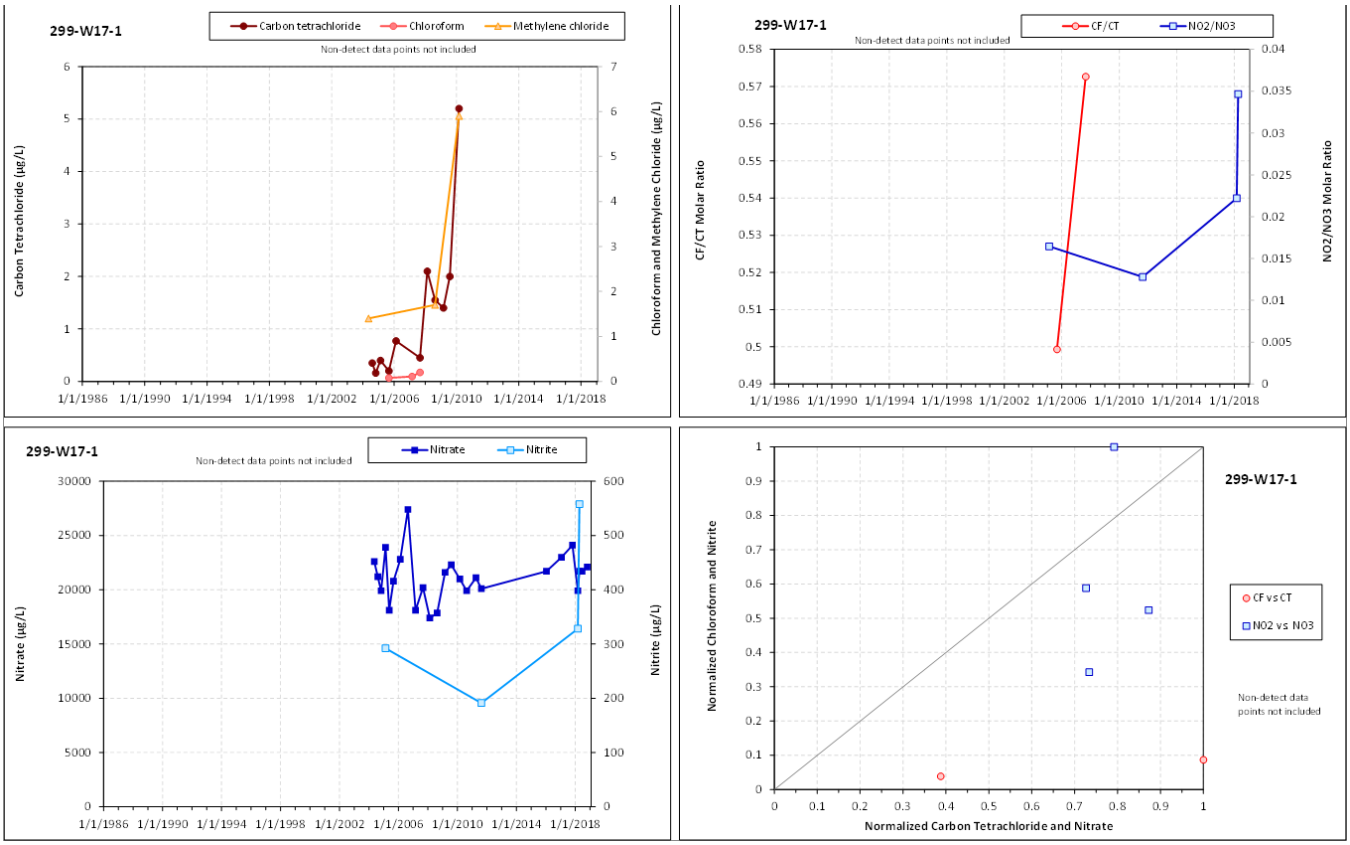
299-W17-1
Carbon tetrachloride
Chloroform
Methylene chloride
Non-detect data points not included
Carbon Tetrachloride (µg/L)
Chloroform and Methylene Chloride (µg/L)
1/1/1986 1/1/1990 1/1/1994 1/1/1998 1/1/2002 1/1/2006 1/1/2010 1/1/2014 1/1/2018
299-W17-1
CF/CT
NO2/NO3
Non-detect data points not included
CF/CT Molar Ratio
NO2/NO3 Molar Ratio
299-W17-1
Nitrate
Nitrite
Non-detect data points not included
Nitrate (µg/L)
Nitrite (µg/L)
299-W17-1
CF vs CT
NO2 vs NO3
Non-detect data points not included
Normalized Chloroform and Nitrite
Normalized Carbon Tetrachloride and Nitrate

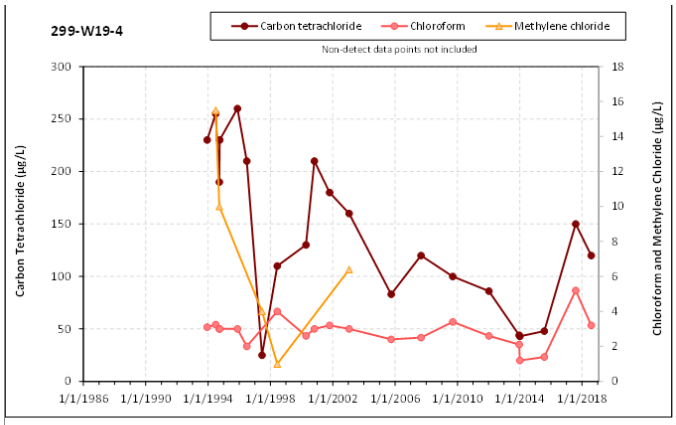
299-W19-4
Carbon tetrachloride
Chloroform
Methylene chloride
Non-detect data points not included
Carbon Tetrachloride (µg/L)
Chloroform and Methylene Chloride (µg/L)
1/1/1986 1/1/1990 1/1/1994 1/1/1998 1/1/2002 1/1/2006 1/1/2010 1/1/2014 1/1/2018

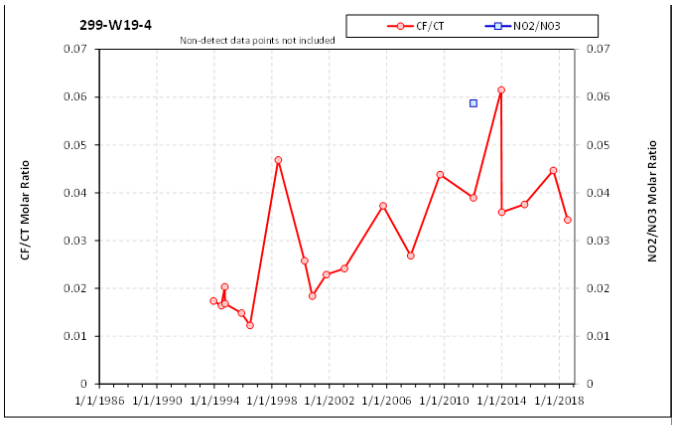
299-W19-4
CF/CT
NO2/NO3
Non-detect data points not included
CF/CT Molar Ratio
NO2/NO3 Molar Ratio
1/1/1986 1/1/1990 1/1/1994 1/1/1998 1/1/2002 1/1/2006 1/1/2010 1/1/2014 1/1/2018

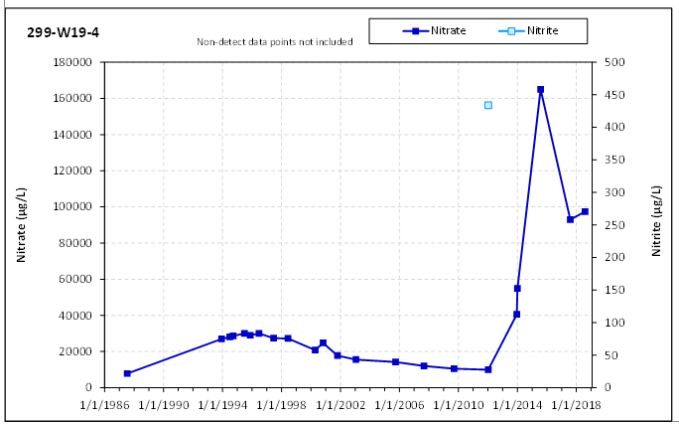
299-W19-4
Nitrate
Nitrite
Non-detect data points not included
Nitrate (µg/L)
Nitrite (µg/L)
1/1/1986 1/1/1990 1/1/1994 1/1/1998 1/1/2002 1/1/2006 1/1/2010 1/1/2014 1/1/2018

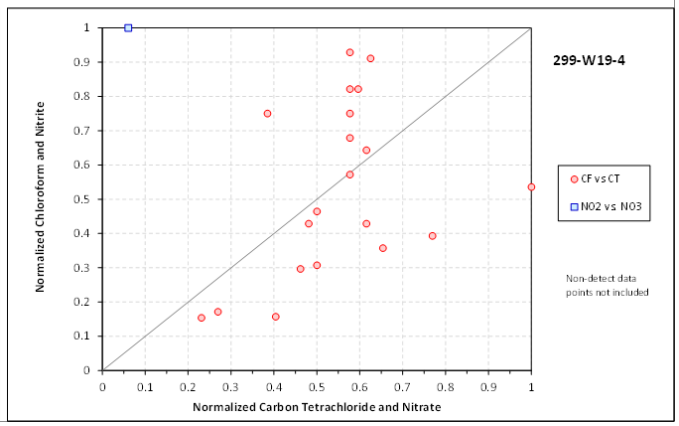
299-W19-4
Normalized Chloroform and Nitrite
Normalized Carbon Tetrachloride and Nitrate
CF vs CT
NO2 vs NO3
Non-detect data points not included

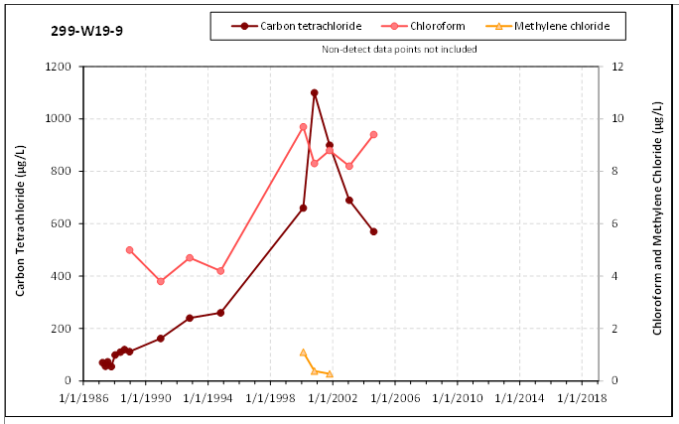
299-W19-9
Carbon tetrachloride
Chloroform
Methylene chloride
Non-detect data points not included
Carbon Tetrachloride (µg/L)
Chloroform and Methylene Chloride (µg/L)
1/1/1986 1/1/1990 1/1/1994 1/1/1998 1/1/2002 1/1/2006 1/1/2010 1/1/2014 1/1/2018

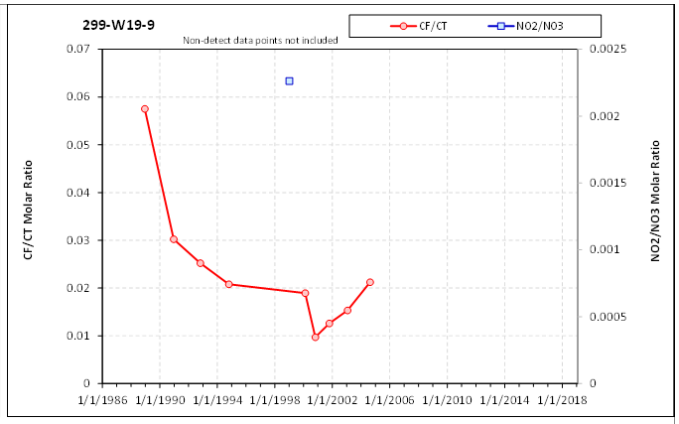
299-W19-9
CF/CT
NO2/NO3
Non-detect data points not included
CF/CT Molar Ratio
NO2/NO3 Molar Ratio
1/1/1986 1/1/1990 1/1/1994 1/1/1998 1/1/2002 1/1/2006 1/1/2010 1/1/2014 1/1/2018

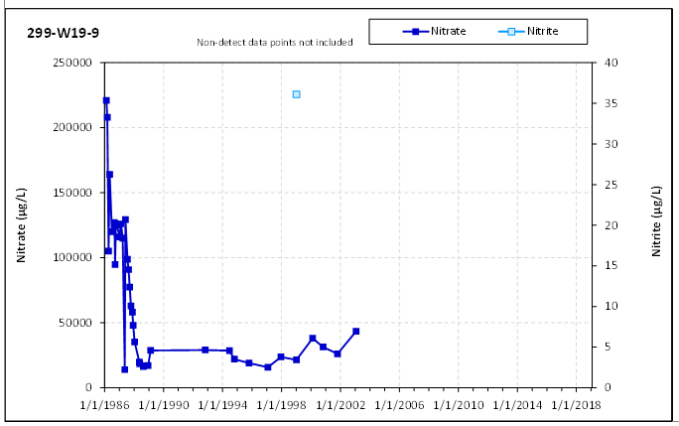
299-W19-9
Nitrate
Nitrite
Non-detect data points not included
Nitrate (µg/L)
Nitrite (µg/L)
1/1/1986 1/1/1990 1/1/1994 1/1/1998 1/1/2002 1/1/2006 1/1/2010 1/1/2014 1/1/2018

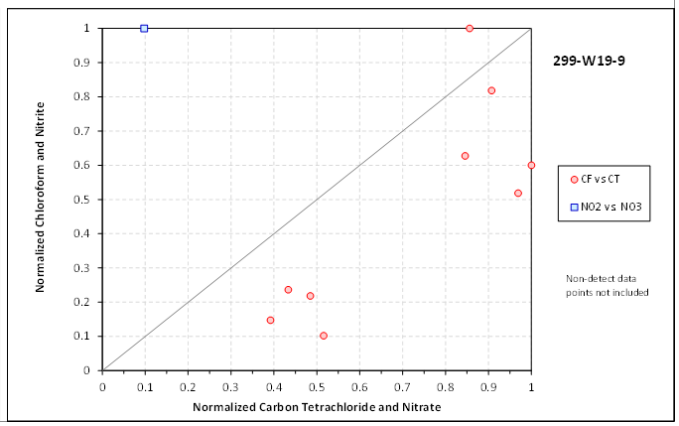
299-W19-9
Normalized Chloroform and Nitrite
Normalized Carbon Tetrachloride and Nitrate
CF vs CT
NO2 vs NO3
Non-detect data points not included

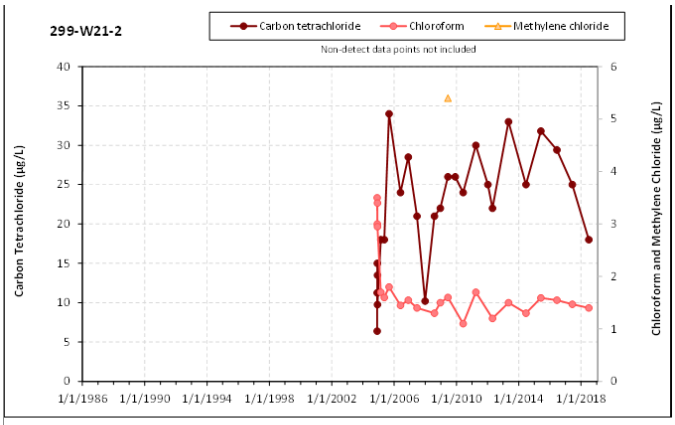
299-W21-2
Carbon tetrachloride
Chloroform
Methylene chloride
Non-detect data points not included
Carbon Tetrachloride (µg/L)
Chloroform and Methylene Chloride (µg/L)
1/1/1986 1/1/1990 1/1/1994 1/1/1998 1/1/2002 1/1/2006 1/1/2010 1/1/2014 1/1/2018

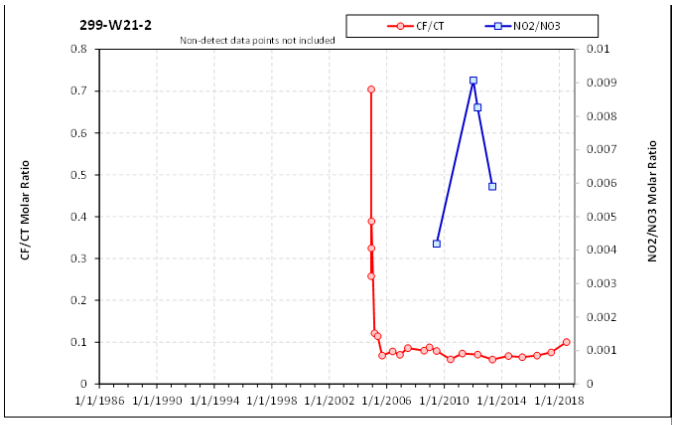
299-W21-2
CF/CT
NO2/NO3
Non-detect data points not included
CF/CT Molar Ratio
NO2/NO3 Molar Ratio
1/1/1986 1/1/1990 1/1/1994 1/1/1998 1/1/2002 1/1/2006 1/1/2010 1/1/2014 1/1/2018

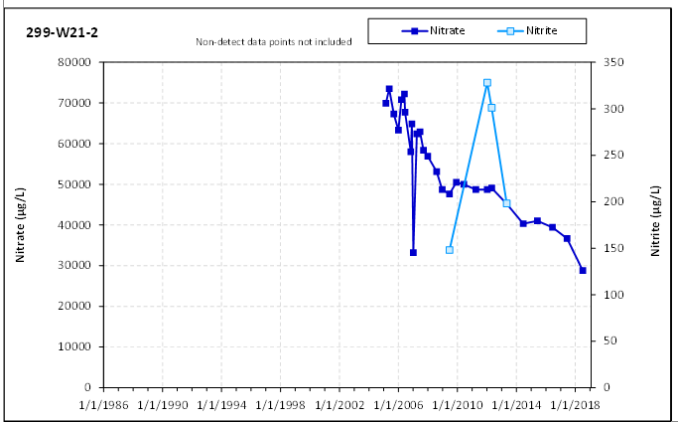
299-W21-2
Nitrate
Nitrite
Non-detect data points not included
Nitrate (µg/L)
Nitrite (µg/L)
1/1/1986 1/1/1990 1/1/1994 1/1/1998 1/1/2002 1/1/2006 1/1/2010 1/1/2014 1/1/2018

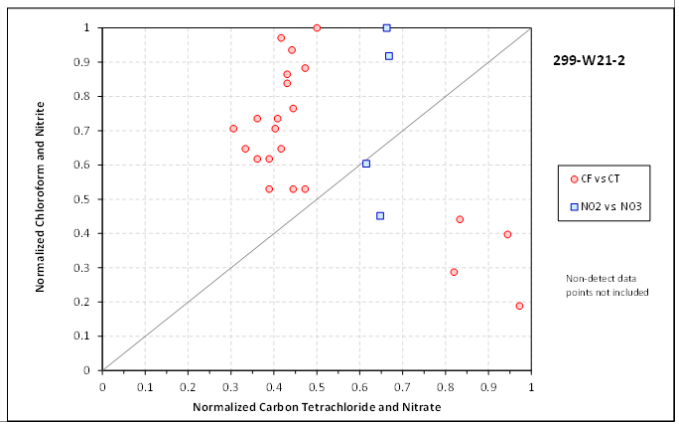
299-W21-2
Normalized Chloroform and Nitrite
Normalized Carbon Tetrachloride and Nitrate
CF vs CT
NO2 vs NO3
Non-detect data points not included

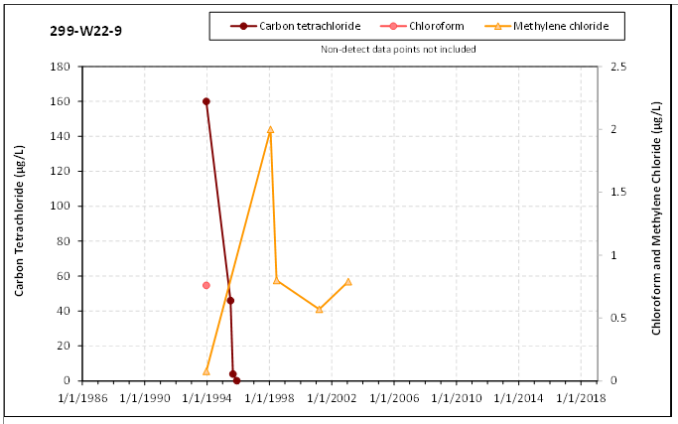
299-W22-9
Carbon tetrachloride
Chloroform
Methylene chloride
Non-detect data points not included
Carbon Tetrachloride (µg/L)
Chloroform and Methylene Chloride (µg/L)
1/1/1986 1/1/1990 1/1/1994 1/1/1998 1/1/2002 1/1/2006 1/1/2010 1/1/2014 1/1/2018

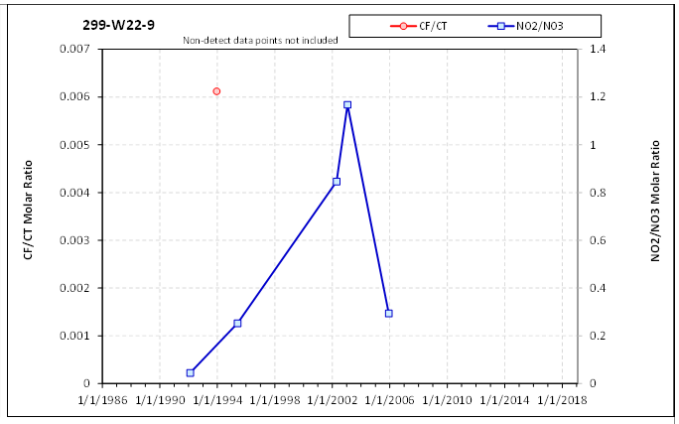
299-W22-9
CF/CT
NO2/NO3
Non-detect data points not included
CF/CT Molar Ratio
NO2/NO3 Molar Ratio
1/1/1986 1/1/1990 1/1/1994 1/1/1998 1/1/2002 1/1/2006 1/1/2010 1/1/2014 1/1/2018

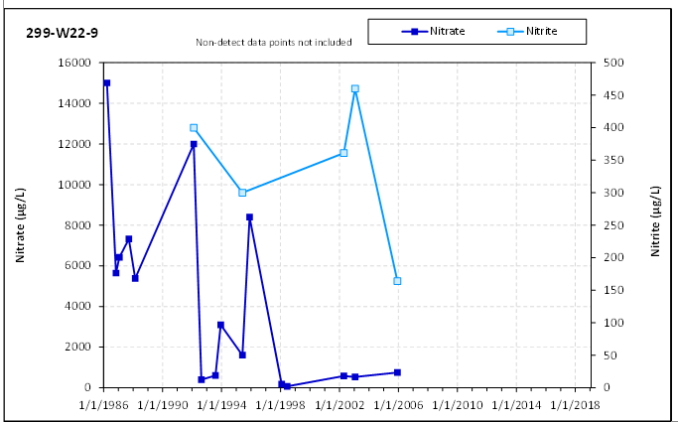
299-W22-9
Nitrate
Nitrite
Non-detect data points not included
Nitrate (µg/L)
Nitrite (µg/L)
1/1/1986 1/1/1990 1/1/1994 1/1/1998 1/1/2002 1/1/2006 1/1/2010 1/1/2014 1/1/2018

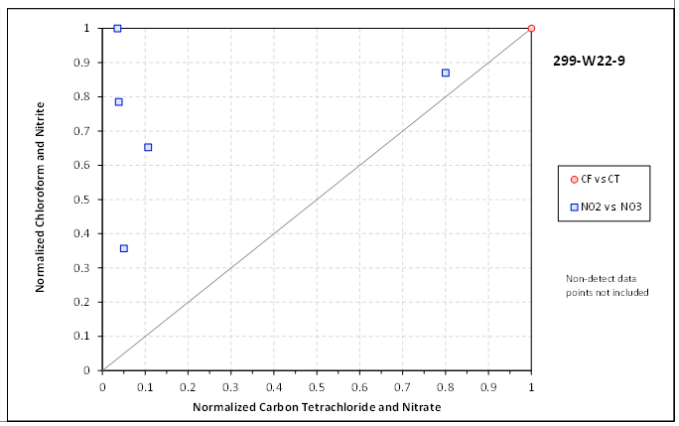
299-W22-9
Normalized Chloroform and Nitrite
Normalized Carbon Tetrachloride and Nitrate
CF vs CT
NO2 vs NO3
Non-detect data points not included

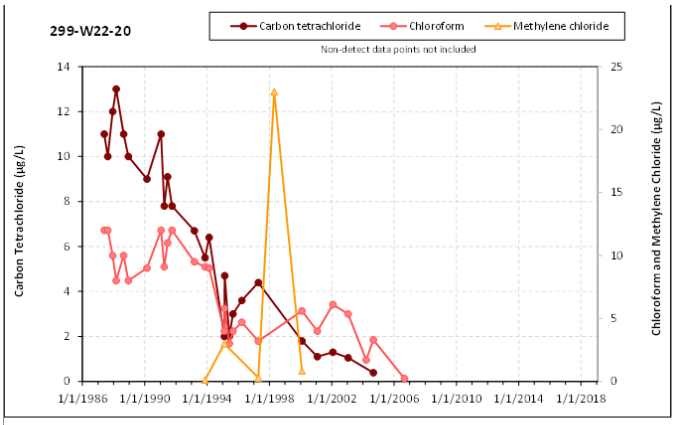
299-W22-20
Carbon tetrachloride
Chloroform
Methylene chloride
Non-detect data points not included
Carbon Tetrachloride (µg/L)
Chloroform and Methylene Chloride (µg/L)
1/1/1986 1/1/1990 1/1/1994 1/1/1998 1/1/2002 1/1/2006 1/1/2010 1/1/2014 1/1/2018

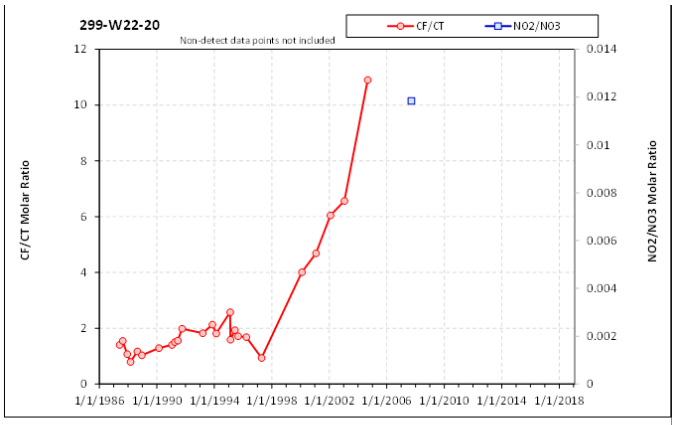
299-W22-20
CF/CT
NO2/NO3
Non-detect data points not included
CF/CT Molar Ratio
NO2/NO3 Molar Ratio
1/1/1986 1/1/1990 1/1/1994 1/1/1998 1/1/2002 1/1/2006 1/1/2010 1/1/2014 1/1/2018

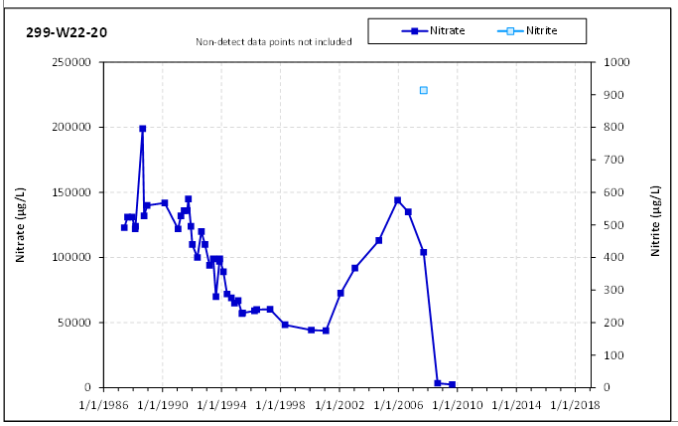
299-W22-20
Nitrate
Nitrite
Non-detect data points not included
Nitrate (µg/L)
Nitrite (µg/L)
1/1/1986 1/1/1990 1/1/1994 1/1/1998 1/1/2002 1/1/2006 1/1/2010 1/1/2014 1/1/2018

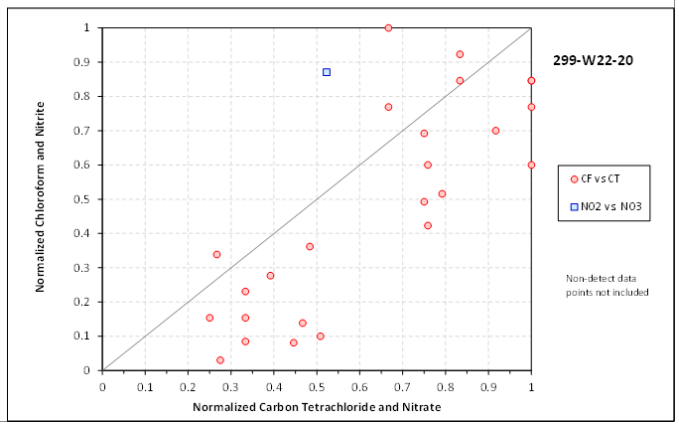
299-W22-20
Normalized Chloroform and Nitrite
Normalized Carbon Tetrachloride and Nitrate
CF vs CT
NO2 vs NO3
Non-detect data points not included

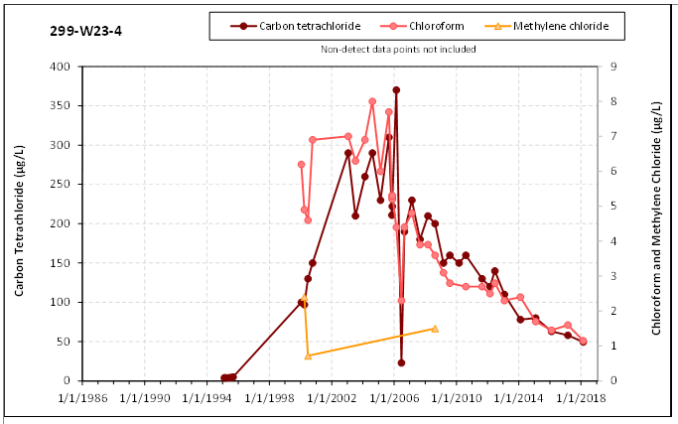
299-W23-4
Carbon tetrachloride
Chloroform
Methylene chloride
Non-detect data points not included
Carbon Tetrachloride (µg/L)
Chloroform and Methylene Chloride (µg/L)
1/1/1986 1/1/1990 1/1/1994 1/1/1998 1/1/2002 1/1/2006 1/1/2010 1/1/2014 1/1/2018

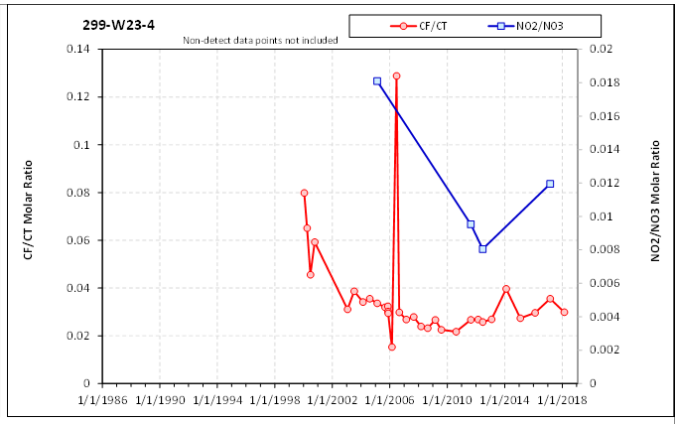
299-W23-4
CF/CT
NO2/NO3
Non-detect data points not included
CF/CT Molar Ratio
NO2/NO3 Molar Ratio
1/1/1986 1/1/1990 1/1/1994 1/1/1998 1/1/2002 1/1/2006 1/1/2010 1/1/2014 1/1/2018

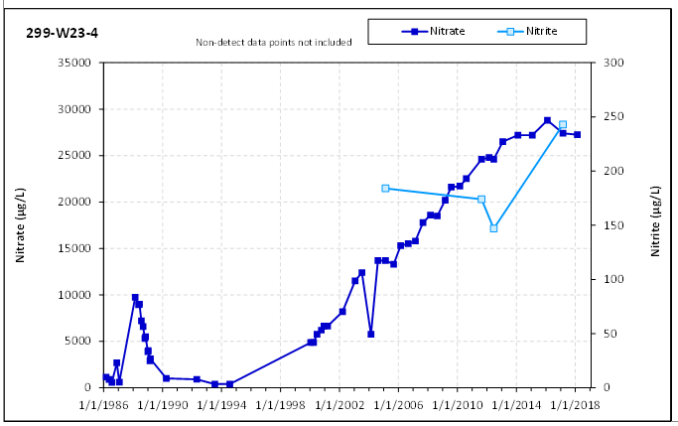
299-W23-4
Nitrate
Nitrite
Non-detect data points not included
Nitrate (µg/L)
Nitrite (µg/L)
1/1/1986 1/1/1990 1/1/1994 1/1/1998 1/1/2002 1/1/2006 1/1/2010 1/1/2014 1/1/2018

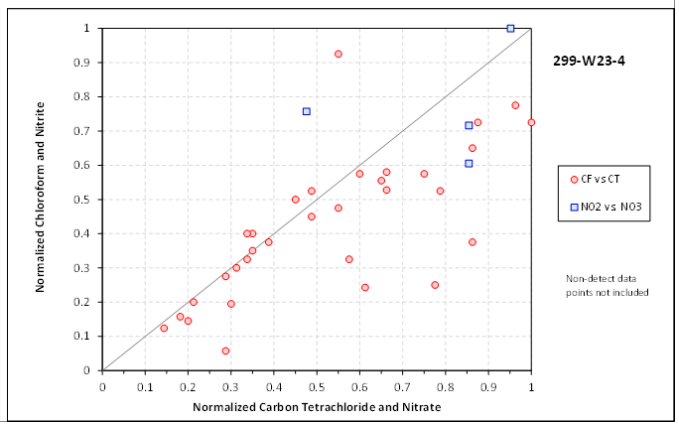
299-W23-4
Normalized Chloroform and Nitrite
Normalized Carbon Tetrachloride and Nitrate
CF vs CT
NO2 vs NO3
Non-detect data points not included

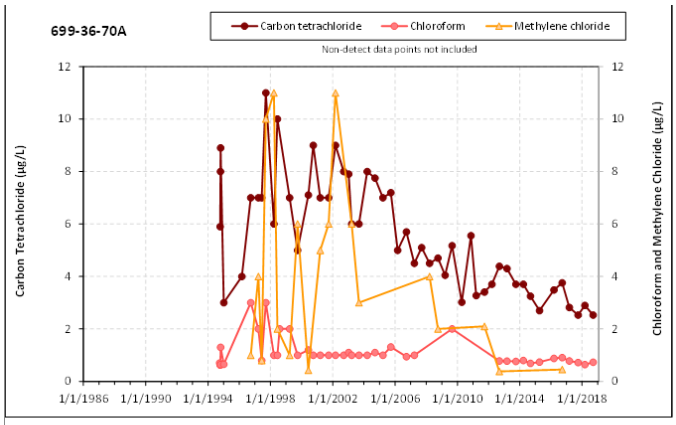
699-36-70A
Carbon tetrachloride
Chloroform
Methylene chloride
Non-detect data points not included
Carbon Tetrachloride (µg/L)
Chloroform and Methylene Chloride (µg/L)
1/1/1986 1/1/1990 1/1/1994 1/1/1998 1/1/2002 1/1/2006 1/1/2010 1/1/2014 1/1/2018

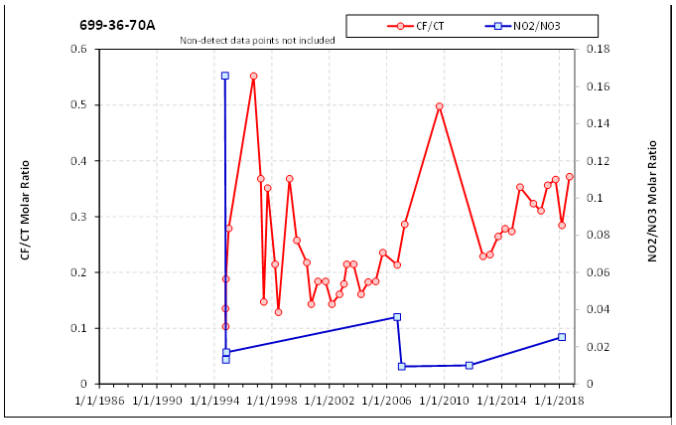
699-36-70A
CF/CT
NO2/NO3
Non-detect data points not included
CF/CT Molar Ratio
NO2/NO3 Molar Ratio
1/1/1986 1/1/1990 1/1/1994 1/1/1998 1/1/2002 1/1/2006 1/1/2010 1/1/2014 1/1/2018

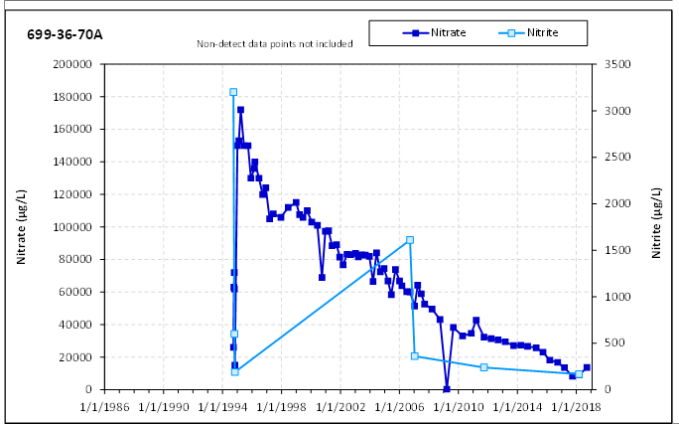
699-36-70A
Nitrate
Nitrite
Non-detect data points not included
Nitrate (µg/L)
Nitrite (µg/L)
1/1/1986 1/1/1990 1/1/1994 1/1/1998 1/1/2002 1/1/2006 1/1/2010 1/1/2014 1/1/2018

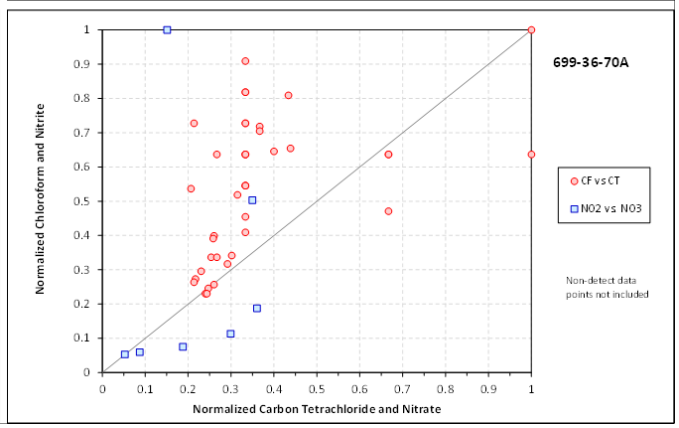
699-36-70A
Normalized Chloroform and Nitrite
Normalized Carbon Tetrachloride and Nitrate
CF vs CT
NO2 vs NO3
Non-detect data points not included

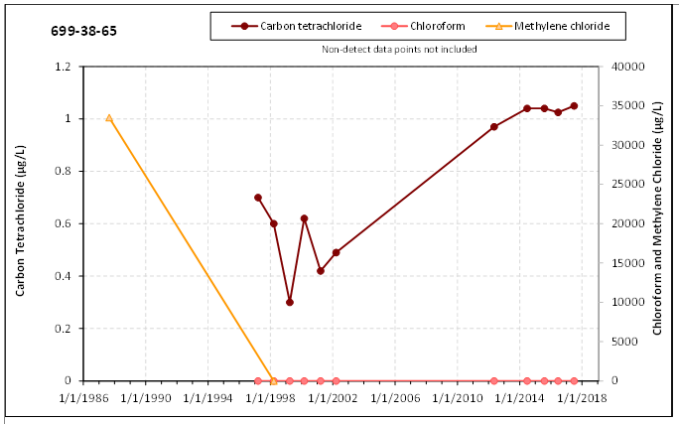
699-38-65
Carbon tetrachloride
Chloroform
Methylene chloride
Non-detect data points not included
Carbon Tetrachloride (µg/L)
Chloroform and Methylene Chloride (µg/L)
1/1/1986 1/1/1990 1/1/1994 1/1/1998 1/1/2002 1/1/2006 1/1/2010 1/1/2014 1/1/2018

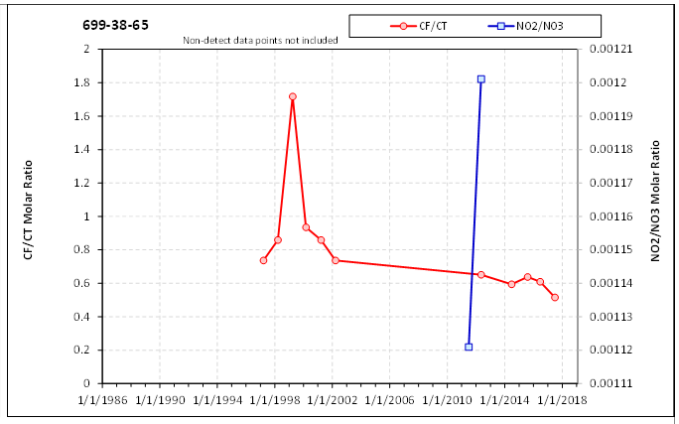
699-38-65
CF/CT
NO2/NO3
Non-detect data points not included
CF/CT Molar Ratio
NO2/NO3 Molar Ratio
1/1/1986 1/1/1990 1/1/1994 1/1/1998 1/1/2002 1/1/2006 1/1/2010 1/1/2014 1/1/2018

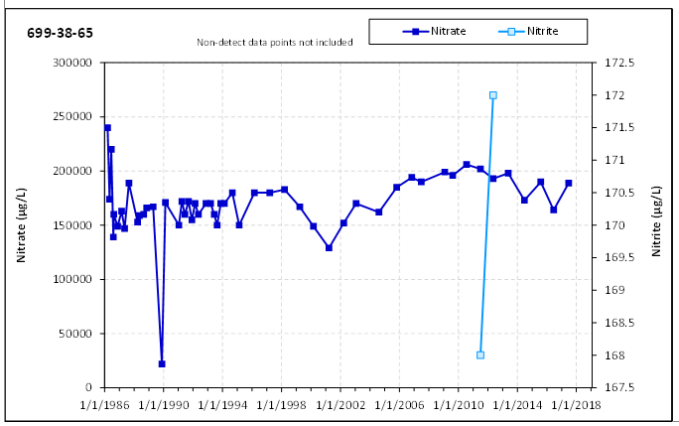
699-38-65
Nitrate
Nitrite
Non-detect data points not included
Nitrate (µg/L)
Nitrite (µg/L)
1/1/1986 1/1/1990 1/1/1994 1/1/1998 1/1/2002 1/1/2006 1/1/2010 1/1/2014 1/1/2018

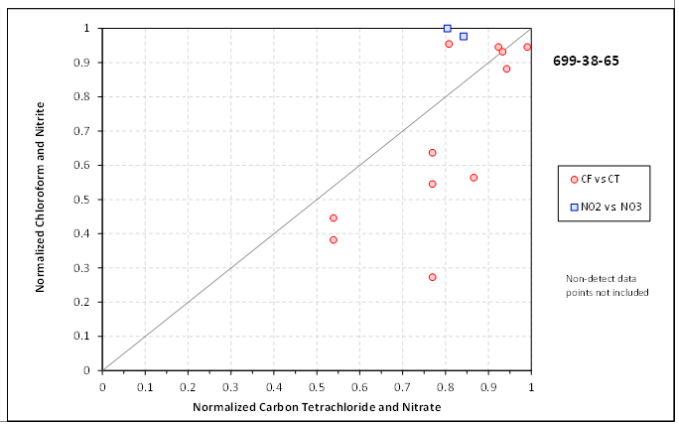
699-38-65
Normalized Chloroform and Nitrite
Normalized Carbon Tetrachloride and Nitrate
CF vs CT
NO2 vs NO3
Non-detect data points not included

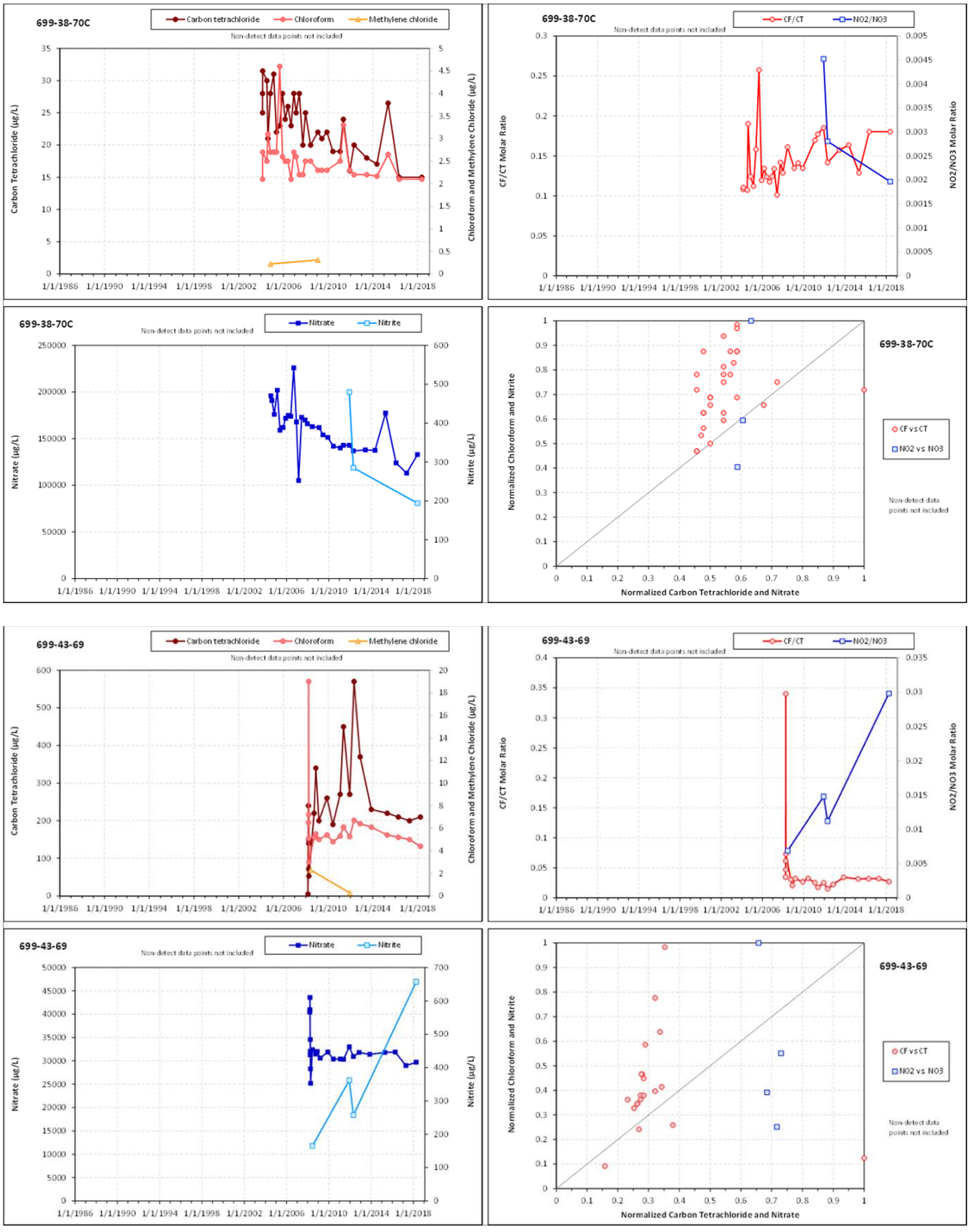
699-38-70C
Carbon tetrachloride
Chloroform
Methylene chloride
Non-detect data points not included
Carbon Tetrachloride (µg/L)
Chloroform and Methylene Chloride (µg/L)
699-38-70C
CF/CT
NO2/NO3
Non-detect data points not included
CF/CT Molar Ratio
NO2/NO3 Molar Ratio
699-38-70C
Nitrate
Nitrite
Non-detect data points not included
Nitrate (µg/L)
Nitrite (µg/L)
699-38-70C
Normalized Chloroform and Nitrite
Normalized Carbon Tetrachloride and Nitrate
CF vs CT
NO2 vs NO3
Non-detect data points not included
699-43-69
Carbon tetrachloride
Chloroform
Methylene chloride
Non-detect data points not included
Carbon Tetrachloride (µg/L)
Chloroform and Methylene Chloride (µg/L)
699-43-69
CF/CT
NO2/NO3
Non-detect data points not included
CF/CT Molar Ratio
NO2/NO3 Molar Ratio
699-43-69
Nitrate
Nitrite
Non-detect data points not included
Nitrate (µg/L)
Nitrite (µg/L)
699-43-69
Normalized Chloroform and Nitrite
Normalized Carbon Tetrachloride and Nitrate
CF vs CT
NO2 vs NO3
Non-detect data points not included

B.3 Multi-Indicator Plots for Northern Well Group

Multi-indicator plots for groundwater data from selected well locations in the northern grouping of wells (total 113 wells, 70 with CT detections) in the 200 West Area. Data from the northern grouping of wells is most relevant through the IRA P&T, 1986-2012.

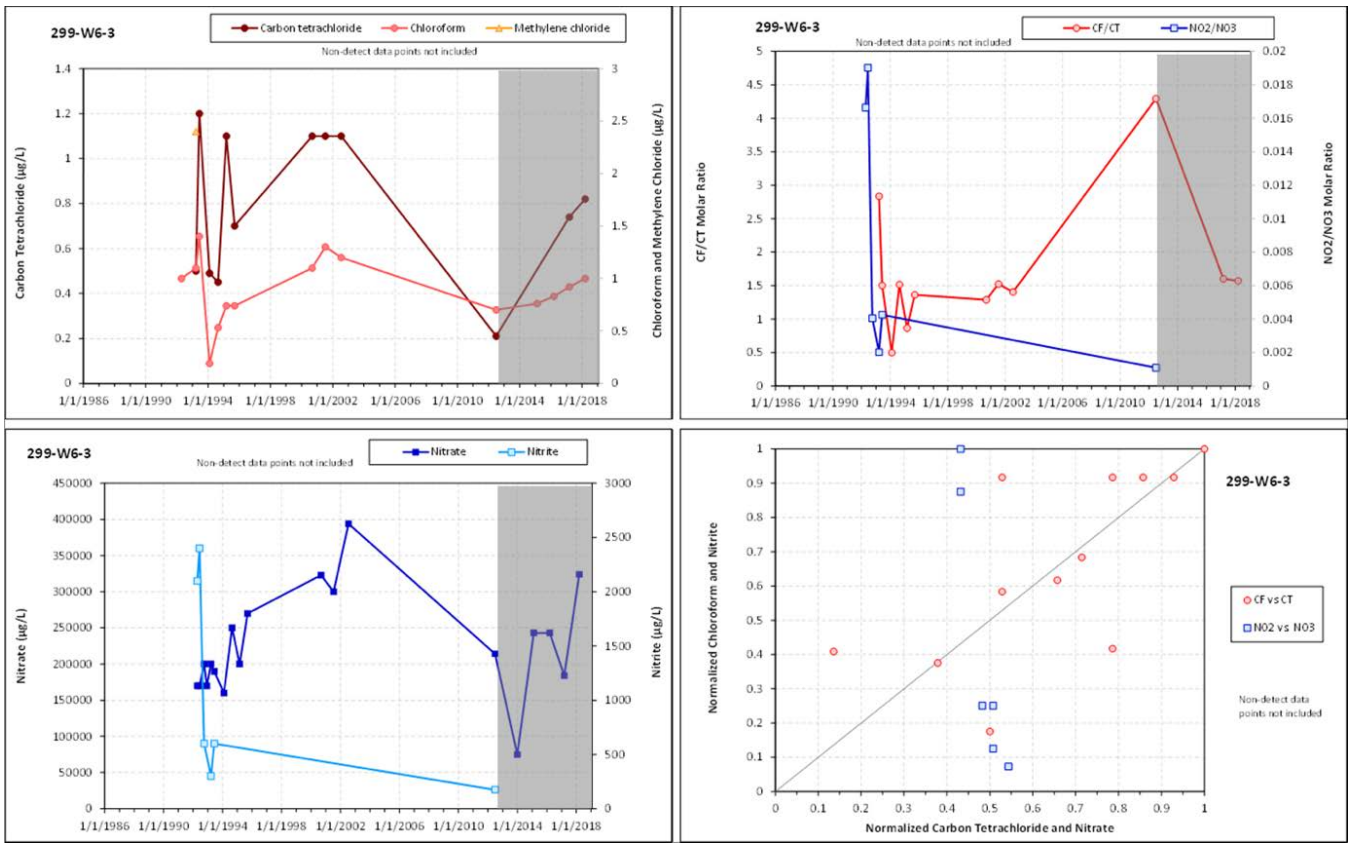

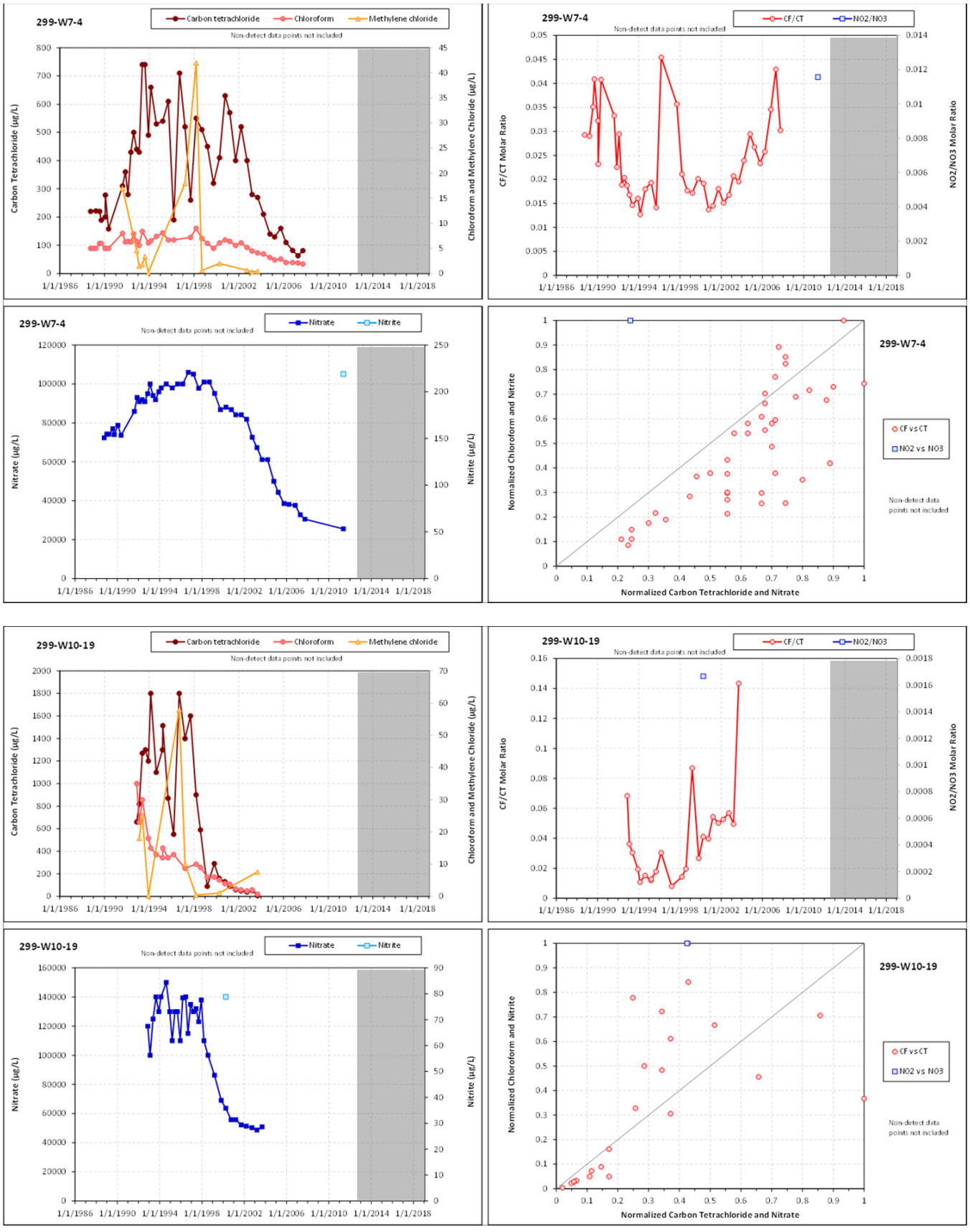
299-W7-4
Carbon tetrachloride
Chloroform
Methylene chloride
Non-detect data points not included
Carbon Tetrachloride (µg/L)
Chloroform and Methylene Chloride (µg/L)
299-W7-4
CF/CT
NO2/NO3
Non-detect data points not included
CF/CT Molar Ratio
NO2/NO3 Molar Ratio
299-W7-4
Nitrate
Nitrite
Non-detect data points not included
Nitrate (µg/L)
Nitrite (µg/L)
299-W7-4
Normalized Chloroform and Nitrite
Normalized Carbon Tetrachloride and Nitrate
CF vs CT
NO2 vs NO3
Non-detect data points not included
299-W10-19
Carbon tetrachloride
Chloroform
Methylene chloride
Non-detect data points not included
Carbon Tetrachloride (µg/L)
Chloroform and Methylene Chloride (µg/L)
299-W10-19
CF/CT
NO2/NO3
Non-detect data points not included
CF/CT Molar Ratio
NO2/NO3 Molar Ratio
299-W10-19
Nitrate
Nitrite
Non-detect data points not included
Nitrate (µg/L)
Nitrite (µg/L)
299-W10-19
Normalized Chloroform and Nitrite
Normalized Carbon Tetrachloride and Nitrate
CF vs CT
NO2 vs NO3
Non-detect data points not included

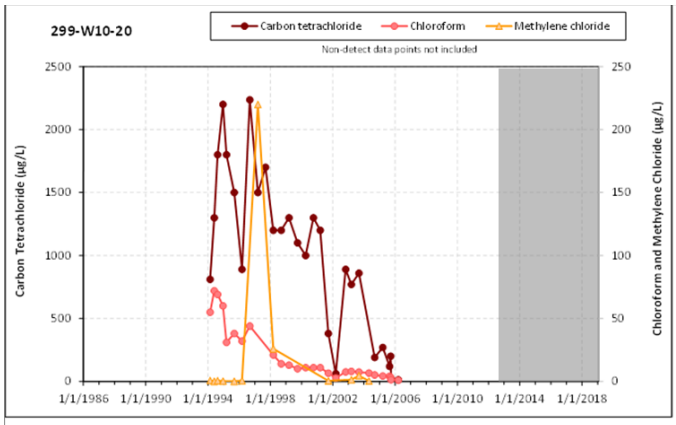
299-W10-20
Carbon tetrachloride
Chloroform
Methylene chloride
Non-detect data points not included
Carbon Tetrachloride (µg/L)
Chloroform and Methylene Chloride (µg/L)

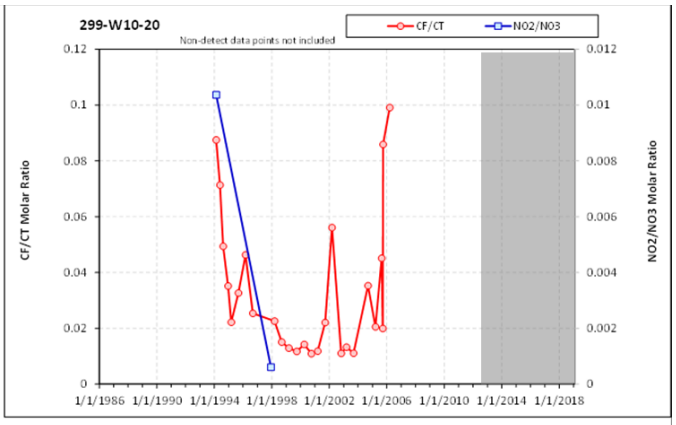
299-W10-20
CF/CT
NO2/NO3
Non-detect data points not included
CF/CT Molar Ratio
NO2/NO3 Molar Ratio

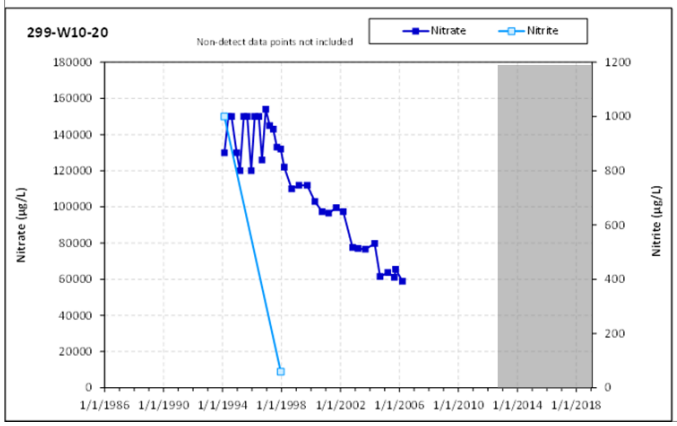
299-W10-20
Nitrate
Nitrite
Non-detect data points not included
Nitrate (µg/L)
Nitrite (µg/L)

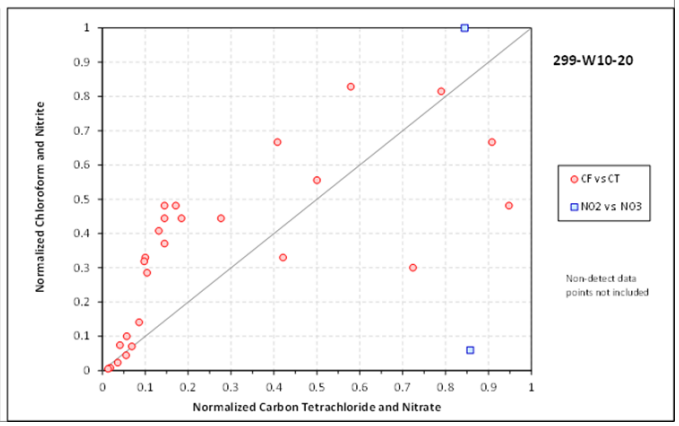
299-W10-20
CF vs CT
NO2 vs NO3
Non-detect data points not included
Normalized Chloroform and Nitrite
Normalized Carbon Tetrachloride and Nitrate

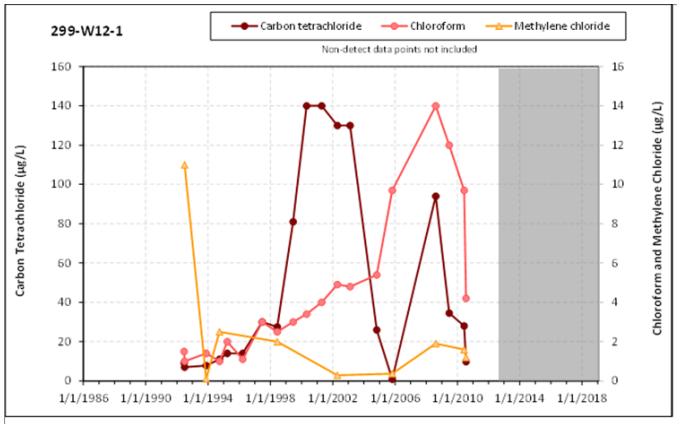
299-W12-1
Carbon tetrachloride
Chloroform
Methylene chloride
Non-detect data points not included
Carbon Tetrachloride (µg/L)
Chloroform and Methylene Chloride (µg/L)

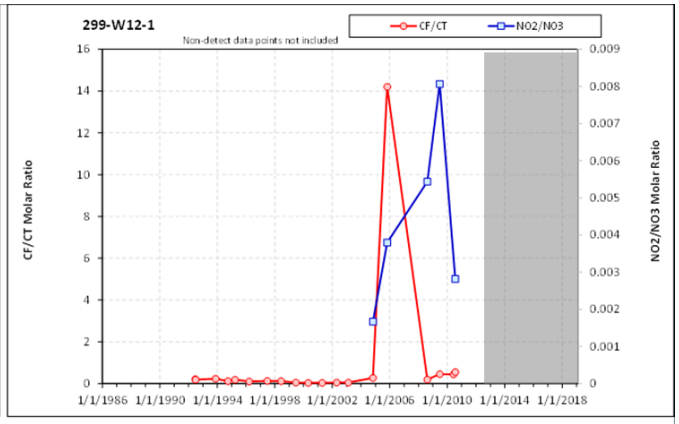
299-W12-1
CF/CT
NO2/NO3
Non-detect data points not included
CF/CT Molar Ratio
NO2/NO3 Molar Ratio

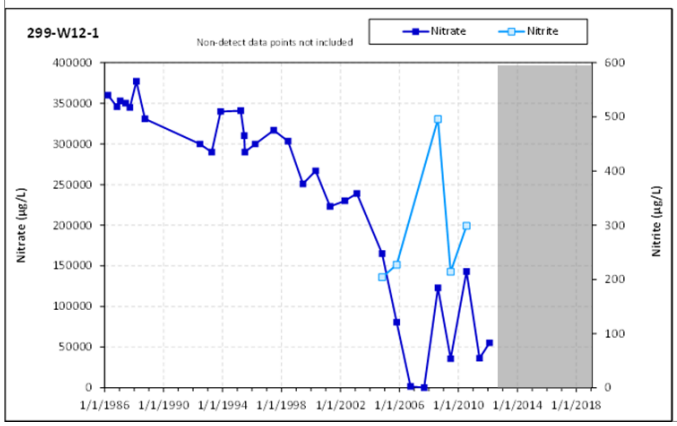
299-W12-1
Nitrate
Nitrite
Non-detect data points not included
Nitrate (µg/L)
Nitrite (µg/L)

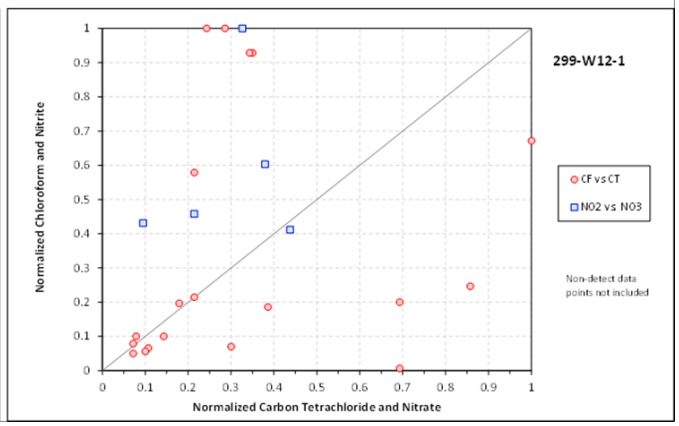
299-W12-1
CF vs CT
NO2 vs NO3
Non-detect data points not included
Normalized Chloroform and Nitrite
Normalized Carbon Tetrachloride and Nitrate

– Silt Assessment

A preliminary analysis was conducted to evaluate the presence and extent of potential silt or clay lenses in the 200 West aquifer, where anoxic, reduced conditions may develop to support biotic degradation of carbon tetrachloride. The analysis quantified the fraction of silt units for a subset of boreholes where composite log data was available (Table C.1). The selected lithologic categories representative of silt in this analysis are listed in Table C.2. These silt categories were selected out of 96 different lithologic categories listed in the existing borehole logs for the 200 West Area (in the Wells with Composite Logs dataset in Table C.1) and represent a conservative subset where anoxic, reduced conditions may develop. These lithologic units are referred in this section collectively as silt units.

Table C.3. Summary of the datasets that were used in this analysis.

Dataset Name	Description of the Dataset	Number of Wells in the Dataset
Wells TD>400ft	A set of wells within the selected boundary that have total depths greater than 400 ft.	295
Formation Tops	A set of wells with measured depths to at least one of the following units Rwie, Rwia, and Rlm identified. Not all formation tops were identified for all wells.	304
Wells with Composite Logs	A set of wells with composite log information. The number of wells in this data set that had the top of the Rwie, Rwia, and Rlm identified were 115, 96, and 30, respectively.	124*

*Only 115 of these wells, with the top of Rwie identified, were used in the final analysis. Four wells had data entry typos for at least one lithologic unit. These were corrected and these wells were included in the final analysis.
TD: Total Depth
Rwie: Ringold Unit E
Rwia: Ringold Unit A
Rlm: Ringold Lower Mud

Table C.4. Lithologic categories selected to represent potential anoxic, reduced silt zones in the 200 West aquifer.

Selected Lithologic Categories
Silt
Silt Lens
Very Silty Sand
Slightly Sandy Silt
Silty Clay
Silt and Clay
Sand Silt Clay
Sandy Silt
Sand Clay Silt

A subsection of the 200 West Area (Table C.1), encompassing the CT degradation data analysis area shown in Figure 7 (in the main body of the report), was selected to identify the boreholes that extend into or below Ringold Unit E (Rwie). These boreholes in the subsection were selected based on their total depth being greater than 400 ft. As a result, 295 boreholes were identified in this dataset (Table C.1). An additional dataset was also gathered from the site geologic data that identified at least one of the three formation tops for Rwie, Ringold Unit A (Rwia), and/or Ringold Lower Mud (Rlm). This information was important to conducting the silt analysis for specific formations where data is available.

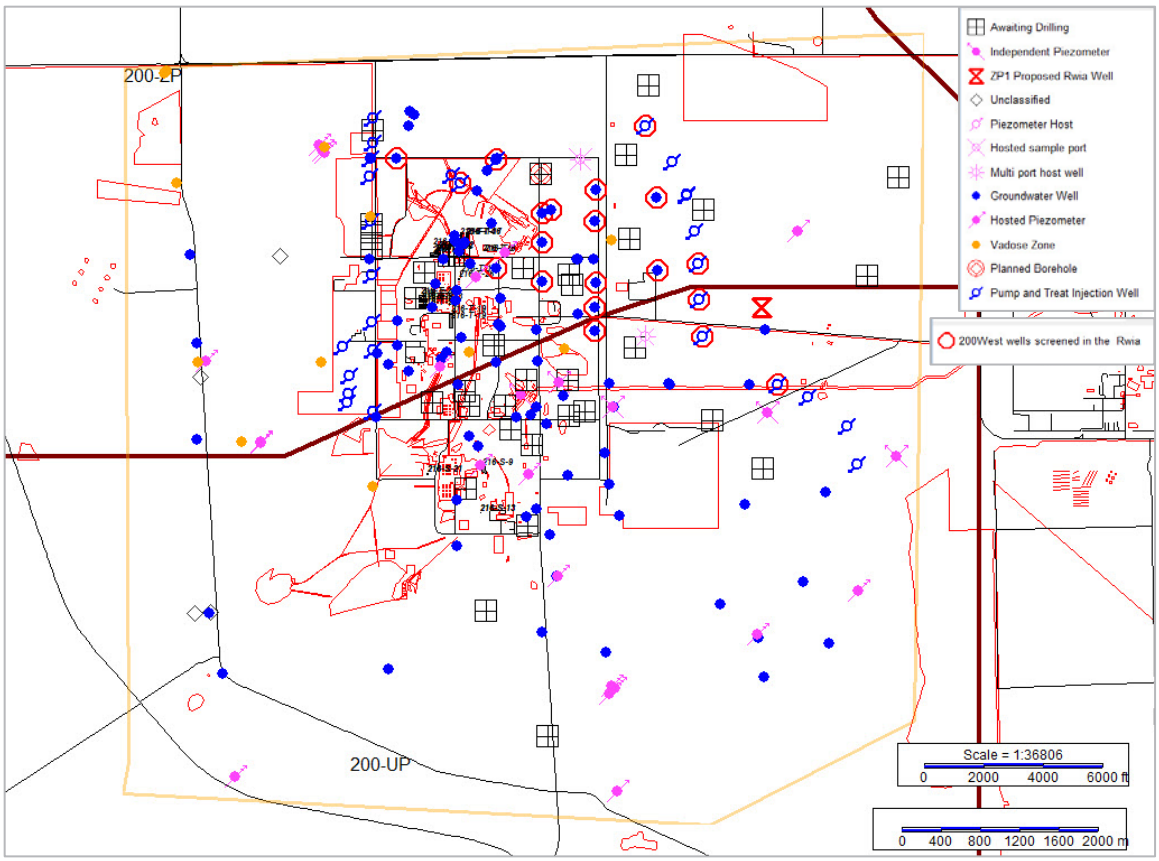

Figure C.1. Boundaries of the selected zone for evaluation of silt layers shown in yellow.

A subset of the 295 wells (with total depths greater than 400 ft) were also identified based on the availability of sufficient lithologic information to support this analysis. This subset, 124 wells, had composite log information for the entirety of their depth. However, 9 wells in this dataset didn't have the top of Rwie identified (in the Formation Tops dataset). As a result, a total of 115 wells were selected for the final silt analysis. This final set of wells had composite log information, the depth for the top of Rwie, and total depth information. Since not all of these 115 wells also had Rwia identified (Table C.1), two separate analyses were conducted to represent the extent of silt units in the 200 West aquifer:
(1) calculating the aggregate silt fraction below the top of Rwie across the total depth (below Rwie) for each well; and (2) calculating the aggregate silt fractions for Rwie (including Rlm where applicable) and Rwia for a subset for a subset of wells for which the top of the Rwia was identified. A summary of analyses and datasets used is given in Figure C.2.

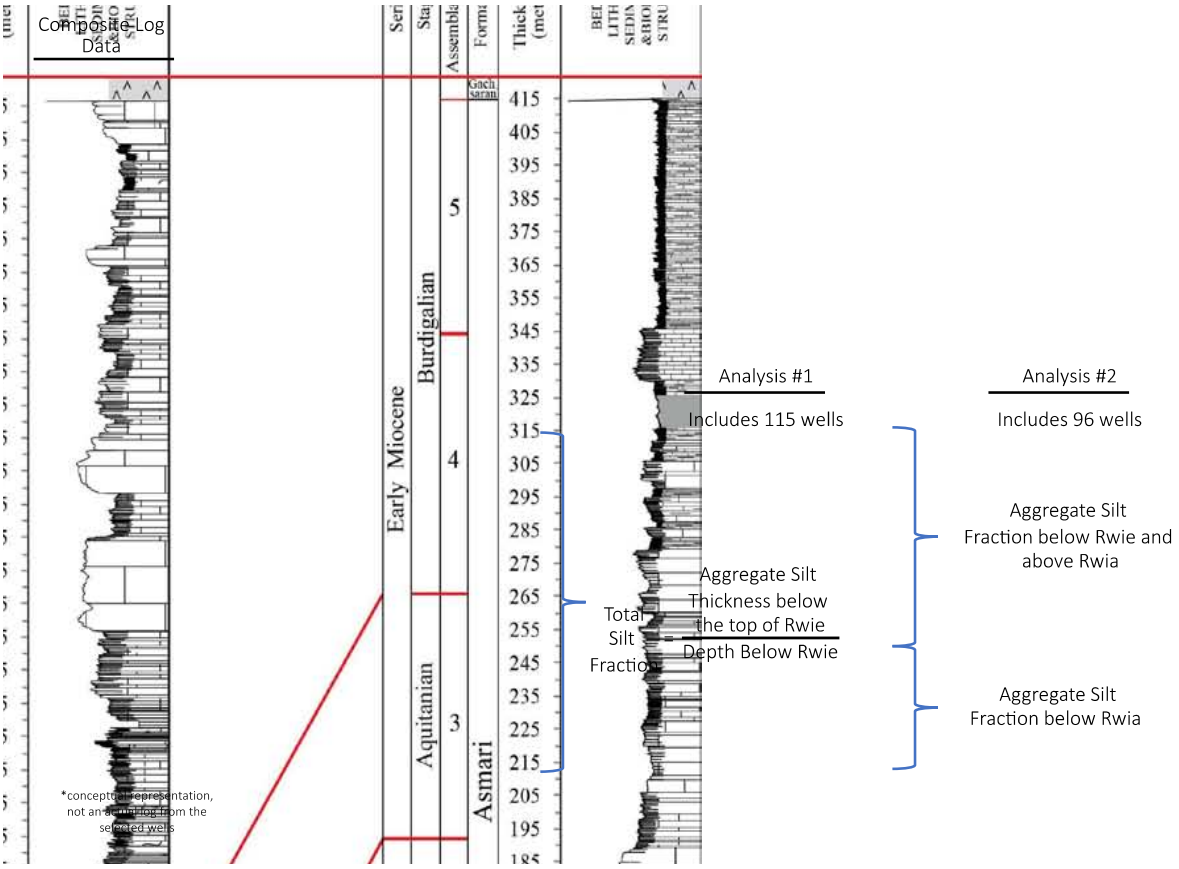

Figure C.2. Summary of datasets and analyses used in the silt assessment.

Among the 115 wells used in the first analysis, a total of 59 wells had one or more of the selected silt units. The analysis only included the silt units that started below the top of Rwie; units that started above and continued into Rwie were excluded. The total silt fractions (i.e., fraction of aggregate silt thickness for below the top of Rwie portion of the well) ranged from 0% to 36% (Figure C.3). A total of 49 wells had less than 10% silt content (with 20 of those <2%), while 8 had 10%-20%, and 2 had more than 20%. Higher silt fractions may indicate Rlm contribution to these numbers where certain layers within Rlm were defined as one of the selected silt categories. Note that Rlm was not consistently identified in the dataset; therefore, it was not included in the analysis as a separate unit.

The second analysis focused on evaluating the silt content for Rwie and Rwia separately for a smaller subset of 96 wells based on the availability of Rwia information. For this analysis, Rwie was defined from the top of the unit until the top of Rwia. The average thickness of Rwie for the 96 wells was about 239 ft. Rwia was defined from the top of the unit until the total depth of each well. The average thickness of this section for the 96 wells was about 49 ft. The distribution of aggregate silt fractions for the both units are given in Figure C.4 and Figure C.5. Forty-two wells had at least one silt unit in the Rwie formation. The distribution of the silt fractions among these 42 wells looked similar to the first analysis results with the majority of the wells (29) having less than 10% silt. For Rwia estimates, only a total of 19 wells showed any silt content over an average of 49 ft thickness. The aggregate silt fraction showed relatively more even distribution ranging from 0% to close to 100%.

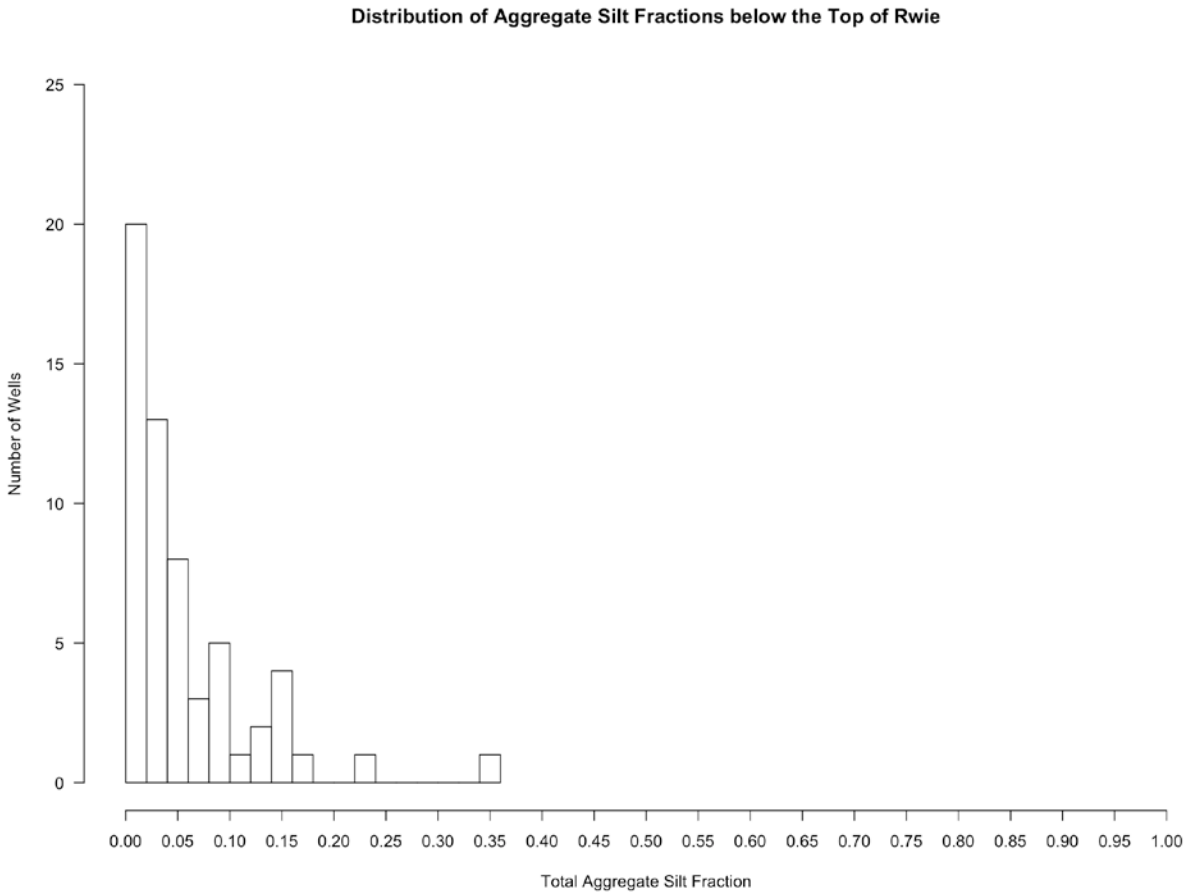

Figure C.3. Fraction of aggregate silt content below the top of Rwie, calculated for 115 wells. Wells with no silt content are excluded.

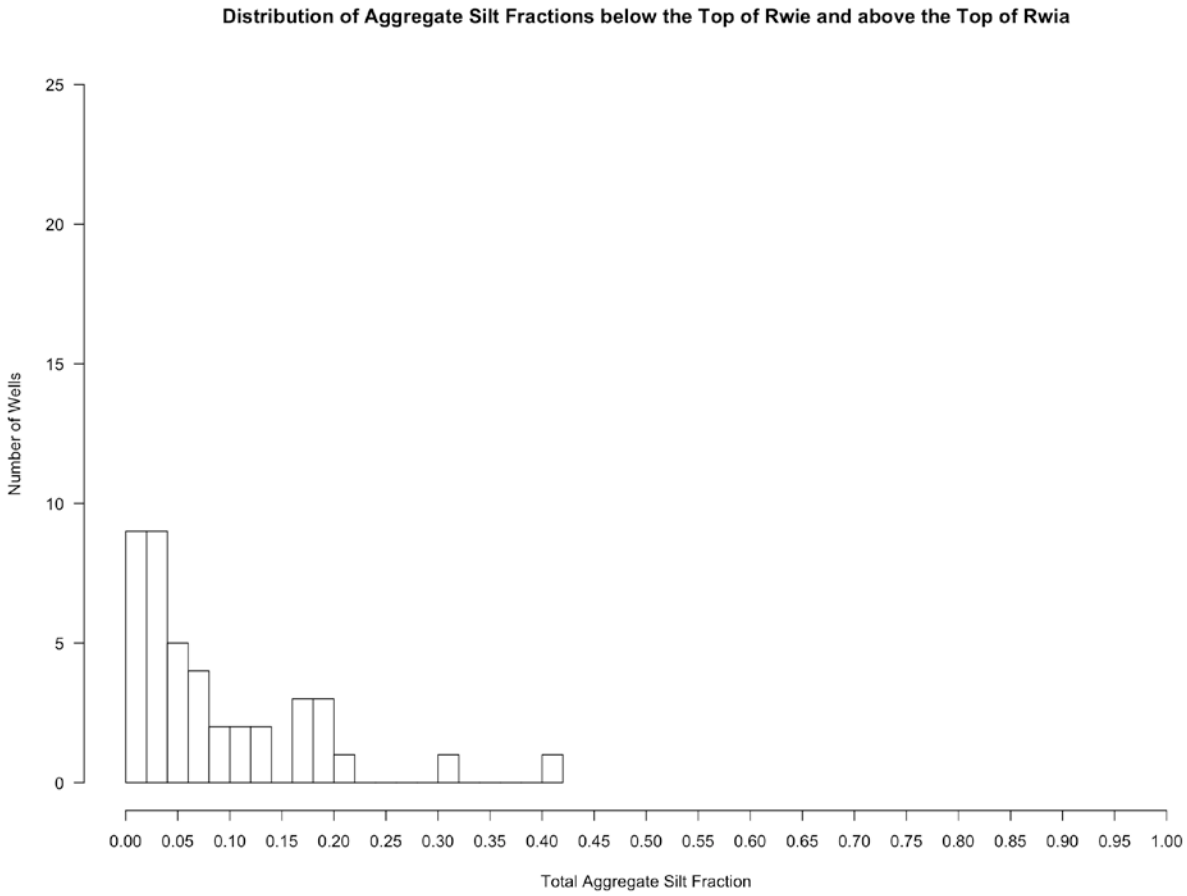

Figure C.4. Fraction of aggregate silt thickness below the top of Rwie and above the top of Rwia, calculated for 96 wells (Average evaluated thickness for Rwie = 239 ft). Wells with no silt content are excluded.

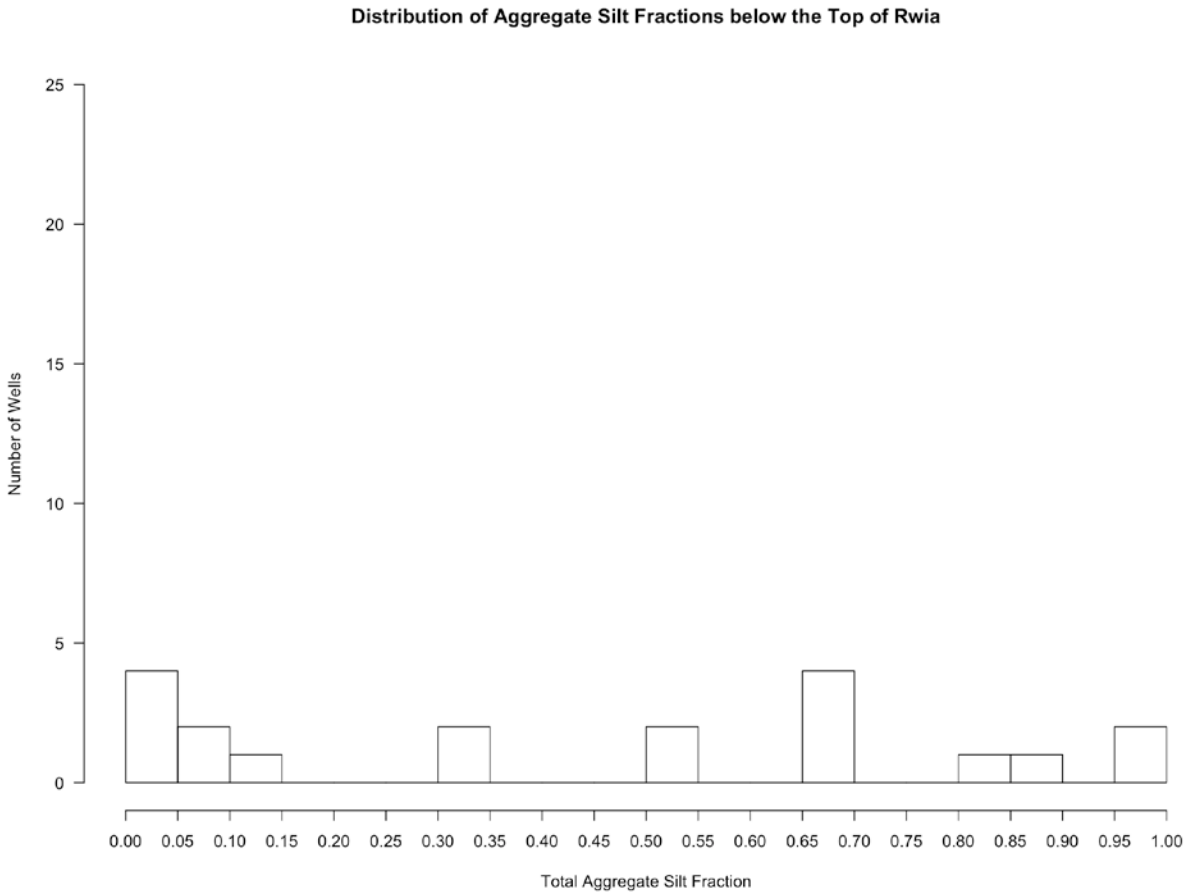

Figure C.5. Fraction of aggregate silt thickness below the top of Rwia until the total well depth, calculated for 96 wells (Average evaluated thickness = 49 ft). Wells with no silt content are excluded.

Figure C.6(a) shows the distribution of wells and their silt fractions analyzed for below the top of Rwie across the total depth (i.e., 115 wells in analysis #1). The distribution of silt for these wells showed some areas where silt content might be relatively higher, but these wells represent only a small percentage of overall wells (<21% of the wells showed higher than 5% silt fraction). The location of the wells identified with any silt content (59 wells out of 114) are shown in Figure C.6(b) and compared to the CT degradation indicators. There is very little or no correlation observed between the degradation indicators and the location of the wells with silt content. However, it is important to note that the subset of wells analyzed for silt content and the wells analyzed for the indicators are not the same.

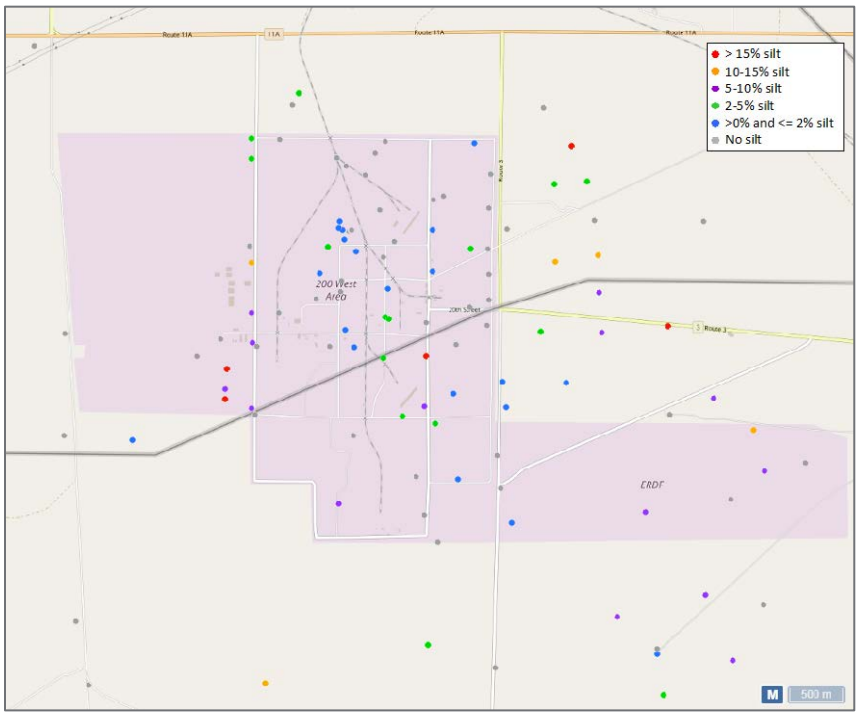

(a)

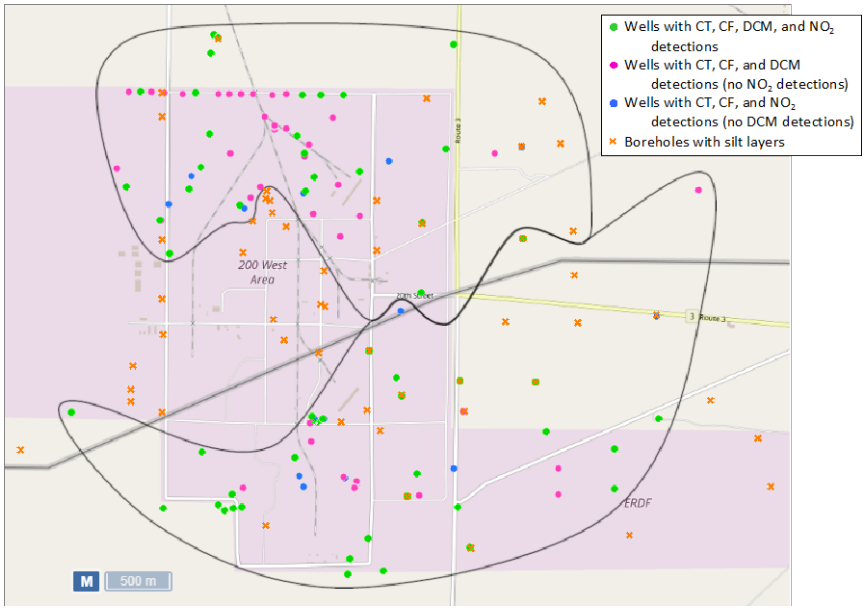

(b)

Figure C.6. (a) All wells analyzed in the 200 West aquifer (below the top of Rwie) for their silt content (114 wells included in analysis #1); (b) Distribution of the wells with any silt content (from analysis #1) compared to the CT degradation indicators used in this assessment.

PNNL-28846
73793-RPT-0001, Rev 0.0

Pacific Northwest National Laboratory

902 Battelle Boulevard
P.O. Box 999
Richland, WA 99354
1-888-375-PNNL (7665)

www.pnnl.gov